



CryoSat Calibration & Validation Concept

Prepared by:

CryoSat Science Advisory Group

•
Centre for Polar Observation & Modelling
Department of Space & Climate Physics
University College London
Pearson Building, Gower St.
London WC1E 6BT

•
14 November 2001



Authorship

The CryoSat Science Advisory Group (SAG) has prepared this document. Its members are: Prof. D.J. Wingham (Lead Investigator), University College London, UK; Dr. Rene Forsberg, National Survey & Cadastre (KMS), Denmark; Dr. Seymour Laxon, University College London; Prof. Peter Lemke, Institute of Marine Research, Germany; Prof. Heinrich Miller, Alfred Wegener Institute, Germany; Prof. Keith Raney, Johns Hopkins University, US; Dr. Stein Sandven, Nansen Centre, Norway; Remko Scharroo, Technical University of Delft, The Netherlands; Dr. Patrick Vincent, CNES, France and Dr. Helge Rebhan (convenor), ESA-ESTEC, Noordwijk, The Netherlands.

The Science Advisory Group would like to express their appreciation to the ESA CryoSat Project Team for their support in preparing this document. They would also like to thank those scientists who have contributed material to this document: Dr. R. Arthern, British Antarctic Survey; Prof. S. Gogineni, University of Kansas, USA; Dr. W. Krabill, NASA Goddard Flight Centre, USA; Dr. N. Peacock, University College London; Dr. A. Shepherd, University College London; and Dr. H. J. Zwally, NASA Goddard Flight Centre, USA.



Table of Contents

1	Introduction to the CryoSat Calibration and Validation Concept.....	1
1.1	ABOUT THIS DOCUMENT.	2
1.2	OTHER SOURCES OF INFORMATION.....	8
2	The General Objective and Character of CryoSat Calibration and Validation.	9
2.1	GENERAL OBJECTIVE OF THE MEASUREMENT.	9
2.2	GENERAL OBJECTIVE OF THE CALIBRATION AND VALIDATION.....	12
2.3	DEFINITION OF ‘CALIBRATION’ AND ‘VALIDATION’	15
2.4	GENERAL CHARACTER OF THE CALIBRATION AND VALIDATION.....	17
3	Validation of Land Ice Uncertainty	20
3.1	OBJECTIVE AND GENERAL CHARACTER OF LAND ICE VALIDATION.	20
3.2	THE MASS FLUCTUATION.....	25
3.3	THE DENSITY FLUCTUATION	29
3.4	THE RETRIEVAL ERROR.	33
3.4.1	The measurement technique.....	33
3.4.2	The character of the retrieval error.....	37
3.4.3	Validation of the retrieval errors.....	42
3.5	INTERSATELLITE BIAS	46
3.6	TIMING AND LOCATION OF LAND ICE VALIDATION EXPERIMENTS.....	47
4	Validation of Sea Ice Uncertainty.....	49
4.1	OBJECTIVE AND GENERAL CHARACTER OF SEA ICE VALIDATION.	50
4.2	THE SNOW LOAD UNCERTAINTY.	53
4.3	THE DENSITY UNCERTAINTY	55
4.4	THE RETRIEVAL ERROR.	56
4.4.1	The measurement technique.....	57
4.4.2	The character of the retrieval error.....	61
4.4.3	Validation of the retrieval error.....	65
4.5	THE OMISSION ERROR.....	69
4.6	VALIDATION OF THICKNESS MEASUREMENTS	71
4.7	TIMING AND GEOGRAPHICAL EMPHASIS OF THE SEA ICE VALIDATION EXPERIMENTS.....	75
5	Calibration of the satellite measurements.	77



5.1	OBJECTIVE AND GENERAL CHARACTER OF CALIBRATION.....	77
5.2	SOURCE AND SCALES OF FLUCTUATION OF INSTRUMENT SYSTEM ERRORS.....	80
5.2.1	The error in echo delay timing ϵ_t	80
5.2.2	The error in echo direction ϵ_θ	81
5.2.3	The error in radial component of the orbit ϵ_z	82
5.2.4	The along-track position error ϵ_x	82
5.3	INTERNAL AND EXTERNAL CALIBRATION.....	83
6	References.....	86
7	Annex.....	90
7.1	THE VARIANCE OF THE SPATIAL AVERAGE.....	90
7.2	THE VARIANCE OF AN INTEGRAL OF A WHITE STATIONARY PROCESS.....	90
7.3	THE VARIANCE OF A SPATIAL AVERAGE OVER THE SEA ICE AREA.....	91



CryoSat Calibration &
Validation Concept



Doc: CS-PL-UCL-SY-0004

Issue: 1

Date: 14 November 2001

Change Record

Issue	Modification	Issue date
1	Release preceding CVRT AO	14 November 2001

		CryoSat Calibration & Validation Concept	Doc: CS-PL-UCL-SY-0004 Issue: 1 Date: 14 November 2001
--	---	---	--

1 Introduction to the CryoSat Calibration and Validation Concept



The CryoSat mission is aimed at providing to the wider scientific community measurements of mass and thickness fluctuations of the Earth's ice fields. The measurements are of particular importance for the testing and verification of mesoscale and regional numerical models that include cryospheric components. This wider community is concerned to receive measurements that require no further processing for their application and which are supported by estimates of their uncertainty.

The purpose of the calibration and validation of the CryoSat data is to provide confidence in estimates of the uncertainty of CryoSat data products. In principle, this may be determined by examining the difference between the CryoSat data product and a suitably large number of independent, accurate measurements. In practise such a scheme is scarcely possible; if it were, there would be limited point in flying the satellite.

In practice, a sensible approach is to try to characterise at least the temporal and spatial scale of the uncertainties. This reduces the number of independent estimates of errors to a minimum that, on the basis of a physical argument, may be extrapolated to the satellite data as a whole. Nonetheless the validation requires a wide range of surface measurements of ice character, geometry and distribution, and the change of these properties with time. The limited resources for experimental work in the polar regions means that CryoSat calibration and validation will require the support of polar scientists, and make best use of existing and planned measurement campaigns at high latitudes.

The purpose of this document is assist this process by describing:

- A framework for the treatment of CryoSat errors and their breakdown into components.
- The expected nature of uncertainty in the CryoSat measurements and their likely spatial and temporal scales.
- The experiments, sensors and platforms that may most usefully estimate the uncertainties.



		CryoSat Calibration & Validation Concept	Doc: CS-PL-UCL-SY-0004 Issue: 1 Date: 14 November 2001
--	---	---	--

1.1 About this document.

In writing this document, our intention is to provide a description of a calibration and validation approach that is understandable by wider scientific users of the CryoSat data. In the case of the ice sheets, the wider user is interested primarily in the average mass change over a region. In the case of sea ice, it is the average thickness and mass over a region that is the principal interest. Moreover, since the wider user is likely to be concerned with comparing the results of the CryoSat mission with numerical models, or with assimilating the CryoSat observations, they will be concerned to have estimates of the covariance of the errors in the CryoSat data, rather than simply their variance. In breaking down the various errors in the CryoSat data, and in structuring our approach to the calibration and validation, we have worked downwards from the variables of the average mass change over an area, or the average thickness or mass within an area. We have also emphasised throughout the importance of gaining some practical understanding of the error covariance associated with the data.

This is by no means the only way to approach this task. A possibly more conventional approach is to start with the instrument errors and work upwards, emphasising rather more the variance of the errors in a point measurement. For this reason, we provide in section 2 an introduction to the importance and use of the covariance function in determining the errors of spatial averages in general, and, in general terms, the nature of the error covariances that are characteristic of ice radar altimetry. In a first reading of the document, this section could be skipped. It introduces the error covariance function and describes why, in the case of land ice, one is concerned with the covariance of a trend measurement, whereas in the case of sea ice it is the covariance of the thickness itself that is the primary interest. This section also distinguishes ‘validation’, defined here as determining the uncertainty associated with ice specific errors that need *in-situ* experiments, from ‘calibration’, which concerns the uncertainty in the instrument system that may be determined anywhere. It also introduces the terms ‘retrieval error’ to describe a measurement error that requires validation, and ‘system error’ to describe an error that requires calibration.

These ideas inform the way the calibration and validation concept has been developed. Starting in the case of the land ice with the error in the spatial average of mass change, or in the case of sea ice with the spatial average of thickness, the error in either case is successively broken down into components until individual components are identified. For each component, we have then identified ground experiments, or possibly modelling

		CryoSat Calibration & Validation Concept	Doc: CS-PL-UCL-SY-0004 Issue: 1 Date: 14 November 2001
--	---	---	--

studies, that may provide some idea of the variability and spatial and temporal scale of fluctuation of the error component.

So, to each error there is an answering activity. We have tried where possible to identify where particular experiments address particular errors. We would not claim to be complete in our description of the possible experiment or modelling approaches. Where we know of approaches that would contribute to the validation we have identified them, but it may well be that there are methods we are unaware of that could also be important. We *have* tried to be fairly complete in our identification of the error terms (although experience suggests that the number of errors increases with experience and thus with time) so that potential contributors to the validation have an idea of the ‘target’.

The ‘top-down’ approach taken here means that it is some way into the document before the detail of particular errors and their corresponding validation activities are described. It is useful, therefore, to have a brief summary here of the breakdown of the errors and the activities associated with their calibration and validation. On the following two pages this information is presented in a diagrammatic form for land ice (Fig. 1) and sea ice (Fig. 2). Each figure shows (in black) the ‘top-down’ breakdown of the errors and where these errors are described in the document, and (in red) the answering validation or calibration activity. We hope these figures may provide a ‘quick look’ at the calibration and validation concept, as well as providing a route map for using the document. (Further navigation is provided at the start of each chapter with a short summary of its contents.)

Sections 3 and 4 describe the validation of the land ice and sea ice measurements respectively. Each chapter is introduced by describing the quantitative relation between the mass change (or thickness) and the measured elevation change (or measured ice freeboard). In both cases, this naturally leads to a breakdown of the errors into those associated with unknown snow mass fluctuation, an unknown firn (or sea ice) density, and measurement errors. There are also particular uncertainties. In the case of land ice some attention needs to be given to the effect of post-glacial rebound; in the case of sea ice the question arises as to whether the sampling of the ice floes by the radar will bias the ice thickness distribution. Both chapters describe the magnitude and spatial and temporal scale of the snowfall and density uncertainties, in so far as these are known, and how they may be approached experimentally. Traditional glaciological or sea ice methods of ice coring, the revisiting of earlier records, or the development of new, low- and radar-frequency tools to investigate these uncertainties are described.

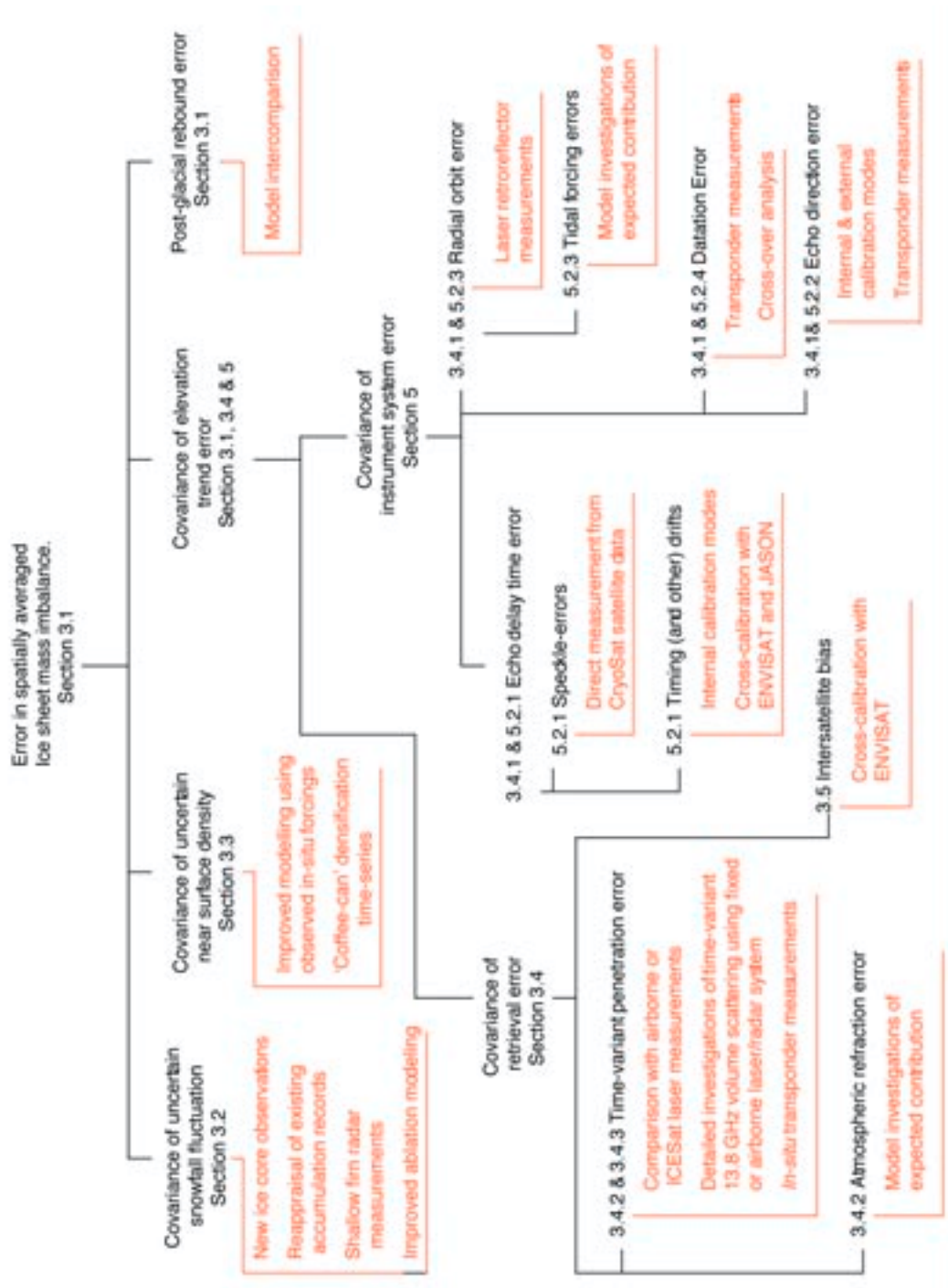


Fig. 1. The breakdown of land ice uncertainties (in black) and their location in the document, and (in red) the proposed calibration and validation activities needed to determine them.

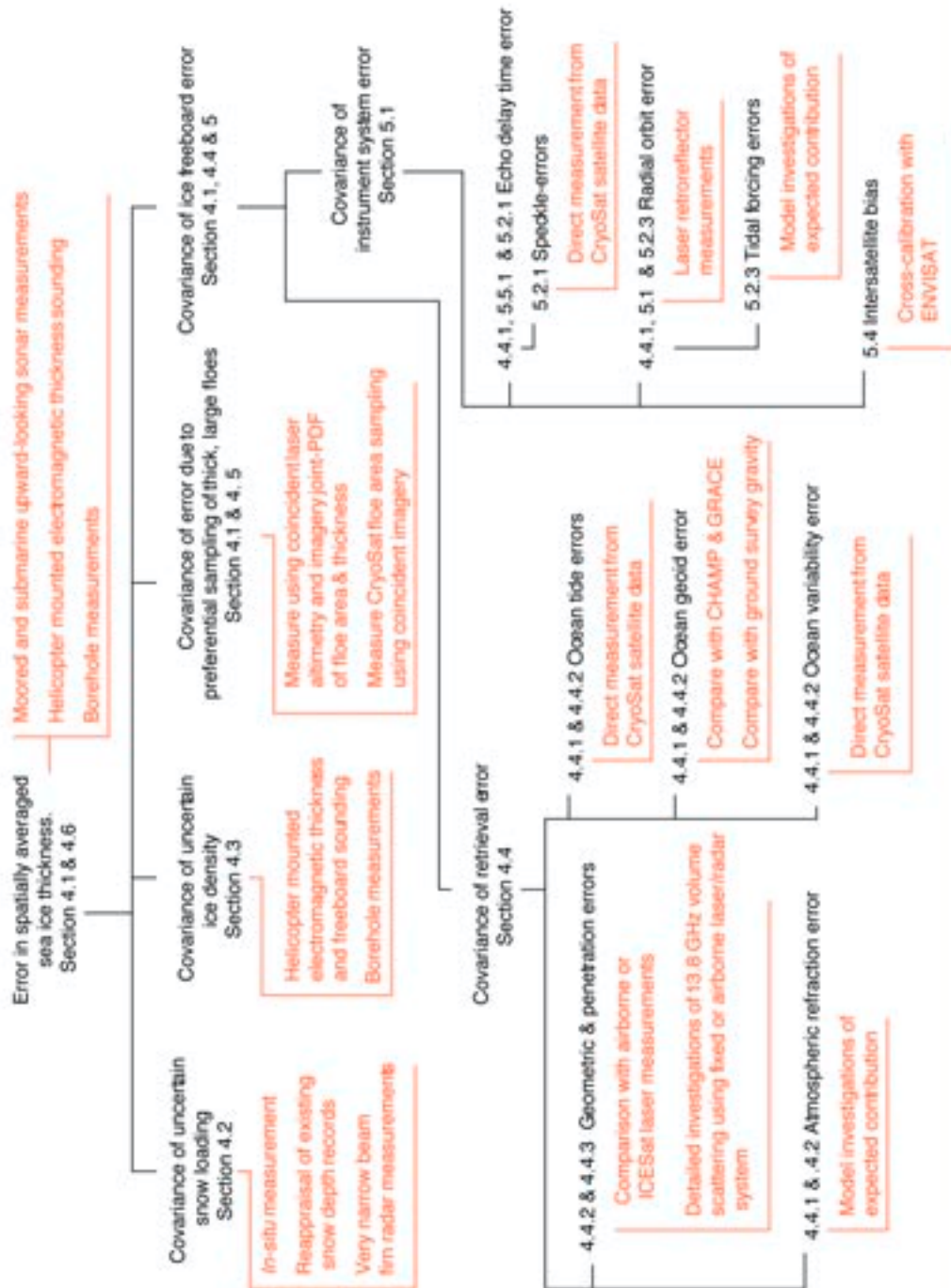




Fig. 2. The breakdown of sea ice uncertainties (in black) and their location in the document, and (in red) the proposed calibration and validation activities needed to determine them.



		CryoSat Calibration & Validation Concept	Doc: CS-PL-UCL-SY-0004 Issue: 1 Date: 14 November 2001
--	---	---	--

Each of chapters then turns to consider the measurement error in the elevation trend and ice freeboard respectively (sections 3.4 and 4.4 respectively). In each case, the sections start with a description of the method of measurement and the measured parameters. These are described as they appear in the ‘level *Ib*’ data. For our purpose here, these data may be quickly defined as the radar echoes and their measurement geometry. (The concept of the ‘level’ of the data is discussed in greater detail in section 2). The new altimeter modes of CryoSat, the SAR and SAR-interferometry modes, are described in outline. This allows us to detail the error breakdown of the measurements, and the various components are divided into ‘retrieval’ errors that arise in converting these measurements to elevation change or ice freeboard, and ‘system’ errors that are present in the level *Ib* measurements themselves.

By and large the retrieval errors fall into two types. Firstly, there are errors that arise because the radar wave penetrates the snow or ice surface in ways that are uncertain. In the case of land ice, the uncertainty arises through changes in the density, layering and grain size of the near surface firn, which causes small but detectable changes in the location of the electromagnetic (as opposed to the material) air-snow interface. In the case of sea ice, the difficulty is that at present it is not altogether clear when snow is present on the ice whether it is the air-snow, or the snow-ice interface is responsible for scattering the radar wave.

In either case we use historical data, or somewhat more speculative arguments, to provide in the form of covariance functions an idea of the magnitude and spatial and temporal scales of these errors. This is important in informing the design of detailed field experiments. These errors may be investigated by a variety of techniques, including airborne laser and radar measurements. The laser altimeter observations of the ICESat mission (Zwally *et al.* 2001) may also be very useful in this context. We also observe in these sections that a considerable amount may learnt from careful experiments that are independent of the satellite measurements themselves – a better understanding is required of the physics of the snow, firn and ice pack, and how the 13.8 GHz radar waves interact with them.

Secondly, there are errors arising from the use of models of the radar wave propagation through the atmosphere, or of the ocean tides, gravity field and dynamic topography. Some of these errors are of the first importance when considering ocean radar altimetry. Although we do not wish to underplay their importance, it is perhaps worth noting here that ice sheet and sea ice trends are an order of magnitude larger than those of the ocean, and that their importance of some of these errors is correspondingly less. They cannot be ignored

		CryoSat Calibration & Validation Concept	Doc: CS-PL-UCL-SY-0004 Issue: 1 Date: 14 November 2001
--	---	---	--

however, and in some instances we recommend that further model investigations would be valuable.



There then follows a section in each case describing the retrieval errors that are particular to the cases of land ice and sea ice. In the case of land ice, the error that arises between different satellite altimeter measurements is of concern. This has often been treated as if it were a calibration problem (*i.e.* a function only of the instrument systems' design). However, in the one case where a direct comparison is possible – a comparison of ERS-1 and ERS-2 radar altimeter measurements over the Antarctic ice sheet – it is clear that the problem lies with the retrieval error. Simply cross-calibrating the instrument systems over a known surface such as the ocean will not deal with the bias. Section 3.5 provides a salutary reminder.

In the case of sea ice, the potential difficulty arises that the radar will preferentially select large, thick ice floes and that the ice thickness distribution will be biased as a result. This is not an easy source of error to predict in advance, because there has been little work previously on the joint probability density of ice floe area and thickness. Section 4.5 describes ways in which using satellite thermal or radar imagery this may be achieved, and then, as a second step, how to determine the way the radar samples the floe area.

Section 4.6 considers ways in which the sea ice thickness may be directly validated using, for example, upward-looking sonar measurements from fixed or submarine platforms. There is no corresponding land ice section. This is because, while using glaciological techniques one can estimate the elevation trend of a region, the measurements are not remotely accurate enough to compare with the satellite measurements.

Finally, sections 3 and 4 are closed with a summary of the considerations that affect the timing and location of the experiments. These sections are brief in that they are restricted to fairly general considerations. For example, we identify areas of Antarctica where better accumulation records would be useful; that Greenland may be a very useful region on logistic grounds; or that the Arctic Ocean north of Greenland contains a wide range of sea ice conditions that are accessible by aircraft or by ship. However, we do not wish to discourage participation by being too prescriptive as to time and place. We recognise that experiments in all regions of the polar latitudes are potentially important to the validation of the CryoSat mission, and that polar logistics are subject to stringent resource limitations.

Section 5 is concerned with the calibration of the instrument system. The section starts with a general description of the nature of these errors, and how these tend, empirically, to have

		CryoSat Calibration & Validation Concept	Doc: CS-PL-UCL-SY-0004 Issue: 1 Date: 14 November 2001
--	---	---	--

scales that are very much less than, of the same order, or very much longer than the orbital period. The concept of describing them by a temporal covariance function is introduced. The introductory section 5.1 summarises the effect of the wrapping of these temporal variations onto the surface of the Earth by the orbital motion, and the way in which these temporal scales of error enter spatial averages of land ice elevation trends and sea ice thickness. Section 5.2 provides a brief summary of how these system errors arise through particular imperfections in the instrument system hardware. This allows us in the final section to describe the approach to calibrating these errors. This will use a combination of internal instrument calibration, external calibration using the ocean surface or a transponder as a ‘known’ signal, and comparison with the contemporary ENVISAT and JASON altimeters’ data.

The document closes with section 6, which contains references that provide more detailed descriptions of many aspects summarised briefly in the text, and section 7, which contains an annex that adds some detail to the mathematics of sections 2 and 3.



1.2 Other sources of information.

There are two other documents that provide important information concerning the CryoSat mission. These are:

CryoSat Mission Requirements (CS-RS-UCL-SY-0001, denoted MRD 1999). This describes the scientific objectives and context of the mission. It also details the derivation of the mission measurement requirements. It is essentially the scientific elements of the CryoSat mission proposal.

CryoSat Mission and Data Description (CS-RP-ESA-SY-0059, denoted MDD 2001). This describes the satellite and instrument system design, satellite operations and the data generated by the ESA ground segment. It is the principal source for technical information concerning the mission implementation.

These, and other supporting information, may be found in their current versions on the CryoSat website (<http://www.esa.int/livingplanet/cryosat>). The CryoSat website in general, and these documents in particular are dynamic. They will be updated from time-to-time as the mission implementation matures. New issues of these documents and activities associated with them will be advertised in the ‘news’ section of the website.

		CryoSat Calibration & Validation Concept	Doc: CS-PL-UCL-SY-0004 Issue: 1 Date: 14 November 2001
--	---	---	--



2 The General Objective and Character of CryoSat Calibration and Validation.

2.1 General character of the measurement. The measurement of thickness and rate-of-change of thickness. Spatial averages. Shorthand description of various practical approaches. 2.2 General objective of the calibration and validation. The uncertainty in spatially-averaged products and their second moment. Assumptions of stationarity and its limitations. The covariance functions of the land ice and sea ice error. 2.3 Definition of 'calibration' and 'validation'. Instrument system and retrieval errors. Treatment of 'biases'. 2.4 General character of the calibration and validation. The importance of repeated independent measurements. The structure of the covariance function and the importance of its independent measurement. Independence of retrieval and system errors and the separation of calibration and validation experiments. Relative importance of validation and calibration activity.

2.1 General character of the measurement.

The objective of the CryoSat mission is to estimate, in the case of land ice, the temporal trends in ice mass averaged at various spatial scales; and, in the case of sea ice, the temporal trends in perennial sea ice thickness and mass. In general, the fundamental objective is to determine a rate of change of mass per unit area through measurements of the rate of change of thickness \dot{h} . In the case of sea ice, the ice thickness h is measured and of interest. In the case of land ice, it is the ellipsoidal elevation that is measured, and changes in elevation are supposed equal to changes in thickness. (In practise, estimates are sometimes made of the motion of the ice sheet bed with respect to the ellipsoid due, for example, to post glacial rebound). In what follows, the symbol h may be taken as ice thickness when referring to sea ice, and ice elevation when referring to land ice.

In general the mass rate is a function of space \mathbf{x} and time t . Here \mathbf{x} should be understood as a vector co-ordinate describing a location on the Earth's reference figure. Generally, the mission aims to make estimates of \dot{h} averaged over an area A . Over land ice, A may typically be a drainage basin; over sea ice A may be a region such as 10^5 km^2 whose trends may usefully be compared with numerical model. The trends will also be averaged over a time interval T that will typically be the mission duration but maybe shorter if the

		CryoSat Calibration & Validation Concept	Doc: CS-PL-UCL-SY-0004 Issue: 1 Date: 14 November 2001
---	---	---	--

annual cycle is of interest, or longer if historical altimeter data can also be brought to bear. The general objective is therefore to measure an average trend

Eqn. 1

$$\begin{aligned} \frac{1}{AT} \int_A dA \int_T dt h(\mathbf{x}, t) &= \frac{1}{A} \int_A dA \frac{(h(\mathbf{x}, t_1 + T) - h(\mathbf{x}, t_1))}{T} \\ &= \frac{1}{T} \left(\frac{1}{A} \int_A dA h(\mathbf{x}, t_1 + T) - \frac{1}{A} \int_A dA h(\mathbf{x}, t_1) \right) \end{aligned}$$

In the second and third forms t_1 is the start of the observation interval. A quantity x averaged in the manner of Eqn. 1 will be denoted by \bar{x} , so that any of the expressions above may be denoted \bar{h} .

The two forms on the right-hand-side (RHS) of Eqn. 9 indicate ways of forming a measurement: by taking the difference of a spatial average, or by taking the spatial average of a difference. As written these are identically equal, but this is no longer the case when observations are only available at particular discrete locations \mathbf{x}_i . In practise, the continuous integrands of Eqn. 1 are approximated by local spatial averages, and there are two distinct possibilities as to how this may be done, namely

Eqn. 2

$$\bar{h} \sim \frac{1}{AT} \int_A dA \sum_i w_i(\mathbf{x}) (h(\mathbf{x}_i, t_1 + T) - h(\mathbf{x}_i, t_1))$$

or

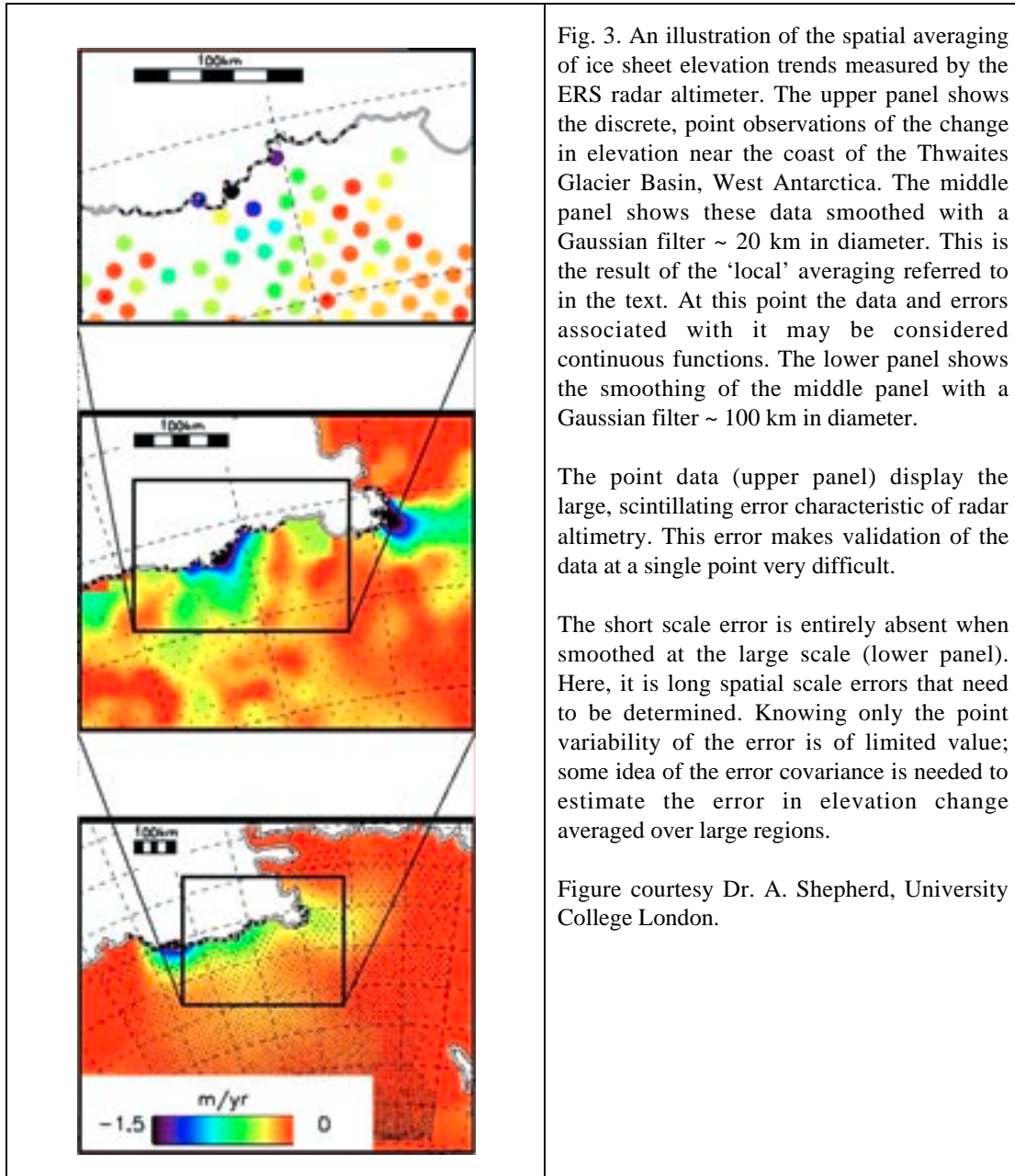
Eqn. 3



$$\bar{h} \sim \frac{1}{T} \left(\frac{1}{A} \int_A dA \sum_i w_i(\mathbf{x}) h(\mathbf{x}_i, t_1 + T) - \frac{1}{A} \int_A dA \sum_j w_j(\mathbf{x}) h(\mathbf{x}_j, t_1) \right)$$

where the w are the quadrature (numerical integration) weights. The procedure implied by Eqn. 2 is illustrated in Fig. 3. It is obvious that there is some theoretical redundancy in these equations, in that the areal average could be formed directly from the point data. This redundancy is retained in part because the formation of local averages is very common in practice, and in part because it will allow us to discuss the error as a continuous function. (It should also be noted that local averaging, or as is shown in Fig. 3 local smoothing, are essentially the same process. The distinction lies only in whether one regards the argument of the weights as a continuous or a discrete variable.)

The distinction between the two possibilities is that in the first case the quadrature errors are cancelled by insisting that the observations lie at the same discrete locations. In the second the estimated trend contains the difference in quadrature errors, but the measurements are not restricted to lie at the same location. In the case of land ice, the

change in thickness is small in comparison with the elevation. Experience shows that the observations need to be at the same locations. (This is achieved in practise using the method of orbit cross-overs described in section 3.4.1). On the other hand, such an approach is not available in the case of sea ice because the location of the sea ice freeboard measurements are not known *a-priori* (they depend on the location of the ice floes), and the second form, Eqn. 3, is used.



		CryoSat Calibration & Validation Concept	Doc: CS-PL-UCL-SY-0004 Issue: 1 Date: 14 November 2001
---	---	---	--

With this proviso, we will largely assume in this document that the sampling density of the land and sea ice will be sufficient enough to suppose that (for a sensible choice of w) the quadrature errors will be negligible, so that we take

$$\text{Eqn. 4} \quad h(\mathbf{x}, t_1 + T) - h(\mathbf{x}, t_1) = \sum_i w_i(\mathbf{x}) (h(\mathbf{x}_i, t_1 + T) - h(\mathbf{x}_i, t_1))$$

and

$$\text{Eqn. 5} \quad h(\mathbf{x}, t) = \sum_i w_i(\mathbf{x}) h(\mathbf{x}_i, t_i)$$

in the cases of land ice and sea ice respectively. This is in part because we expect this to be mostly true, and in part because situations where quadrature errors become large are usually special and difficult to deal with in a general fashion that might be useful in a document such as this. We do highlight practical circumstances where this assumption may be a poor one (see, for example, section 4.6).

In this document we wish to avoid, for simplicity, introducing too great a degree of detail, and regard the expressions above as a shorthand for a range of practical approaches. In practise, the Earth reference figure will be an ellipsoid and one may take \mathbf{x} as shorthand for elliptical latitude and longitude, and integrals over \mathbf{x} as integrals over an area of the ellipse. Similarly, t_1 may be regarded as shorthand for some fixed time within the observations, rather than only the start time. The local averages of Eqn. 2 and Eqn. 3 may also be temporal averages over short intervals of time (such as the orbit repeat period). The temporal differences of Eqn. 2, Eqn. 3 and Eqn. 4 may be replaced by curve fitting a time series, rather than simply differencing the end points. The details vary from practitioner to practitioner, and the detailed approach may be suggested by the data themselves. However, all these approaches are broadly similar. So far as informing the calibration and validation concept is concerned, the averages above will be taken as a proxy and reasonable description of the effect of all these procedures.

2.2 General objective of the calibration and validation

We shall take as the general objective of the calibration and validation the estimation of the second moment of the uncertainty $\bar{\epsilon}_m$ in the trend in spatially averaged land ice mass, or $\bar{\epsilon}_i$ in the spatially averaged trend in sea ice thickness. This requires some understanding of the covariance of the errors of individual measurements and the purpose of this section is to

introduce this concept¹. The total uncertainty in these trends has contributions from the measurement error, and, in addition, uncertain mass and density fluctuations. In this section we simplify the situation by treating the problem as if the measurement errors were the only contribution to the total error. The more general, distinct cases of the land ice and sea ice are described in detail in sections 3 and 4 respectively.

In general, individual measurements will be in error by an amount ϵ , generally also a function of \mathbf{x} and t . The local approximations to the land ice elevation change or sea ice ice thickness will then contain errors that are respectively

$$\text{Eqn. 6} \quad \Delta(\mathbf{x}, t_1, T) = \sum_i w_i(\mathbf{x}) (\epsilon(\mathbf{x}_i, t_1 + T) - \epsilon(\mathbf{x}_i, t_1))$$



and

$$\text{Eqn. 7} \quad \epsilon(\mathbf{x}, t) = \sum_i w_i(\mathbf{x}) \epsilon(\mathbf{x}_i, t)$$

since by assumption the quadrature errors are negligible. To put that another way, we are assuming that the error of significance is that associated with the measurements, rather than that associated with a lack of them. In line with the remarks above, these expressions for the errors Δ or ϵ may be taken as a shorthand for errors that refer, for example, to an average of observations over some short time interval, or to a curve-fitted trend rather than a difference of end points. By way of illustration, the error $\epsilon(\mathbf{x}_i, t_1 + T) - \epsilon(\mathbf{x}_i, t_1)$ is that associated with the data shown in the upper panel of Fig. 3, and the error Δ is that associated with the middle panel of Fig. 3.

While the distinction between the method of measurement of trends in land ice elevation and sea ice thickness is made because of the large quadrature error that would otherwise result in the case of land ice, it has a second important consequence. The error Δ is independent of any error that is a function of \mathbf{x} only, because any measurement error ϵ that is a function of \mathbf{x} only cancels in Eqn. 6. Over land ice ϵ will certainly contain large terms that depend on the elevation and on the penetration of the radar waves into the firn surface, but which nonetheless cancel when the thickness change is measured at a particular location. It is not only the quadrature errors that are cancelled with this approach. On the other hand, the task of validating the remaining error is made considerably more difficult, because it implies making measurements of elevation change *at the same location*. This is not so easy to arrange on an ice sheet.

¹ A good introduction to the statistical methods of this section is Papoulis (1965).

		CryoSat Calibration & Validation Concept	Doc: CS-PL-UCL-SY-0004 Issue: 1 Date: 14 November 2001
---	---	---	--

The second moments of the spatially averaged measurement errors are the quantities

$$\text{Eqn. 8} \quad E\{\bar{\varepsilon}^2\} = \left(\frac{1}{AT}\right)^2 \int_A dA \int_A dA' E\{\Delta(\mathbf{x}, t_1, T)\Delta(\mathbf{x}', t_1, T)\}$$

or



$$\text{Eqn. 9} \quad E\{\bar{\varepsilon}^2\} = \left(\frac{1}{AT}\right)^2 \int_A dA \int_A dA' E\{(\varepsilon(\mathbf{x}, t_1 + T) - \varepsilon(\mathbf{x}, t_1))(\varepsilon(\mathbf{x}', t_1 + T) - \varepsilon(\mathbf{x}', t_1))\}$$

in the cases of land ice and sea ice respectively. Here $E\{\cdot\}$ denotes expectation.

The task of calibration and validation is to estimate by independent measurement the expectations of Eqn. 8 and Eqn. 9. Since these are generally a function of \mathbf{x} , \mathbf{x}' , t_1 and T , with all that this implies for the space-time sampling of experiments, a main purpose of this document is to reduce the complexity of the problem by simplifying the expectation, mainly by appeal to empirical knowledge.

A considerable immediate simplification would be to suppose that Δ and ε may be regarded as spatially or temporally stationary. There is good reason (explained later in the document) to suppose that both Δ and ε have an annual cycle. On the other hand, it seems reasonable to suppose that error in interannual differences may be regarded as stationary, so long as differences are formed between elevations or thicknesses observed at the same time of year. (This of course conforms to common-sense practise when an annual cycle is present in the observations.) We assume that the covariances of Δ and ε will depend on t_1 only in so far as it determines the time of year, and we restrict interest to intervals T that are an integer number of years. In practise, ‘time-of-year’ may refer to a time interval, such as an orbit repeat period, over which data are averaged on the assumption they are representative of the same ‘time’.

On the other hand, we shall assume that the covariances of Δ and ε are generally spatially stationary. This is will be untrue in general, but later in the document we will show (or at least argue) that the uncertainty has distinct spatial scales, and, for the smaller spatial scales, an assumption of spatial stationarity is appropriate. Implicitly, we are appealing to a ‘local’ stationarity. With these assumptions, we write the covariance functions $E\{\Delta(\mathbf{x}, t_1, T)\Delta(\mathbf{x}', t_1, T)\}$ and $E\{\varepsilon(\mathbf{x}, t_1 + T)\varepsilon(\mathbf{x}', t_1)\}$ as $\Gamma_{\Delta\Delta}(\mathbf{x} - \mathbf{x}', T)$ and $C_{\varepsilon\varepsilon}(\mathbf{x} - \mathbf{x}', T)$ respectively. In this case, Eqn. 8 and Eqn. 9 becomes respectively

		CryoSat Calibration & Validation Concept	Doc: CS-PL-UCL-SY-0004 Issue: 1 Date: 14 November 2001
---	---	---	--

$$\text{Eqn. 10} \quad E\{\bar{\varepsilon}^2\} = \left(\frac{1}{T}\right)^2 \int_{\text{Earth}} dA W(\mathbf{s}) \Gamma_{\Delta\Delta}(\mathbf{s}, T)$$

and

$$\text{Eqn. 11} \quad E\{\bar{\varepsilon}^2\} = 2\left(\frac{1}{T}\right)^2 \int_{\text{Earth}} dA W(\mathbf{s}) (C_{\varepsilon\varepsilon}(\mathbf{s}, 0) - C_{\varepsilon\varepsilon}(\mathbf{s}, T))$$

The integral in Eqn. 10 and Eqn. 11 is over the Earth figure but in any practical case the weighting function is zero except in the vicinity the measurements. The weighting function W is described more fully in section 7.1. (In the handling of the covariance function we are ignoring the fact that the Earth figure is curved. The form $C_{\varepsilon\varepsilon}(\mathbf{x} - \mathbf{x}')$, for example, is a statement of spatial stationarity on a plane but not, for example, a sphere. The whole problem can be dealt with on a sphere, but at a cost of considerably more algebra. For the most part the regions that concern us are small enough that, at least for the purpose of estimating errors, a plane approximation will do.)



In a standard statistical treatment, one would further separate in the contribution of the mean and fluctuation about the mean, and reserve in the process the term ‘covariance’ to describe the contribution of the fluctuation. Generally, however, we shall not make the distinction, preferring to appeal to the properties of the covariance function to determine what, in practise, may be regarded as ‘constant’ in any given situation. For example, if over the area A a component y of the uncertainty is perfectly correlated, but slowly varying with time, then for this component Eqn. 11 becomes

$$\text{Eqn. 12} \quad E\{\bar{y}^2\} = 2\left(\frac{1}{T}\right)^2 (C_{yy}(\mathbf{0}, 0) - C_{yy}(\mathbf{0}, T))$$

(see section 7.1). The spatial averaging does not reduce the uncertainty resulting from a slowly varying ‘drift’. Its effect on the trend depends on the degree to which it de-correlates over the measurement interval. Practically, this property distinguishes what experimentalists (if not satellite engineers) mean by the term ‘bias’ in any given situation.

2.3 Definition of ‘Calibration’ and ‘Validation’

In general, it is possible to distinguish two contributions to the uncertainty. The satellite system measures the radar echo scattered from a point on the surface. The echo has several physical qualities, such as the echo power, echo delay-time, and echo phase, and these are the actual measurements made by the satellite system. The point ‘measurement’, in time

		CryoSat Calibration & Validation Concept	Doc: CS-PL-UCL-SY-0004 Issue: 1 Date: 14 November 2001
--	---	---	--

and space, of a thickness is h is obtained by an operation L_r , that we term² ‘retrieval’, on the physical qualities of the echo from that point on the surface. The error ε can then arise in two ways. Firstly, there will be measurement errors in the measured quantities. We term these ‘instrument system’ errors, or ‘system’ errors for short, and denote them ε_s . Secondly, errors will arise in the retrieval because it depends on assumptions concerning the relation of the thickness (or elevation) to the echo, and these, in general, will oversimplify the actual situation. These errors we term ‘retrieval’ errors and denote ε_r . The total uncertainty is, at least for a small system error,

$$\text{Eqn. 13} \quad \varepsilon = \varepsilon_r + L_r \cdot \varepsilon_s$$



Where the meaning is clear, we simply write the second term ε_s .

There is a close connection between these errors and the staging of the CryoSat data processing. The sequence of measured echoes along the satellite orbit, together with their ancillary measurements, are termed ‘level 1b’ data, and the processor that converts the satellite telemetry to the echo sequence is termed the ‘level 1b’ processor. The sequence of thicknesses (or elevations) along the satellite orbit, together with their ancillary data, are termed the ‘level 2’ data, and the processor that converts the level 1b data to the level 2 data is termed the ‘level 2’ processor. Thus in a generic fashion ε_s may also be termed the ‘level 1b’ error, and ε_r the ‘level 2’ error.

The terminology comes from the generic classification of satellite data and the equivalence is not exact because the retrieval operator L_r may well depend on data, such as a mean sea level for example, that is technically level 3 or 4. There is scope for confusion in the terms. However, this is inevitable given the various engineering and scientific practices involved in a satellite mission. What is important to recognise practically is that the retrieval operator L_r is defined by the algorithms in the level 2 processor, and thus the design of the level 2 processing algorithms and the understanding of the retrieval error ε_r gained by validation experiments are closely linked.

We shall use the term ‘calibration’ to describe the estimation of system errors, and the term ‘validation’ to describe the estimation of retrieval errors. In general, the system error arises from imperfect engineering, the retrieval error from an imperfect description of the scattering from the surface. On the assumption that second order errors (*i.e.* products of retrieval and system errors) are negligible, these two errors are uncorrelated. Thus Eqn. 10 and Eqn. 11 become respectively

² This operation is termed the ‘retracking’ by altimeter specialists for historical reasons.

		CryoSat Calibration & Validation Concept	Doc: CS-PL-UCL-SY-0004 Issue: 1 Date: 14 November 2001
---	---	---	--

$$\text{Eqn. 14} \quad E\{\bar{\varepsilon}^2\} = \left(\frac{1}{T}\right)^2 \int_{\text{Earth}} dA W(\mathbf{s})(\Gamma_{rr}(\mathbf{s}, T) + \Gamma_{ss}(\mathbf{s}, T))$$

and

$$\text{Eqn. 15} \quad E\{\bar{\varepsilon}^2\} = 2\left(\frac{1}{T}\right)^2 \int_{\text{Earth}} dA W(\mathbf{s})(C_{rr}(\mathbf{s}, 0) - C_{rr}(\mathbf{s}, T) + C_{ss}(\mathbf{s}, 0) - C_{ss}(\mathbf{s}, T))$$

where Γ_{rr} and C_{rr} , and Γ_{ss} and C_{ss} , are the respectively the covariances of the retrieval and system contributions to the total error variance.

2.4 General character of the calibration and validation

The preceding discussion is of a rather general nature. Nonetheless, a number of important features of the calibration and validation problem have already emerged and it is worthwhile here to emphasise these before, in the following chapters, looking at the land- and sea-ice problems in detail.

The first feature is that, because an objective of the mission is to measure a trend, validation experiments will need to be repeated. This is almost a statement of the obvious but nonetheless is worth further discussion. Firstly, for a short mission of, for example, 3 years duration, it will scarcely be possible to gain sufficient samples to estimate the temporal covariance function. Indeed, given that the errors are seasonally variable, only three temporal measurements are possible. However, the difference in the character of the land- and sea-ice covariance functions places a different emphasis on the nature of the repetition.

In the case of sea ice, one or two estimates will have to be enough (on the basis of some argument and with the risk of offending statisticians) to make an estimate of $C_{\varepsilon\varepsilon}(\mathbf{s}, 0)$. (When resources are limited, it may be better to concentrate on ‘determining’ $C_{\varepsilon\varepsilon}(\mathbf{s}, 0)$ for different times of year.) If an estimate of $C_{\varepsilon\varepsilon}(\mathbf{s}, 0)$ is available, the worst case value of $C_{\varepsilon\varepsilon}(\mathbf{s}, 0) - C_{\varepsilon\varepsilon}(\mathbf{s}, T)$ is $C_{\varepsilon\varepsilon}(\mathbf{s}, 0)$, which occurs when the error de-correlates completely in the interval T . Thus, for sea-ice, the estimate of uncertainty becomes

$$\text{Eqn. 16} \quad E\{\bar{\varepsilon}^2\} = 2\left(\frac{1}{T}\right)^2 \int_{\text{Earth}} dA W(\mathbf{s})(C_{rr}(\mathbf{s}, 0) + C_{ss}(\mathbf{s}, 0))$$

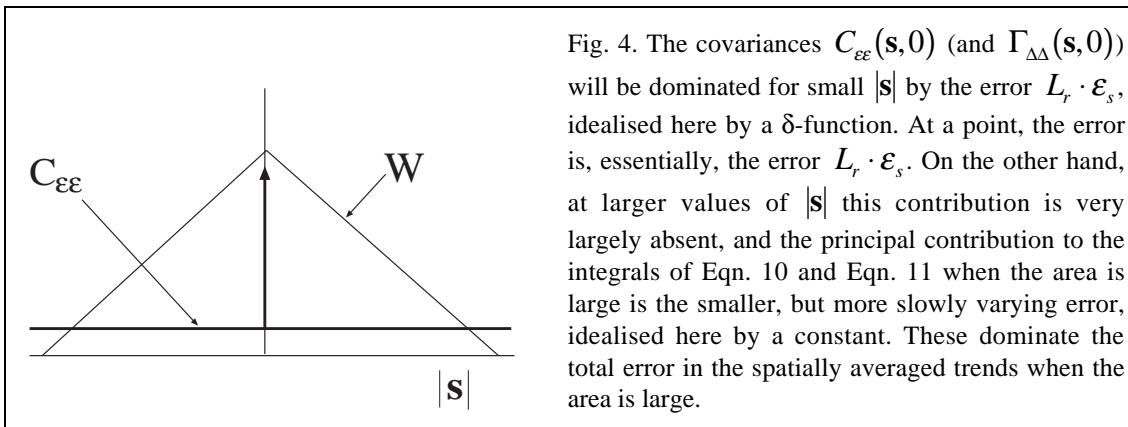
On the other hand, no such luxury is possible in the case of the land ice. A single temporal measurement of ε will contain the large, absolute component of the error and will be, from the point of view of validating the trend measurement, practically useless. Repeated measurements are essential to estimating the land ice uncertainties. In the case of land ice, however, a good deal of experience exists as to the source of the errors. Here, the emphasis





is on experiments that provide a better understanding of them so that, possibly, they may be modelled.

The second feature is that, because an objective of the mission is to measure a spatial average, it is the spatial *covariance*, and not simply the variance of the error that needs to be estimated. While it *may* be possible in the case of sea ice to estimate $C_{\epsilon\epsilon}(\mathbf{s},0)$ from a single temporal sample, this is still a function of space, and estimating it requires many measurements. The covariance function has a structure that may be hidden in a point spatial measurement. In consequence, a point measurement may offer little information as to the error in the spatial average. This will be emphasised in later sections, but it is sufficiently important that it is worth illustrating here (Fig. 4).

In practical terms, the source of most of the short scale error idealised in Fig. 4 is the speckle on the radar echoes. Independent measurements that are dominated by radar speckle are of limited use unless there are sufficient number to average out the speckle fluctuations. This makes the land ice problem particularly challenging in practice, because it is the correlation function of the temporal difference in elevation *at the same locations* that is required. It is not sufficient to make measurements in the same region at different times; they must be at numerous, *identical* locations at different times.





Finally, two points emerge with respect to the activities of calibration and validation. Firstly, the assumption that the system and retrieval errors are independent implies that calibration experiments can be performed separately, in time and space, from validation experiments. This implies, for example, that it is not necessary to travel to the Antarctic to calibrate the instrument system. On the other hand, the effect of the errors on the measurement will depend on the situation and the way individual errors are combined. If the calibration is performed independently (as is the planned case with CryoSat) there is still the task of estimating their effect on the measurement. In the language of Eqn. 13, if ϵ_s

		CryoSat Calibration & Validation Concept	Doc: CS-PL-UCL-SY-0004 Issue: 1 Date: 14 November 2001
--	---	---	--

has been determined through calibration, one still needs to estimate the error $L_r \cdot \epsilon_s$ in the data.

Secondly, it is a fact that, of all the errors, the system error ϵ_s is the most accurately calculable in advance. This occurs because the instrument system is *designed* to meet performance requirements that are specified in terms of the magnitude of the system error ϵ_s . It follows that, if resources are limited, it is sensible to place an emphasis on the validation, which addresses greater uncertainty. This is not to say that in-orbit calibration experiments are unnecessary: the unexpected does occur with payload or instrument hardware following the launch. However, it is the reason that in this document, a greater emphasis is placed on the validation of the products than the calibration of the instrument system.

		CryoSat Calibration & Validation Concept	Doc: CS-PL-UCL-SY-0004 Issue: 1 Date: 14 November 2001
--	---	---	--

3 Validation of Land Ice Uncertainty

3.1 Objective and general character of land ice validation. *The mass imbalance and its relation to the change in elevation. Contributions of measurement errors, snowfall fluctuations and surface temperature fluctuations. Empirical evidence for the general form of the error covariance.* **3.2 The mass fluctuation covariance.** *Deterministic and statistical characterisation. The fluctuation variance. Present knowledge of the covariance and need for further investigation. Possible importance of historical glaciological data. Potential importance of new accumulation radar systems. Fluctuations in regions of ablation* **3.3 The density fluctuation.** *The effect of surface fluctuations on the density and elevation. Relative importance in dry and wet accumulation regions. Potential importance of ‘coffee can’ measurements.* **3.4 The retrieval error.** *Separation of retrieval and system errors.* **3.4.1 The measurement technique and the origin of measurement error.** *Source of retrieval errors. Timing errors. Ionospheric and tropospheric errors.* **3.4.2 Character of retrieval errors.** *Use of crossovers. Pulse-limited echoes from ice sheets. Effects arising from changes in near surface firn. Geographical extent of retrieval errors in Antarctica and Greenland. Empirical correction of retrieval errors. Need for independent measurements. Smallness of ionospheric and tropospheric errors.* **3.4.3 Validation of retrieval errors.** *Importance of airborne laser altimetry. Conceptual validation of retrieval error in areas of accumulation and importance of careful experiment design. Contribution of ICESAT measurements. Absolute validation of interferometer elevation.* **3.5 Inter-satellite bias.** *Cross calibration with ENVISAT mission.* **3.6 Timing and location of land ice validation experiments.** *Dependence or otherwise on contemporary satellite measurements. Regions of special importance. Benefit of simultaneous experiments. Practical usefulness of Greenland as a focus for campaigns.*

3.1 Objective and general character of land ice validation.

In this section the error in spatial averages of the land ice mass trend and its validation are described. In contrast to section 2, which considered only the contribution of the measurement error, this section introduces two other uncertainties that effect the determination of the trend: snowfall fluctuations and density variations. The approach is to describe first the relationship between the measured quantity, the trend in ice sheet thickness, and the desired quantity, the longer-term trend in mass imbalance. This then leads in this subsection to a more complete description of the error covariance than given in section 2 that includes the contributions of snowfall and density fluctuations. In the

following sub-sections, each of the contributions and their validation is described in more detail.

The mass imbalance of large ice sheets is the difference between two processes: the arrival (or departure) of mass at a rate \dot{m} at the surface of the ice arising from atmospheric mass transports, and the loss of mass at a rate \dot{M}_l arising from the flow of ice (or basal melting). At a point, the state of mass imbalance is often written by glaciologists and ice sheet modellers in terms of the rate of change of thickness \dot{h} of ice

$$\text{Eqn. 17} \quad \dot{h}(\mathbf{x}, t) = \dot{m}(\mathbf{x}, t) - \dot{M}_l(\mathbf{x}, t)$$

In Eqn. 17, \dot{m} and \dot{M}_l have the dimensions of velocity and the actual mass transports per unit area of bed are obtained from them by multiplying by the density of ice.

The essential idea of using altimetry to determine ice sheet mass imbalance is to overcome the difficulty (see *e.g.* Jacobs 1992) of measuring the two mass transports on the right hand side of Eqn. 17 by measuring the left hand side directly. In fact, Eqn. 17 holds only for areas of bare ice or for variations long enough that the fluctuations in the near surface density of firn can be ignored (van der Veen 1993, Wingham 2000). For the short-term observations provided to date by satellites, however, these fluctuations cannot be ignored. In general, including them in a description of the thickness rate is a complex matter. However, in dry firn at least, a good deal of the actual variation in thickness is captured by replacing Eqn. 17 with

$$\text{Eqn. 18} \quad \dot{h}(\mathbf{x}, t) = \dot{m}_0(\mathbf{x}) - \dot{M}_l(\mathbf{x}) + \frac{\rho_{ice}}{\rho_{snow}} \dot{m}_s(\mathbf{x}, t) + \int_0^{\infty} d\tau k(\tau, \mathbf{x}) T_s(t - \tau, \mathbf{x})$$

In Eqn. 18, the surface accumulation \dot{m} , surface density and surface temperature T_0 have been split into longer-term trends \dot{m}_o , ρ_{snow} and T_o and short-term fluctuations of which the mass and temperature $\dot{m}_o(t)$ and $T_s(t)$ are important. The kernel $k(t)$ describes the effect of the history of surface temperature on the elevation change and is described further below. ‘Long-term’ here means greater than 30 years, and while the long-term trends are generally functions of t this fact is immaterial for the short measurement time intervals provided to date by satellites. Except in the unusual circumstances of glacier surges \dot{M}_l has no short-term variation and is treated in the same way. For longer measurement intervals the ‘amplification’ in the elevation change of the short term mass fluctuations by the factor ρ_{ice} / ρ_{snow} overestimates the fluctuation, and an integral formulation similar to that connected with the surface temperature must be used in that case. More detailed justifications of Eqn. 18 and limitations connected with it may be found in Arthern & Wingham (1998) and Wingham (2000).

The great majority of the Antarctic ice sheet is a region of surface mass accumulation. At lower altitudes in central and southern Greenland, however, are regions of net surface ablation. In regions of ablation, at least for those times of year where winter snowfall has disappeared Eqn. 18 must be replaced with

$$\text{Eqn. 19} \quad \dot{h}(\mathbf{x}, t) = \dot{m}_0(\mathbf{x}) - \dot{M}_l(\mathbf{x}) + \dot{m}_s(\mathbf{x}, t)$$

(\dot{m} and \dot{M}_l are *both* negative in regions of ablation). The situation is considerably simpler, because there are no variations arising from the differences in the densities of firn and ice.

We shall use Eqn. 18 and Eqn. 19 as a description of the ice sheet elevation change observed by altimeters. Because the more important questions concerning the ice sheets are concerned with the long-term trends in mass imbalance, uncertainties in the mass fluctuations and effects of densification (discussed further below) introduce uncertainty into the measurement of the longer term imbalance $\dot{m}_0 - \dot{M}_l$. These are in addition to the error $\dot{\epsilon}(\mathbf{x}, t)$ in the measurement of \dot{h} itself. In general, the total imbalance uncertainty is

$$\begin{aligned} \text{Eqn. 20} \quad \dot{\epsilon}_m(\mathbf{x}, t) &= \dot{h}(\mathbf{x}, t) + \dot{\epsilon}(\mathbf{x}, t) - \dot{m}_0(\mathbf{x}) - \dot{M}_l(\mathbf{x}) \\ &= \frac{\rho_{ice}}{\rho_{snow}} \dot{m}_s(\mathbf{x}, t) + \int_0^{\infty} d\tau k(\tau, \mathbf{x}) T_s(t - \tau, \mathbf{x}) + \dot{\epsilon}(\mathbf{x}, t) \end{aligned}$$

in regions of accumulation. It may be noted that the CryoSat measurement requirements were defined by requiring the measurement error $\dot{\epsilon}(\mathbf{x}, t)$ to contribute no more than 10% of the total mass imbalance uncertainty.

Eqn. 20 assumes that the bed of the ice sheet is fixed with respect to the ellipsoidal reference frame of the altimeter measurements. This is not generally true, as the ‘solid’ Earth is itself moving with respect to the ellipsoidal reference frame, due to post-glacial rebound, tectonics and other causes. In general, however, these motions are small in comparison with other terms in (see, for example, Bentley & Wahr 1998). They are ignored here. That is not to say that they may not be important in some localities. It simply means that we consider beyond the remit of the validation of the CryoSat mission.

Eqn. 20 is the uncertainty in the longer-term elevation trend. It may be argued that is overly pessimistic, in that the purpose of the altimeter is to measure the mass imbalance contemporary with the measurements, that is, the quantity $\dot{m}_0 + \dot{m}_s - \dot{M}_l$. This would be the case if the interest were, for example, to examine the annual cycle of accumulation. However, to the extent that the surface mass fluctuation is unknown, which is the normal case over the great majority of the ice sheets, there is not much difference in the errors in



practise. The expression for the error in the contemporary mass imbalance in regions of accumulation is different from that in Eqn. 20 only in that the term $(\rho_{ice} / \rho_{snow}) \dot{m}_s$ is replaced with the term $((\rho_{ice} / \rho_{snow}) - 1) \dot{m}_s$. Since $\rho_{ice} / \rho_{snow} \sim 3$, the contribution of the surface mass fluctuation to the error in the contemporary imbalance remains approximately two thirds of its contribution to the longer-term error.

In keeping with the general objective of the calibration and validation described in section 2.2, we take as the purpose of the land ice calibration and validation activity the estimation of the second moment of the uncertainty in mass imbalance. This is for regions of accumulation

Eqn. 21

$$E\{\bar{\epsilon}_m^2\} = \left(\frac{1}{AT}\right)^2 \int_A dA \int_T dt \int_A dA' \int_T dt' E\{\dot{\epsilon}_m(\mathbf{x}, t) \dot{\epsilon}_m(\mathbf{x}', t')\}$$

$$= \left(\frac{1}{T}\right)^2 \int_{Earth} dA W(\mathbf{s}) Cov \left[\frac{\rho_{ice}}{\rho_{snow}} \int_{t_1}^{t_1+T} dt \dot{m}_s(\mathbf{x}, t) + \int_{t_1}^{t_1+T} dt \int_0^\infty d\tau k(\tau, \mathbf{x}) T_s(t - \tau, \mathbf{x}) + \Delta(\mathbf{x}, t_1, t_1 + T) \right]$$

following the general method of section 2.2, and using the function Δ introduced there. It is probably reasonable to assume that the three uncertainties may be regarded as independent. In this case,

$$Eqn. 22 \quad E\{\bar{\epsilon}_m^2\} = \left(\frac{1}{T}\right)^2 \int_{Earth} dA W(\mathbf{s}) (\Gamma_{mm}(\mathbf{x}, T) + \Gamma_{\rho\rho}(\mathbf{x}, T) + \Gamma_{\Delta\Delta}(\mathbf{x}, T))$$

where Γ_{mm} , $\Gamma_{\rho\rho}$ and $\Gamma_{\Delta\Delta}$ are respectively the covariances of the trends in the mass and density fluctuations and the measurement error. The assumption of statistical independence is quite an important assumption in practise. It means that their experimental investigation need not be simultaneous.

In the following sections the magnitude of the individual terms in the covariance function of Eqn. 21, their scales of variation, and approaches to their experimental estimation are discussed. Before doing so, however, it is useful here to discuss in broad terms the experience gained from previous altimeter missions in the practical behaviour of the covariance functions.

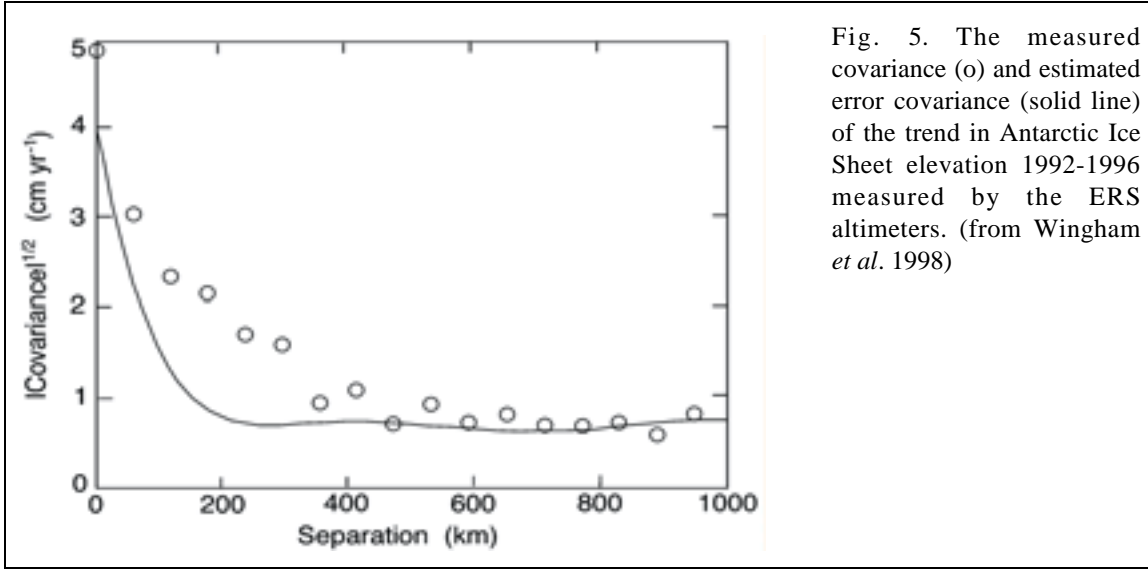


Fig. 5. The measured covariance (o) and estimated error covariance (solid line) of the trend in Antarctic Ice Sheet elevation 1992-1996 measured by the ERS altimeters. (from Wingham *et al.* 1998)



Fig. 5 shows the covariance of the 5-year elevation rate (1992 to 1996 inclusive) measured by the ERS altimeter averaged over 63% of the interior of the Antarctic ice sheet. The term ‘covariance’ applied to these observed data means the function

$$\Gamma(r) = \frac{1}{2\pi T^2} \int_{\text{Measurement Area}} dA \int_0^{2\pi} d\phi \{h_m(\mathbf{s}, t_1 + T) - h_m(\mathbf{s}, t_1)\} \{h_m(\mathbf{s} + \mathbf{r}, t_1 + T) - h_m(\mathbf{s} + \mathbf{r}, t_1)\}$$

Here $\mathbf{r} = \mathbf{i}r \cos \phi + \mathbf{j}r \sin \phi$ in a Cartesian system, and h_m are the measured elevations, *i.e.* the measurements including the errors. The ‘separation’ in the figure means the value of r .

Apart from a notable regional exception (described later), the observed trends were very small (see Wingham *et al.* 1998), and for this reason, the covariance of Fig. 5 may be regarded as a proxy for the uncertainty covariance of Eqn. 21. The measured covariance has three components. One is the large, short length scale component that is significant only at small spatial scales. The second, smaller in magnitude but substantial, extends largely over length scales of some 300 km but has a significant element at larger scales. The third, smaller in magnitude, is practically constant up to length scales of 1000 km: essentially it is a bias.

The solid line in Fig. 5 is a calculation of the contribution to the uncertainty of the system error, that is, of the function Γ_{ss} of Eqn. 14. It has, essentially, two components: the small spatial scale signal arising from radar speckle error, and a smaller, essentially constant component arising from an estimate of instrument system drift and orbit-related errors (the slight ripple arose from the estimate of orbit error covariance). The figure shows that, at the

		CryoSat Calibration & Validation Concept	Doc: CS-PL-UCL-SY-0004 Issue: 1 Date: 14 November 2001
---	---	---	--

smallest and largest spatial scales, the instrument system error dominates the uncertainty. It also shows that at intermediate scales the dominant uncertainty arises from the other terms of Eqn. 21. Wingham *et al.* (1988) used Fig. 5 to show that, at drainage basin scales and larger, it was this intermediate-scale error that dominated the total mass-imbalance error. This has important implications for the validation of CryoSat data. The covariance function has significant energy at spatial scales up to 500 km. This immediately gives some idea of the distances over which the covariance function needs sampling. This figure also illustrates the general remarks of section 2.4 concerning the need to consider spatial scales larger than those at which the speckle error is the dominant term.



3.2 The mass fluctuation.

Ice sheets contain in a solid form the history of their precipitation over many thousands of years. This means that it is possible in principle to determine in any region the behaviour of the mass fluctuation \dot{m}_s in relation to the longer-term mean \dot{m}_0 , and, again in principle, to remove its contribution to the imbalance error. But the practical difficulties in achieving this are substantial and underlie the justification, mentioned in the previous section, for using altimetry to measure the mass imbalance. A simpler approach is to at least determine the fluctuations statistically. It is then at least possible, in any given situation, to determine if the thickness trend may be reasonably explained by mass fluctuations. Both approaches are considered here.

The variance of the mass fluctuation \dot{m}_s is well known. It has been established from numerous ice accumulation records assembled over the last 50 years from ice cores from Antarctica and Greenland. A representative sample of the cores from Antarctica can be found in the reference lists in Jacobs (1992) or Wingham *et al.* (1998), or from Greenland in that of van der Veen (1993). From these records, it is well established that in the interior of the ice sheets at least, the mass fluctuations appear to be a white process. The interannual variability (*i.e.* the square root of the variance) is, in Antarctica, approximately 25% of the mean accumulation rate. In Greenland, the proportion is slightly larger. These data are equivalent (see section 7.2) to the statement that

$$\text{Eqn. 23} \quad E \left\{ \left[\frac{\rho_{ice}}{\rho_{snow}} \int_{t_1}^{t_1+T} dt \dot{m}_s(\mathbf{x}, t) \right]^2 \right\} = \Gamma_{mm}(\mathbf{0}, T) \sim 0.25^2 \dot{m}_0^2 \left(\frac{\rho_{ice}}{\rho_{snow}} \right)^2 \left(\frac{T_0}{T} \right)$$

where the numerical value of T_0 is equal to 1 year in the units of the measurement interval T . This expression shows that the contribution of the mass fluctuation to the mass imbalance uncertainty reduces as T , as first observed by van der Veen (1993).

		CryoSat Calibration & Validation Concept	Doc: CS-PL-UCL-SY-0004 Issue: 1 Date: 14 November 2001
--	---	---	--

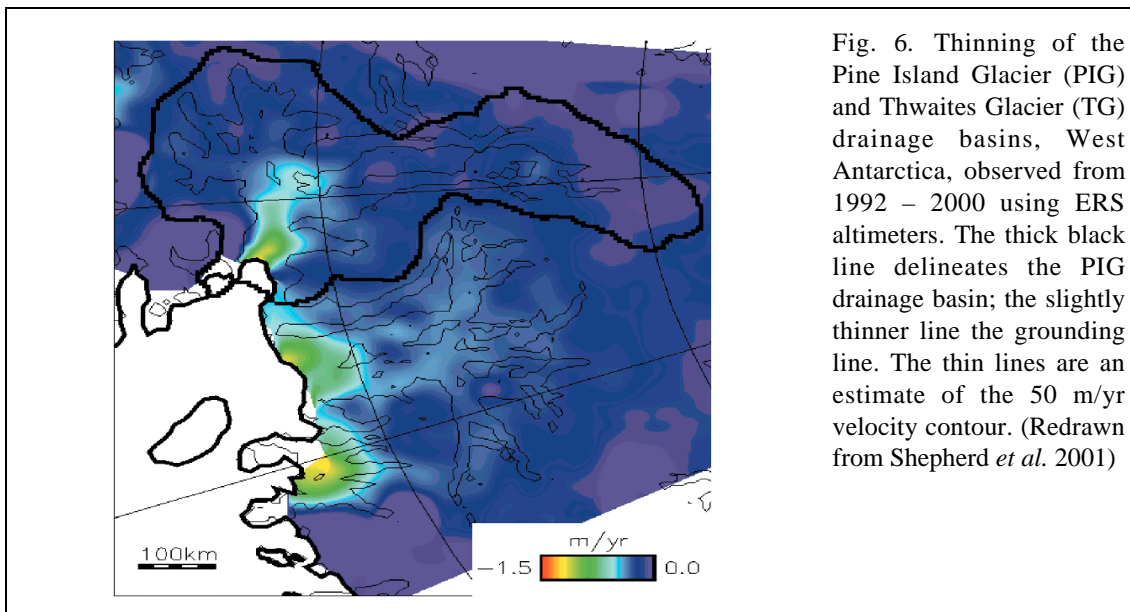
Because at least statistically the mass fluctuation may be related to the mean accumulation, the contribution to the imbalance error at any given point may be estimated using maps of accumulation (*e.g.* Vaughan *et al.* 1999, Ohmura & Reeh 1991), estimated from numerous individual core measurements. The difficulty is, however, that while the temporal covariance of the fluctuation is well-established, little is known for sure concerning the spatial covariability of the *fluctuation* of accumulation. It is worth emphasising that what is important from the point of view of validating altimeter estimates of mass trends is the spatial scale of the fluctuation in the accumulation and *not* that of the mean accumulation. (That is, in our notation, the spatial scale of \dot{m}_s and *not* \dot{m}_0). The need to know the spatial behaviour of the fluctuations is also present in estimating the contribution of Antarctic mass accumulation fluctuations to those of global sea level, as observed originally by Oerlemans (1981).

This is worth emphasising because generally published accounts of accumulation rate measurements present the data in a highly compressed form, and often the short-term fluctuation has been smoothed prior to the presentation of the data. (A good example of such a presentation is that of Petit *et al.* (1982) at Dome C, Antarctica.) This is the case because accumulation rate studies have been typically concerned with determining the long-term mean of the accumulation rate \dot{m}_0 . In that case the fluctuations of interest here are simply a ‘noise’. Usually, to the extent they are considered, they are characterised by their average variability over the time-interval used to smooth the core or stake record.

Because there are a higher density of measurements, the situation is better in Greenland than in Antarctica. McConnell *et al.* (2000) compared a number of core records in southern Greenland to establish that the source of altimeter-measured thickness fluctuations from 1978-88 were the result of fluctuations in snowfall. An example of what may be achieved statistically is that of van der Veen & Blozan (1999), who examined 9 cores in the vicinity of the GRIP ice core site in Greenland to determine the common fluctuations over a large area. There are also a limited number of accurately surveyed traverses in Greenland whose longer-term (40 year) thickness trend may be supposed independent of short-term mass fluctuations and provide a useful comparison with shorter-term measurements (see *e.g.* Paterson & Reeh 2001).

The little information concerning Antarctica that has appeared in the literature (compare, for example, Enomoto (1991) and Morgan *et al.* (1991)) is too sparse to reach any general conclusion. In Antarctica, the best source of information concerning the spatial covariability is the trend observed by previous altimeters. This is discussed further in 3.4.2. The importance of better understanding the spatial scale of accumulation fluctuations in

Antarctica is illustrated by example in Fig. 6, which shows the thinning in the Pine Island Glacier (PIG) and Thwaites Glacier (TG) drainage basins in West Antarctica, observed using ERS altimetry from 1992-2000. The large thinning associated with the lower reaches of the glaciers is clearly the result of ice dynamics (Shepherd *et al.* 2000, Shepherd *et al.* 2001). However, the more widespread thinning in the interior of the TG basin is possibly correlated with the flow, and, if dynamic in origin, is of long-term importance for the future of the drainage basin. On the other hand, the apparent coincidence of the thinning in the deeper interior with the surface velocity may not be conclusive, because surface winds that affect the mass fluctuation may be correlated with topography. At present, the likely magnitude of the fluctuation when averaged on 100 km scales (the averaging scale used in Fig. 6) is not known well enough to settle the matter entirely.



There are two approaches to improving knowledge of the mass fluctuation. One of these is to use glaciological methods: repeated stake measurements and shallow ice cores. There are on-going systematic traverses of the Antarctic ice sheet aimed at (among other things) improving knowledge of accumulation rates (see *e.g.* Mayewski & Goodwin 1996, Oerter *et al.* 1999). In addition, many original observations are archived at polar institutes. A revisiting of original records of repeated traverses with a view to investigating the spatial variability of the accumulation rate *fluctuation* may be of considerable value. This is particularly true if the pattern of stakes and/or cores is such that the very short (metre) scale fluctuations can be distinguished from longer scale fluctuations. (We have already mentioned the example of van der Veen & Blozan (1999).)

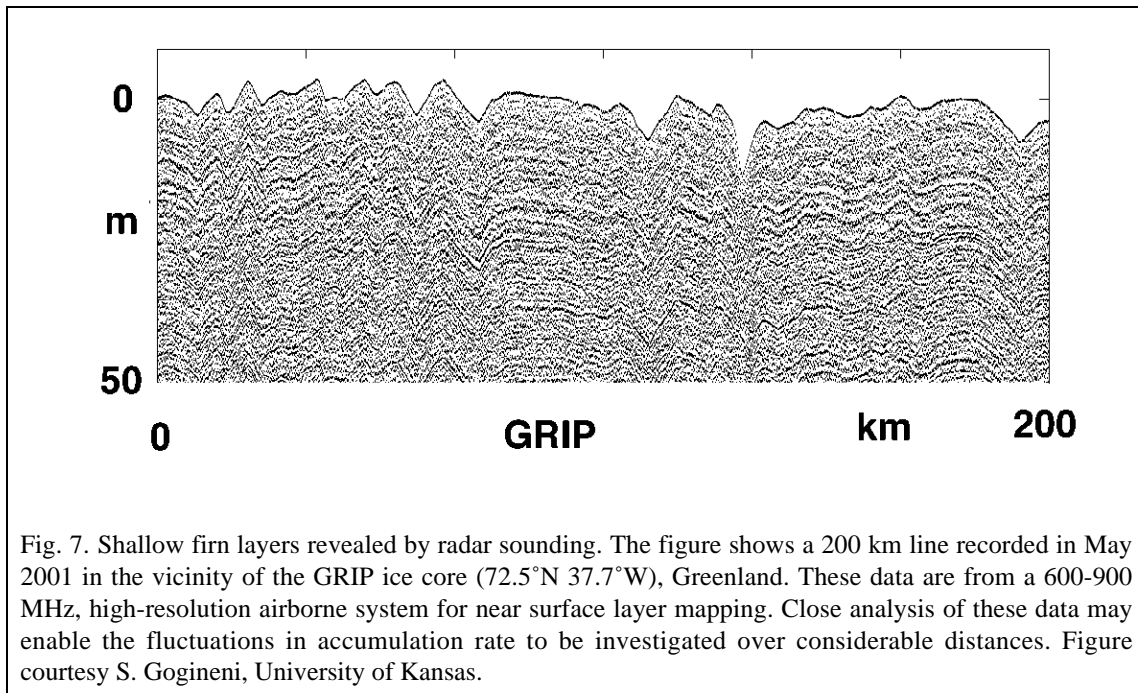




Fig. 7. Shallow firn layers revealed by radar sounding. The figure shows a 200 km line recorded in May 2001 in the vicinity of the GRIP ice core (72.5°N 37.7°W), Greenland. These data are from a 600-900 MHz, high-resolution airborne system for near surface layer mapping. Close analysis of these data may enable the fluctuations in accumulation rate to be investigated over considerable distances. Figure courtesy S. Gogineni, University of Kansas.

A second method of considerable promise is to employ a high-frequency, accumulation-rate radar (Fig. 7). While the need for traverse expeditions remains, the use of a remote measurement technique greatly reduces the difficulty of the measurement itself. It also provides a spatially continuous record, overcoming the difficulty of spatial aliasing that inevitably attends point measurements at stakes or cores. The technique is new and its ability to determine accumulation rate fluctuations over intervals as small as 5 years is presently unproven. In principle, the total accumulation between two layers identified in the radar echoes is determined by dating the layers, and converting the interval between them to mass using some assumed velocity of 'light' and density.

This method has been demonstrated for accumulation intervals spanning decades and centuries (Kanagaratnam *et al.* 2001). Whether the method can be reliably extended to shorter intervals of accumulation and the extent to which the method will require 'calibrating' along the traverse with shallow cores is presently unclear. Present systems (Fig. 7) are presently approaching the bandwidth required to resolve the short-term fluctuations, and it is possible that wider bandwidth (greater than 1 GHz) will be required in due course. Nonetheless, such systems potentially offer a considerable increase in our understanding of the mass fluctuations.

		CryoSat Calibration & Validation Concept	Doc: CS-PL-UCL-SY-0004 Issue: 1 Date: 14 November 2001
--	---	---	--

In regions of ablation, it seems reasonable to assume that the interannual fluctuations are described by a ‘random-walk’ process so that the effect on the fluctuations on the variance of the trend will vary as T^{-1} in the manner of Eqn. 23. It is also probable that the variance can be simply related to the mean ablation rate, although this is not well established. In absolute terms, the fluctuations may be substantial. The area of the regions of ablation is considerably smaller than that of accumulation. Since the ice sheets are approximately in balance, the mass loss per unit area in ablation regions can be as large: 8 m yr^{-1} in some regions of Greenland. In consequence, the fluctuations can also be substantial. Braithwaite (1994) discusses some data from southern Greenland for which the standard deviation of the ablation is 0.5 m yr^{-1} .

The experimental determination of the covariance of ablation fluctuations can in principle be achieved using ‘traditional’ stake measurements, but it is a considerable undertaking to obtain such measurements over substantial areas. As with the accumulation fluctuation, it is possible that a careful examination of historical data could provide useful information. However, unlike accumulation regions, the history of the process is not contained in the ice. What may be a more effective approach to determining this contribution to the trend, in regions of ablation, is to examine the covariance between the observed elevation fluctuations and modelled atmospheric surface temperature. Forecast models show good skill in reproducing observed temperature over the Greenland ice sheet (*e.g.* Hanna & Valdes 2001). A comparison between the interannual variation of elevation observed by the satellite at the end of the summer, and, for example, the degree-days above freezing in the preceding summer, may be very revealing of ablation fluctuations.

3.3 The density fluctuation

Fluctuations in the density of the firn will result in fluctuations in the elevation (Braithwaite 1994, Arthern & Wingham 1998, Wingham 2000). These fluctuations will result from fluctuations in the surface mass accumulation, which affects the densifying pressure experienced by the firn at depth; fluctuations in the density with which the firn is deposited; and fluctuations in the temperature of the firn, which affects the rate at which the firn densifies. For short time periods of less than 10 years, the additional effect on the elevation trend of the mass fluctuation’s *contribution to density fluctuations* is small compared with its direct effect described in the last section. For our purposes, it is the effect of temperature that potentially introduces the greatest uncertainty into the observed trends.

Generally, the elevation fluctuation at any given time depends on the history of the surface fluctuations. Once a density (or thermal) anomaly is created in the firn, its expression in the

elevation continues as the anomaly is carried downwards, until, through densification, the anomaly is reduced to zero as the density approaches that of ice. For this reason, even the simplest linearised description of the process requires an integral formulation such as the one of Eqn. 18. In this description, the kernel $k(\mathbf{x}, t)$ depends on the location through the mean conditions experienced there, and in particular the mean accumulation rate $\dot{m}_0(\mathbf{x})$ and the mean temperature T_0 .

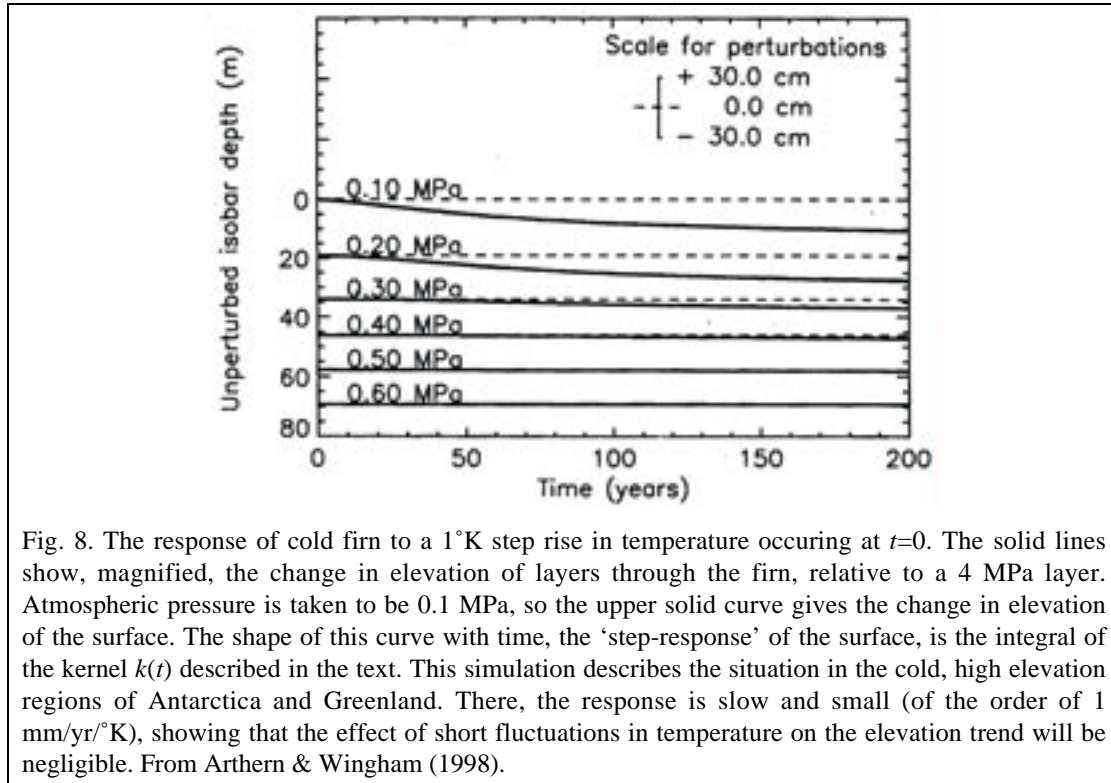


Fig. 8. The response of cold firn to a 1°K step rise in temperature occurring at $t=0$. The solid lines show, magnified, the change in elevation of layers through the firn, relative to a 4 MPa layer. Atmospheric pressure is taken to be 0.1 MPa, so the upper solid curve gives the change in elevation of the surface. The shape of this curve with time, the ‘step-response’ of the surface, is the integral of the kernel $k(t)$ described in the text. This simulation describes the situation in the cold, high elevation regions of Antarctica and Greenland. There, the response is slow and small (of the order of $1 \text{ mm/yr}/^\circ\text{K}$), showing that the effect of short fluctuations in temperature on the elevation trend will be negligible. From Arthern & Wingham (1998).

Arthern & Wingham (1998) investigated theoretically the behaviour of the kernel $k(t)$ in cold, dry firn conditions such as occur in E. Antarctica (Fig. 8). They concluded that throughout much of East Antarctica, and the higher elevations of West Antarctica, the temperature was too cold for temperature fluctuations to much effect the elevation trends. In these cold regions, only temperature trends extending over many decades are long enough for sufficient heat to be conducted or advected into the firn to affect the densification rate. Such slow processes have a negligible effect on the elevation trend in comparison with, for example, the mass fluctuations described in the last section.

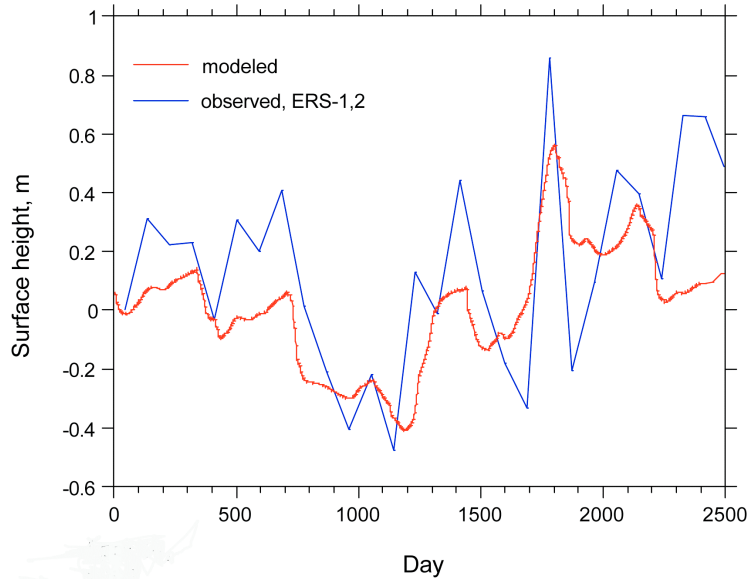


Fig. 9. The calculated elevation change (red) at Greenland summit as a function of time due to the combined effect of observed mass accumulation and modelled density fluctuations driven by the observed temperature variations. The annual signal is predominantly due to the annual cycle of densification. The longer, interannual fluctuation is due to the mass fluctuation. Also shown (blue) is the elevation change observed by ERS-1 altimetry in the vicinity of the locations. There is a measure of agreement between the two, but there is also a clear difference between the two. This may be the result of error in the density modelling or, equally, the retrieval error and/or instrument system errors in the altimetry. Further experiments of the kind illustrated here would be valuable; combining these with the kind of experiments discussed in the next section to investigate the electromagnetic scattering associated with the retrieval error even more so. Figure courtesy H. Zwally, NASA Goddard Space Flight Centre.

This conclusion will not extend to the higher temperature, higher accumulation regions of the Antarctic Peninsula and central and southern Greenland. Densification is thermally activated, at a rate governed by an Arrhenius equation. Various studies have indicated that the activation energy is similar to that for the better studies processes of grain growth and viscous creep. Zwally and Li (2001) have observed grain growth rates show a significant increase in activation energy with temperature (see *e.g.* Jacka & Li 1994) and argued that the activation energy used by Arthern & Wingham underestimates the densification rate at higher temperatures. On this basis, they modelled a 20 cm annual cycle in elevation at Summit, central Greenland (72° 34' N 38° 27' W).



Nonetheless, in regions of dry firn, the effect of density fluctuations on the elevation trend is likely to remain small in comparison with those of mass fluctuations. Interannual fluctuations in temperature are an order of magnitude less than the range of the annual

cycle (a few degrees as opposed to, for example, 30 degrees). To the extent that a linear description holds, interannual differences in elevation arising from temperature-driven densification will also be small in comparison with the annual effects. In a trend measurement over several years, it is likely that the density contribution will be small in comparison with that of the mass fluctuations described in the last section. Fig. 9 shows an example of the total contribution of the two signals in a region of dry firn in central Greenland.

On the other hand, in regions of wet snow or percolation, where the temperature approaches and reaches the melting point, the situation may be different. Here a linear treatment is inappropriate. The average density of annual layers is most probably governed by the number of days the firn temperature reaches the melting point, which varies considerably. Braithwaite (1994) reports on sequences of annual layers, deposited between 1978 and 1985 at the margin of the south west Greenland ice sheet, that have a significantly lower density ($\sim 600 \text{ kg m}^{-3}$) than those deposited in later years ($\sim 800 \text{ kg m}^{-3}$). This fluctuation that would contribute $\sim 20 \text{ cm yr}^{-1}$ to the trend for the period of the measurement. A contribution to the trend of this magnitude, if characteristic of a large area, would be significant. Between the ‘end-cases’ of cold, dry firn and the wet snow zone lie a range of situations in non-linear behaviour - in particular, the increase in densification-rate as the temperature approaches or reaches the melting point - may result in significant interannual variability into the elevation trend.

In general, better knowledge is needed of how the surface conditions affect the elevation through the contribution of densification. Because temperature is reasonably modelled in Greenland in forecast models, and because it has large-scale variation, one may at least hope that the contribution of densification to the spatially-averaged trends may be reasonably estimated by modelling. Further experiments of the kind illustrated in Fig. 9, and those that might directly observe how the surface conditions drive the densification at depth would be particularly useful. The most promising technique to achieve this is an adaption of the ‘coffee-can’ method of measuring mass imbalance (Hamilton & Whillans 2000).

In this method, a ‘coffee-can’ is frozen into the ice at some depth, and the motion of a wire connected to it is observed at the surface, whose inertial velocity is known through a GPS measurement. The original purpose of these measurements was to measure the velocity \dot{M}_l associated with the ice flux divergence. This, combined with the mean accumulation \dot{m}_0 determined from the core removed in burying the can, gives an accurate method of determining, at a point, the long-term mass imbalance of Eqn. 17. However, by adding a

		CryoSat Calibration & Validation Concept	Doc: CS-PL-UCL-SY-0004 Issue: 1 Date: 14 November 2001
--	---	---	--

number of cans at different depths (particularly shallow ones) and by observing the velocities of the cans continuously, the annual and interannual variations in densification may be observed directly. (The first trial of such a continuous measurement will be made in W. Antarctica in 2001/2 (Hamilton, personal communication)). Such measurements, supported by meteorological measurements at the same location, would be of great help in understanding better the contribution of densification to the observed altimeter elevation trend.

3.4 The retrieval error.

The general discussion of section 2.3 separated the measurement error into two components. A retrieval error arises because the reduction of the echo to an elevation depends on simplified assumptions concerning the relation of the echo to the surface. An instrument system error arises because the measurements of echo power, phase angle, *etc.* are in error. By assumption (section 2.3), these errors are independent, and the measurement error covariance function of may be separated into two terms:

$$\text{Eqn. 24} \quad \Gamma_{\Delta\Delta}(\mathbf{x}, T) = \Gamma_{rr}(\mathbf{x}, T) + \Gamma_{ss}(\mathbf{x}, T)$$

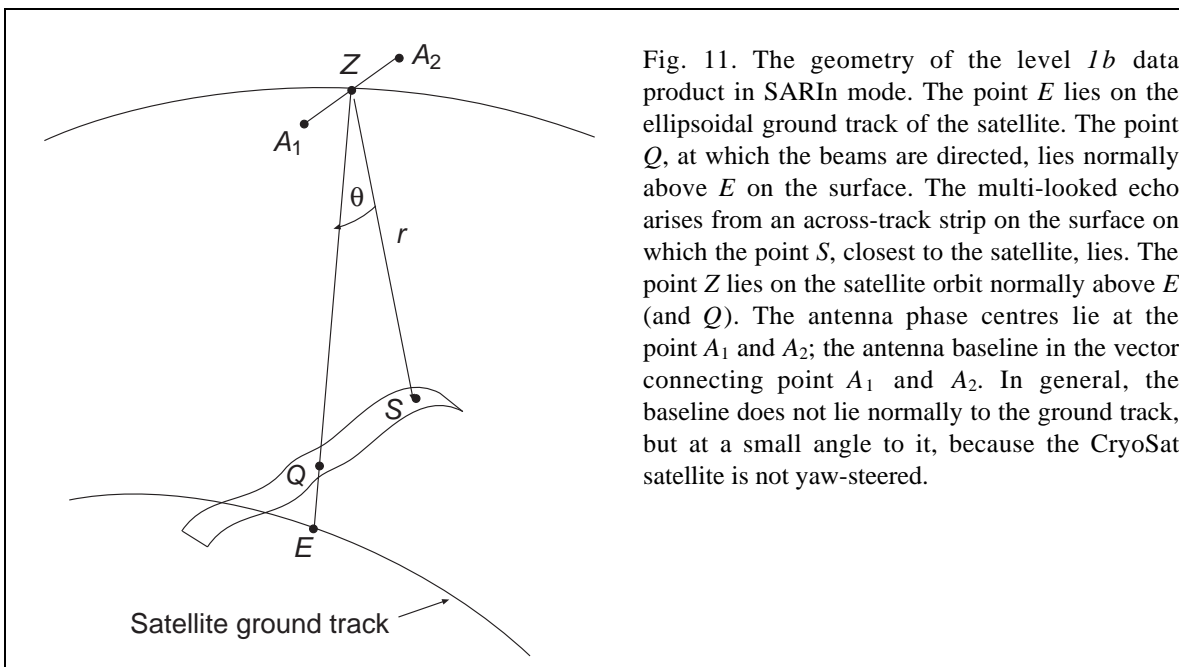
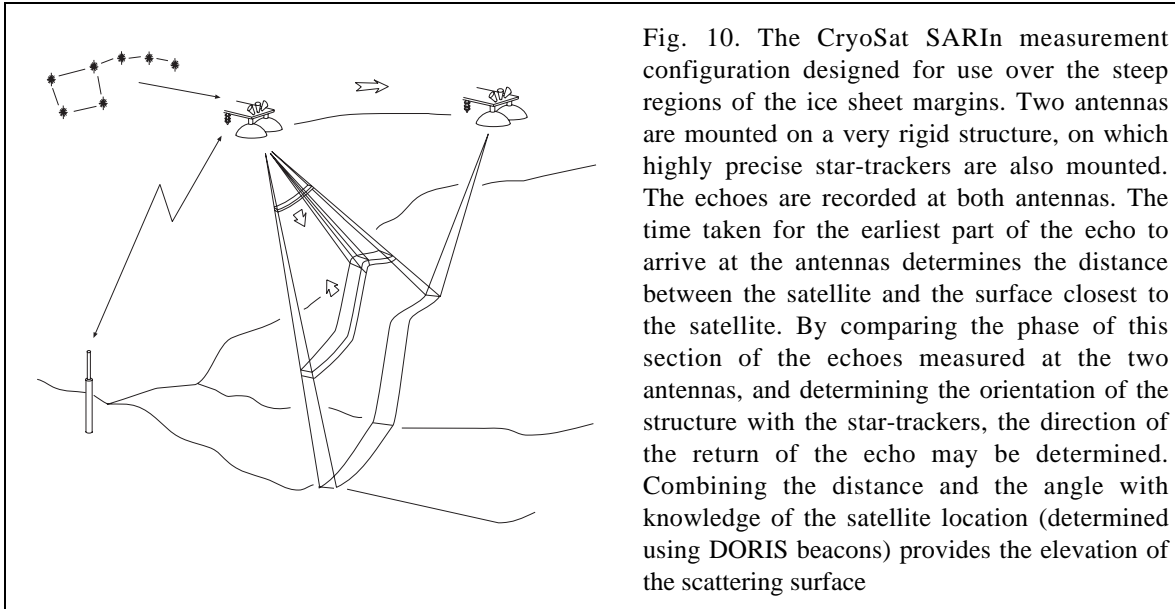
in which Γ_{rr} is the retrieval error covariance and Γ_{ss} is the system error covariance.

Both these errors both emerge at the same stage of the retrieval: the conversion of the radar echo to a distance from the satellite. They are nonetheless distinct. The source of the retrieval error lies in the passage of the radar wave through the polar atmosphere and its interaction with the ice surface, and its validation requires *in-situ* investigations. The source of the system error lies with the imperfections of the instrument, which can be determined separately. The separation of the retrieval and system errors is discussed in the following subsection, and the *in-situ* investigation of the retrieval error is the subject of the remainder this section. The system error is dealt with in section 5.

3.4.1 The measurement technique and the origin of measurement error.

The concept of the measurement of ice sheet elevation over the ice sheet margins is illustrated in Fig. 10. Over the margins of the ice sheets, CryoSat will use an interferometric mode of operation. (The technical operation of this mode is described in more detail in the MDD.) A narrow across-track strip of the surface is illuminated by the radar in this mode. A thin pulse-shell is transmitted by the radar and the amplitude and phase of the echo scattered back to the radar from the strip is recorded at the two antennas as a function of the echo delay time. The same strip on the surface is illuminated many

times by the radar as the satellite flies overhead, and an averaged ('multi-looked') echo is determined.



The level *1b* data contains, essentially, the multi-looked echoes, together with the geometrical information concerning the satellite location and orientation. It amounts to the following parameters

$$\phi_{1b}(\mathbf{x}, t, \tau) \equiv \begin{cases} \psi^{(1)}(\mathbf{x}, t, \tau) \\ \psi^{(2)}(\mathbf{x}, t, \tau) \\ z(\mathbf{x}, t) \\ \mathbf{b}(\mathbf{x}, t) \end{cases}$$

(More details as to the actual contents of the level *1b* data may be found in the MDD). Here, \mathbf{x} is the location of a point *E* in Fig. 11 that lies on the satellite ellipsoidal ground track. z is the normal altitude of the satellite at the point *Z* normally above *E*. t is the time at which the satellite is located at the point *Z*. $\psi^{(1)}$ and $\psi^{(2)}$ are the complex echoes measured at the two antennas located at the points A_1 and A_2 ; these echoes are functions of the echo delay time τ from the instant of transmission. \mathbf{b} is the baseline vector that separates the points A_1 and A_2 . (As Fig. 10 implies, in dealing with lower than level *1b* data products, the point *E*, the satellite nadir point, and the point *Q*, at which the beams are directed, must be distinguished. These geometrical effects are corrected for in the level *1b* products).

The elevation is determined from these data by determining the value of echo delay time, τ_r , from the shape of the average echo $\psi(\tau)$ received at the point *Z* from the surface at the point *S*. This echo delay is used to determine the range r in Fig. 11 using the velocity of light c according to

Eqn. 25 $r = c\tau_r / 2$

The second step is to determine the angle θ in using the phase difference ϕ between the two echoes at the delay time τ_r using the interferometer equation:

Eqn. 26 $\theta = \arcsin\left(\frac{\lambda\phi}{2\pi|\mathbf{b}|}\right)$

Because the elevation of the point *S* is defined in an elliptical co-ordinate system its expression in terms of r and θ is somewhat complicated. To highest order, however, the expression for the error in the elevation in terms of the measured parameters c , τ_r , θ , z and $\mathbf{x}(t)$ and their errors ϵ_τ , ϵ_c , ϵ_θ , ϵ_z and ϵ_x is simple. It is:

Eqn. 27 $\epsilon_e(\mathbf{x}, t) = c\epsilon_\tau(\mathbf{x}, t)/2 + \tau_r\epsilon_c(\mathbf{x}, t)/2 + c\tau_r\epsilon_\theta^2(\mathbf{x}, t)/4 + \epsilon_z(\mathbf{x}, t) + \gamma\epsilon_x$

In the expression above for the level *1b* data \mathbf{x} and t appear as independent parameters. Errors in \mathbf{x} that arise from the orbit computation are expected to be small and are ignored.

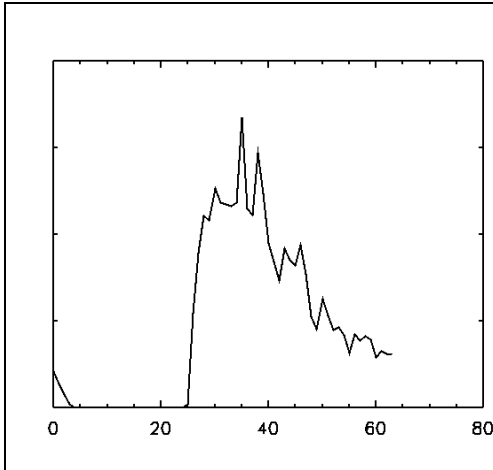




Fig. 12. Average of 50 ERS-2 altimeter ‘ice-mode’ echoes from 77° S, 100° W, West Antarctica, recorded on 4 March 1997. The echo is resolved into 63 samples of 12.5 ns duration, equivalent to 1.86 m of range. The initial part of the rising edge (samples 25 and 26) arises from the surface. The later part (samples 27 onwards) contain energy scattered from the surface and the snow volume. The obvious jitter on the echo is speckle noise. The precursor in samples 0 to 4 is an instrument artifact.

However, because the satellite travels along the orbit \mathbf{x} is a function of t , errors in \mathbf{x} may arise from errors in t , the so-called ‘datation’ error. This is the error accounted for by ϵ_x . The coefficient γ is the derivative of the elevation at the point S in the along-track direction; with this definition ϵ_x is a scalar. Note that the error is second-order in ϵ_θ because the tangent of the surface at the point of closest approach S is normal to the line ZS .

Of these terms, it is the errors ϵ_τ and ϵ_c which give rise to the retrieval error. The ‘first-arrival time’ τ_r is determined by examining in detail the shape of the echo. An example of a pulse-limited echo from the Antarctic ice sheet is shown in Fig. 12. In this case, τ_r lies around sample 26. To determine it exactly requires some assumptions concerning the geometry of the surface and the nature of the scattering. Historically, the retrieval has assumed the surface to be locally plane. This assumption was first used by Martin *et al.* (1983) in their retrieval, and although a number of detailed changes have been made over the years by a number of practitioners (see *e.g.* Femenias *et al.* 1993, Bamber 1994, Davis 1995, Davis 1997) this essential assumption has not been altered. (For a detailed discussion of this assumption see Wingham 1995). As this assumption will generally not describe in detail the actual situation, a retrieval error ϵ_r will result in τ_r . There is, in addition, an instrument contribution to the travel time error in τ_r and generally

$$\text{Eqn. 28} \quad \epsilon_\tau(\mathbf{x}, t) = \epsilon_r(\mathbf{x}, t) + \epsilon_i(\mathbf{x}, t)$$

The velocity of light c is affected by the degree to which the ionosphere is ionised, by the density of dry air and by the humidity, and variations in c due to these causes is accounted for. The total electron content of the ionosphere will be provided by the DORIS receiver network, while the tropospheric contributions will be provided by the ECMWF forecast model. Nonetheless, a residual error ϵ_c will remain.

		CryoSat Calibration & Validation Concept	Doc: CS-PL-UCL-SY-0004 Issue: 1 Date: 14 November 2001
--	---	---	--

In the remainder of this section, the character and validation of the retrieval errors ϵ_r and ϵ_c is described. The contribution of ϵ_i in Eqn. 28 and the remaining terms in Eqn. 27 are the subject of section 5.

3.4.2 The character of the retrieval error.

There are two sources of the retrieval error ϵ_r . The first arises because the topography of ice sheets is not, in fact, planar, and the shape of the echo will depart from its assumed shape. To first order this error depends only on the time-invariant topography of an ice sheet. The second error arises because at 13.8 GHz, altimeter echoes from ice sheets result from scattering from the air-snow interface, and from scattering within the snow volume below the interface to a depth of several metres (Ridley & Partington 1988). This may be corrected for to some extent (although not entirely – see Arthern & Wingham 2001) but in any case to the extent that the scattering as a function of depth into the firn is time-invariant, the retrieval error from either source is time-invariant.

Such time-invariant errors will cancel in the formation of the local trend, as described in section 2.2, provided a method is used that ensures the measurements are made at the same locations. In principal, the elevation change may be determined from repeated satellite tracks. However, in the past and generally speaking, the orbits do not strictly repeat themselves. In consequence, such ‘repeat track’ differences are largely dominated by differences in the topography of the ice sheet between the two tracks (*i.e.*, in the language of section 2, retain large quadrature errors). This difficulty is overcome using the method of cross-overs (Fig. 13). The technique was introduced over ice sheets by Zwally *et al.* (1989) and has been used, essentially unchanged, since that date.

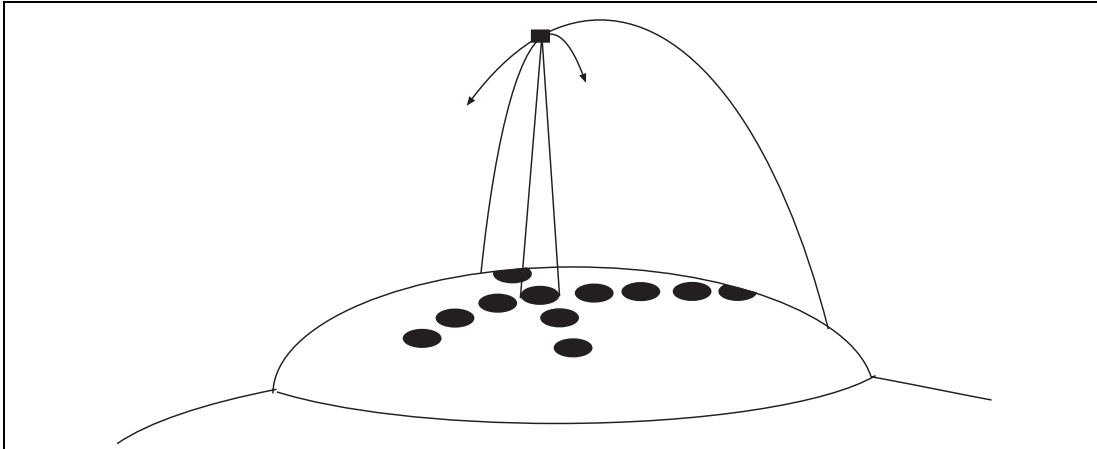


Fig. 13. The elevation of the surface at the location of individual echoes (black circles, above) may contain a large, spatially invariant term associated with ice sheet elevation. For this reason, measurements of elevation change are made at a crossing point of the ascending and descending satellite orbits. At this point, the elevation of the ice sheet is the same. The elevation of the ice sheet is cancelled when the elevation change is measured by differencing the two elevations observed at the crossing point at two different times.

However, time variant retrieval errors will occur if changes in the relative power scattered from the surface and volume causes a time-variant redistribution of the energy in the echo. Processes that can cause such a redistribution include changes in the cm-scale roughness of the surface, and changes in the near surface layering and density, any or all of which may arise from variations in snowfall, surface wind and surface temperature. Because these processes alter the absolute power of the echo, as well as its shape, these retrieval errors are marked by observed elevation changes being correlated with changes in the echo power (Legresy & Remy 1998, Wingham *et al.* 1998). Calculations show that the sensitivity of the retrieved elevation to changes in scattered power at or near (within 1 m) of the surface is of the order of 0.4 m/dB, depending on the total power scattered from the volume.

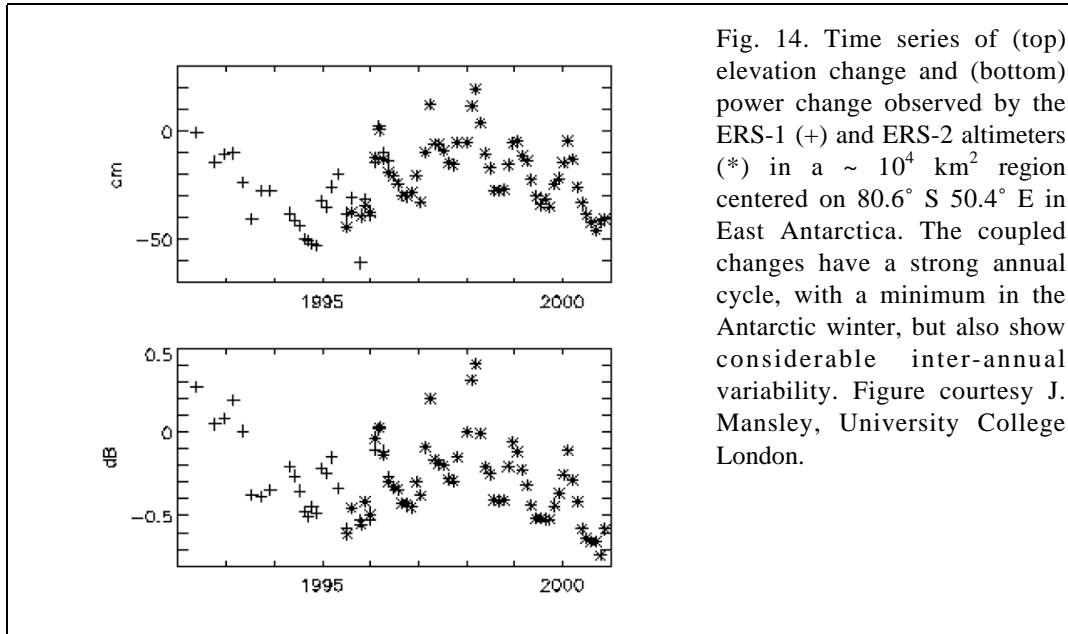


Fig. 14. Time series of (top) elevation change and (bottom) power change observed by the ERS-1 (+) and ERS-2 altimeters (*) in a $\sim 10^4$ km² region centered on 80.6° S 50.4° E in East Antarctica. The coupled changes have a strong annual cycle, with a minimum in the Antarctic winter, but also show considerable inter-annual variability. Figure courtesy J. Mansley, University College London.

Fig. 14 shows 5-year time series of elevation change and power change in a region of $\sim 10^4$ km² centered at 80.6° S 50.4° W in East Antarctica. Both time series show a marked annual cycle with an amplitude of ~ 20 cm, and an interannual fluctuation of a similar magnitude. A straight-line regression of the elevation change with the power change has a gradient of 0.5 m/dB and a correlation coefficient of 0.96. The value of the gradient strongly suggests these fluctuations are an artefact of scattering changes at or near the surface. Arthern *et al.* (2001) have confirmed this directly by using deconvolution techniques to examine changes in the distribution of echo power.

This behaviour is widespread in the high, cold, low accumulation regions of Antarctica and Greenland. Fig. 15 shows the correlation coefficient between elevation change and power change observed over 5 years in the ERS-2 altimeter data.

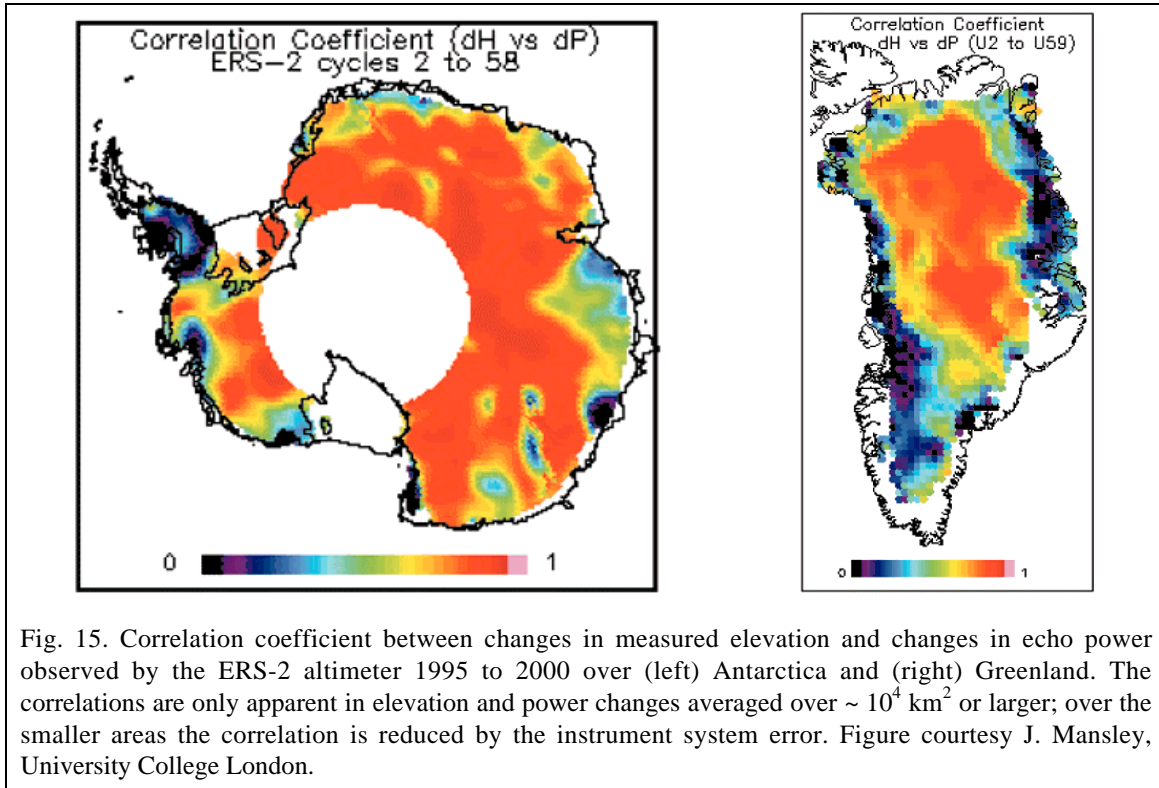


Fig. 15. Correlation coefficient between changes in measured elevation and changes in echo power observed by the ERS-2 altimeter 1995 to 2000 over (left) Antarctica and (right) Greenland. The correlations are only apparent in elevation and power changes averaged over $\sim 10^4$ km² or larger; over the smaller areas the correlation is reduced by the instrument system error. Figure courtesy J. Mansley, University College London.

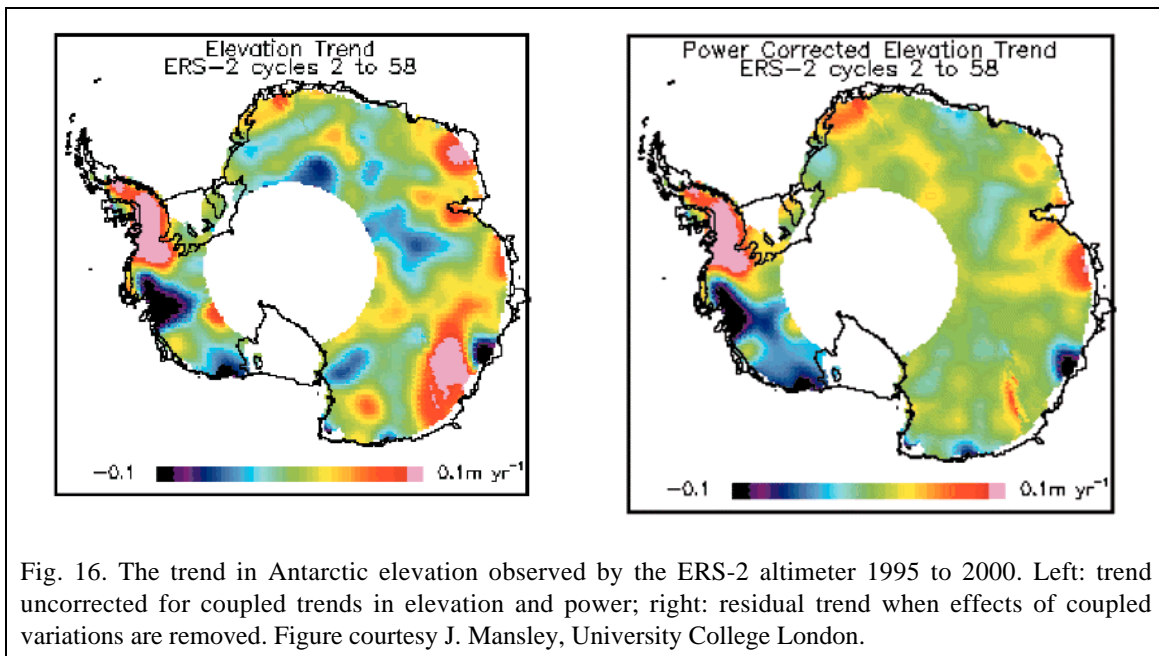


Fig. 16. The trend in Antarctic elevation observed by the ERS-2 altimeter 1995 to 2000. Left: trend uncorrected for coupled trends in elevation and power; right: residual trend when effects of coupled variations are removed. Figure courtesy J. Mansley, University College London.

From the point of view of the trend error, it is the interannual variability that is of greatest importance. Wingham *et al.* (1998) modelled empirically the retrieval error as

$$\text{Eqn. 29} \quad \varepsilon_r(\mathbf{x}, t_1 + T) - \varepsilon_r(\mathbf{x}, t_1) = \left\langle \frac{\Delta h}{\Delta \sigma}(\mathbf{x}) \right\rangle (\sigma(\mathbf{x}, t_1 + T) - \sigma(\mathbf{x}, t_1))$$

where σ is the echo power, and the expression $\langle \cdot \rangle$ is the gradient of the regression of elevation changes and power changes over the interval T . They used this expression to correct the trends for the variations in power. Fig. 16 shows the difference made by the correction to the 5-year trends in Antarctic elevation. This figure shows that the apparent elevation changes in East Antarctic in the uncorrected trends are largely the result of interannual changes in scattered power at or near the surface of the firn.

The residual trends shown on the right-hand side of Fig. 16 have been interpreted glaciologically using arguments supported by ancillary measurements. Wingham *et al.* (1998) examined the observed covariance $\Gamma(r)$ shown in Fig. 5. They showed that the observed value of $\Gamma(0)$ was closely equal to $\Gamma_{mm}(\mathbf{0}) + \Gamma_{ss}(\mathbf{0})$ when Eqn. 23 was used to calculate $\Gamma_{mm}(|0|)$. On this basis they argued that the intermediate scale fluctuation in Fig. 5 was the contribution $\Gamma_{mm}(|s|)$ of the mass fluctuation, and that its spatial scale was of the order of 200 km. They assigned most of the fluctuation seen on the right-hand side of Fig. 16 to fluctuations in snowfall. Shepherd *et al.* (2000, 2001) showed that the Pine Island and Thwaites glaciers basins were the exception. The correlation of the pattern of thinning near the coast with ice velocity shown in Fig. 6 showed this thinning to be ice dynamic in origin.

The correlation of the pattern of thinning with ice velocity makes the interpretation of dynamic thinning fairly secure. This is not the case with residual trends whose origin is supposed to be fluctuations in snowfall. The correction (Eqn. 29) assumes that the source of the fluctuations in echo power is at or close to the surface. In East Antarctica, where conditions are very cold, temporal fluctuations in the firn are limited to 25 cm or so (Alley, personal communication) this assumption is reasonable. It is much more questionable in warmer areas with higher accumulation rates. Over a period of some years, it is conceivable that in regions with an annual accumulation of, for example, 2 metres of snow, fluctuations in volume scattering may extent several metres into the firn. To some degree, the behaviour of the volume scattering may be investigated independently of the surface scattering (Legresy & Remy 1999, Arthern *et al.* 2001). To this extent, examining the satellite measurements themselves may check the assumption. Nonetheless, independent measurements that will provide a detailed understanding of fluctuations in the vertical distribution of scattering are of particular importance.

Because of its importance to the study of sea level, the propagation error ε_c has been extensively studied over the oceans, and a considerable literature exists (see, for example,

2nd Special issue on TOPEX/Poseidon, Journal of Geophysical Research, 100, C12, 1995; Fu & Cazenave 2001). For ocean altimetry, which aims to determine changes of a few millimetres, the error in these corrections is important, and their validation forms an important part of the validation activities. For the ice sheets however, the situation is somewhat different. This is in part because the changes of interest are an order of magnitude larger than those of the ocean, and in part because in polar regions the atmosphere is dry (Fig. 17) and the total ionospheric content is low. The contribution of these errors to the total error in the trend is expected to be small, and a specific validation activity seems unnecessary.

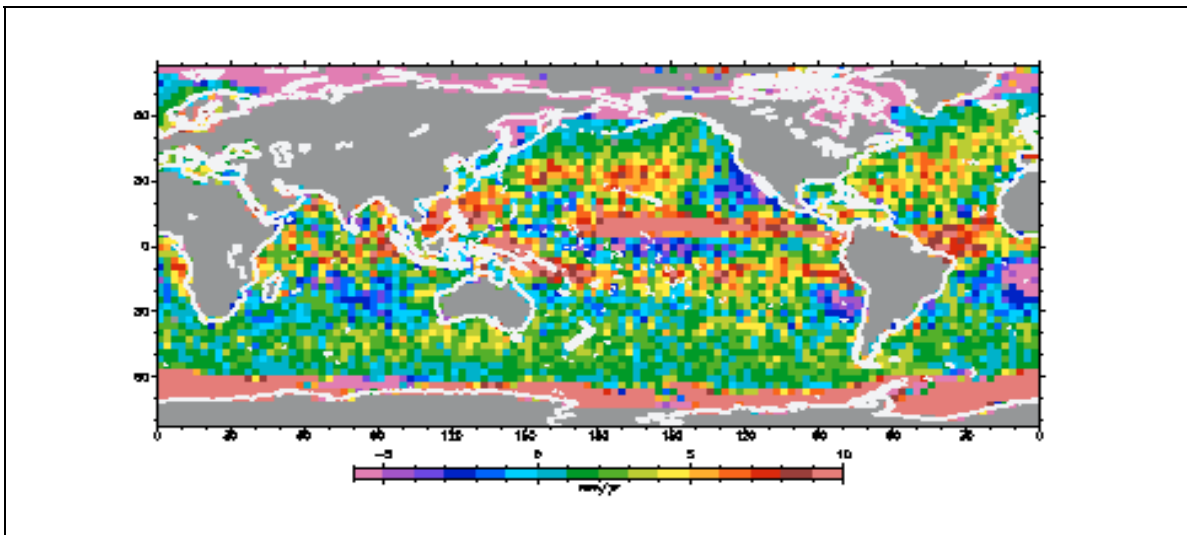
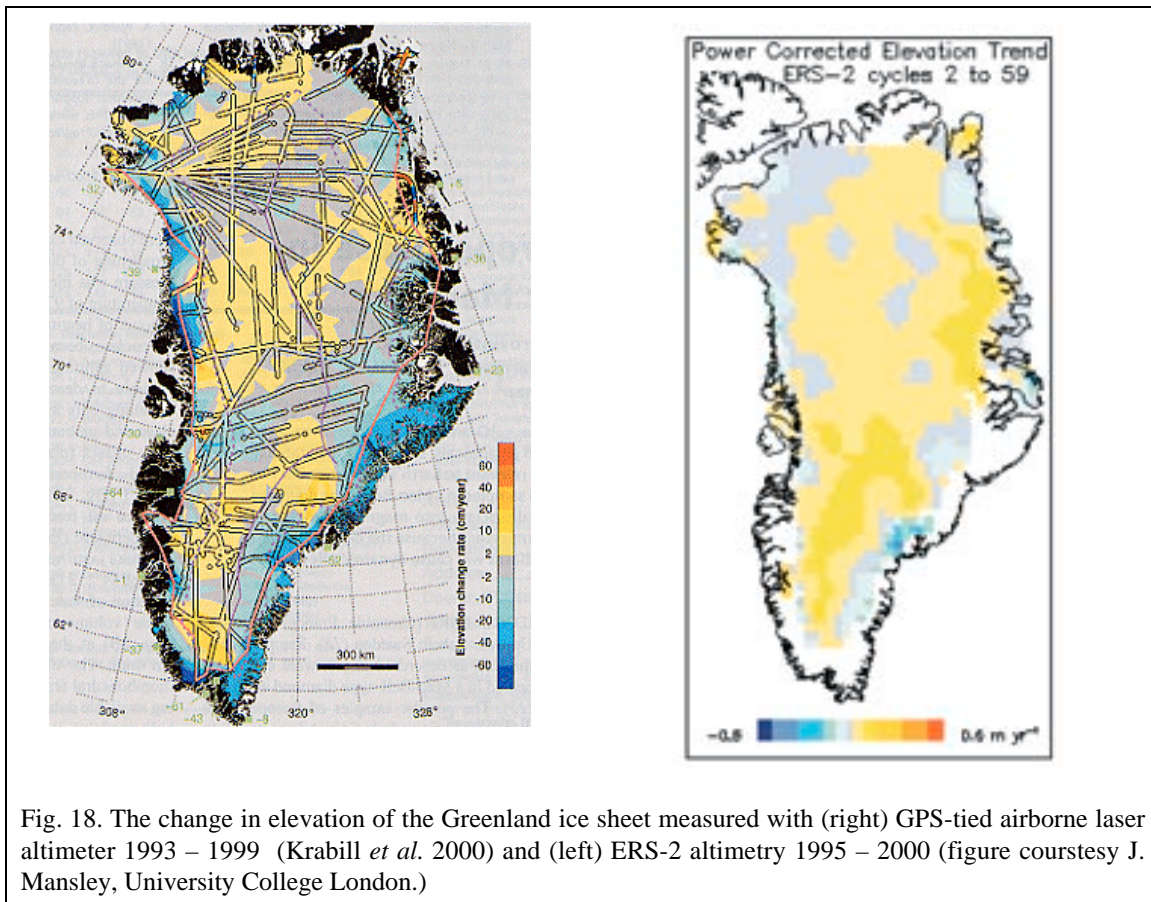


Fig. 17. A comparison of modelled (ECMWF) and measured (MWR) wet tropospheric path delays for 3 years of ERS-2 data (1995-1998). Differences between modelled and measured values were computed and averaged in 35-day batches over 3×3 degree cells ($\sim 10^5 \text{ km}^2$). Trends were passed through the averages. These trends are largely due to the modelled field errors. The extremes of the colour bar are -0.5 and 1.0 cm yr^{-1} . At high latitudes (except in regions of sea ice contamination of the MWR) the trends are very small, $\sim 0.1 \text{ cm yr}^{-1}$. A worst case assumption is that trends at scales larger than at 10^4 km^2 are independent, in which case the trends will be order $\sim 0.3 \text{ cm yr}^{-1}$ at 10^4 km^2 . At 10^7 km^2 , this error is comfortably expected to be less than 0.05 cm yr^{-1} . At latitudes higher than those shown, the correction becomes very small due to the low atmospheric temperatures. (Taken from MRD 1999)



3.4.3 Validation of the retrieval errors.

Until recently, the independent validation of ice sheet elevation trends measured by radar altimeters has been very difficult. A large, short scale, instrument system error is present in the satellite radar observations. This is clearly seen in the observed covariance of Fig. 5.

The presence of this error makes comparisons of the satellite trends with independent observations at point locations in space of limited value. The difficulty has only recently been overcome with the advent of GPS-tied airborne laser altimeter systems, which have allowed, at least over Greenland, repeated areal surveys of elevation change to be conducted (Krabill *et al.* 2000).



These provide, for the first time, measurements that may be directly compared with the satellite measured trends over large areas. Because the laser reflection occurs strictly from the surface, these observations do not contain the retrieval errors present in the satellite radar measurements. Fig. 18 shows the comparison between the elevation changes observed in Greenland by Krabill *et al.* (2000) and the trends observed by the ERS-2 altimeter over a similar time-scale. In general, there is a considerable measure of agreement, particularly in the thickening in central southern Greenland, and the thinning in south-west, north-west and north-east Greenland. Clearly, continuation of these laser measurements is of considerable importance.

		CryoSat Calibration & Validation Concept	Doc: CS-PL-UCL-SY-0004 Issue: 1 Date: 14 November 2001
--	---	---	--

Clearly there are also differences between the two measurements sets in Fig. 18, particularly in regions of snow accumulation. There are space-time differences between the sampling of the laser and satellite measurements, and it is possible to argue that much of the difference arises from the different sampling of the fluctuation in snowfall (section 3.2), or, possibly, density fluctuations (section 3.3). On the other hand, there is a considerable disagreement in the magnitude and extent of thickening in south- and central-east Greenland. This may be evidence of unresolved retrieval errors in the satellite trends in regions of accumulation.

This comparison of the satellite and aircraft measurements underlines the importance of understanding the extent and magnitude of the retrieval error. It requires, essentially, a better understanding of the relationship between changes in the elevation of the surface, and fluctuations in the scattering with depth. Experiments designed to investigate this behaviour would be of importance not only to the CryoSat mission, but also to understanding the historical measurements of the Seasat, Geosat and ERS altimeter missions. Such experiments need not be coincident, temporally or spatially with the satellite observations, although that would add value to such experiments.

Conceptually, such experiments would employ a radar at the same frequency as the satellite radar (13.8 GHz) with, preferably, a wider bandwidth than that of the satellite. The surface elevation could be determined at a static location with a sonic or optical device; for airborne experiments a laser altimeter would be used. Static sites are suited to investigate continuously the temporal variation (Fig. 14); airborne surveys to investigate at intervals the spatial variation (Fig. 15 and Fig. 16). At static sites a range of ancillary meteorological information (accumulation, temperature *etc.*) may also be measured continuously. This would also permit investigations of the mass and density fluctuations at a co-incident location (see Fig. 9) and the combination of all these measurements in a single location would be of particular value.

Nonetheless, such experiments will need careful design. There is a great deal of metre scale variability in near surface firn. Changes affecting the data at large length scales may not be the largest changes seen at a particular location. Some way of connecting the variability seen at an individual location with that seen over larger scales will be needed. Aircraft experiments that aim at understanding the wider scale behaviour will need to ensure that repeated measurements are made *at the same location*. Otherwise it is likely that repeated experiments will largely measure the spatial variation of the scatter, rather than the temporal fluctuations of the scatter.

Another new and important set of observations may be provided by the laser altimeter carried by the ICESAT mission (Zwally *et al.* 2001), which will be contemporary at least in part with CryoSat. These measurements may overcome some of the space-time problems associated with the airborne measurements. As important, they may provide independent measurements over large areas of the Antarctic ice sheet that, at present, are beyond the reach of repeated survey by aircraft.

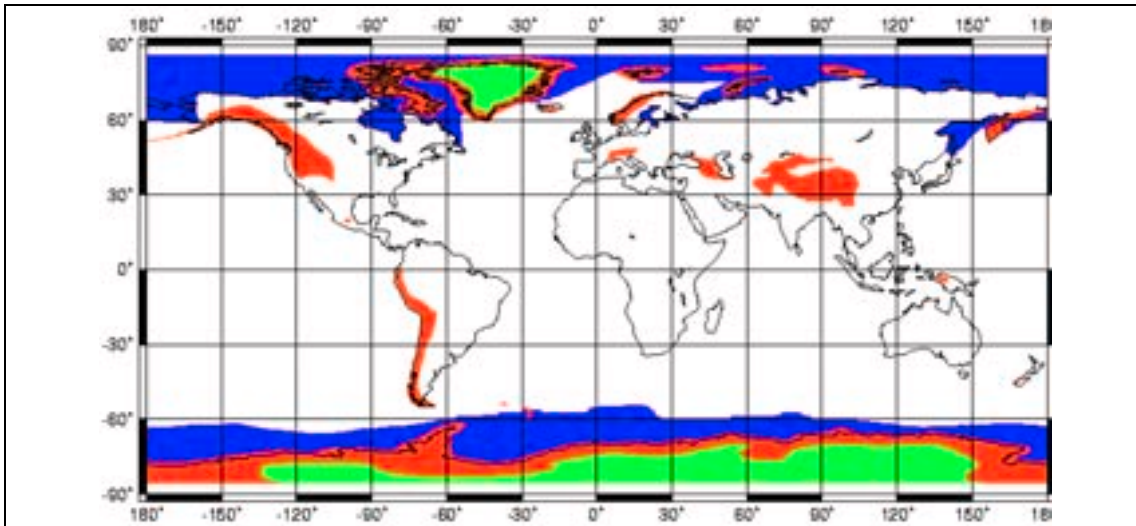
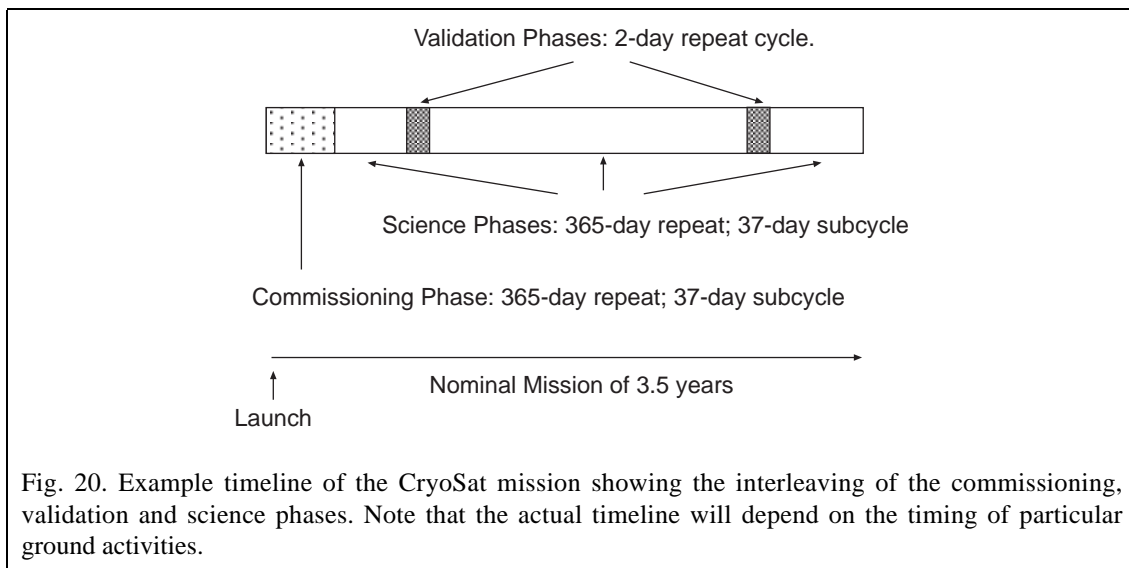


Fig. 19. CryoSat operating mode mask. The coloured regions of the plot shows the location of the Earth's ice surfaces. In those regions shaded red, the interferometric mode of operation will be used. In the blue regions, the synthetic aperture radar mode will be used. In the green regions, the conventional pulse-limited mode will be used. A conventional pulse-limited mode will be used over the global ocean. The figure shows the masks used to size on the on-board memory of the satellite. Detailed changes to accommodate particular experiments will be possible.

The main aim of CryoSat is to measure trends in ice elevation. For this reason, we have not emphasised the independent measurement of the elevation error itself. A number of absolute and relative comparisons between pulse-limited satellite measurements and ground measurements have been made over the years (*e.g.* Gundestrup *et al.* 1986, Phillips *et al.* 1998). These measurements have provided a detailed understanding of the limitations of the pulse-limited altimeter measurements of elevation. It is unlikely that repeating such experiments in the case of CryoSat will provide much new information. On the other hand, the opposite is true in the case of the interferometric mode. In areas of complex topography, the echoes will have considerably more variability in shape than those of pulse-limited systems. The retrievals are likely to be more complicated than for the pulse-limited case, and may suffer from particular defects. Penetration may effect the error in the phase angle retrieval of Eqn. 26. An absolute comparison with independent measurements may be of

great value in improving the retrievals. Well-surveyed sites in the ice sheet margins will be of particular use. By ‘margin’ we mean the red zone in Fig. 19, which indicates the region of interferometer coverage.

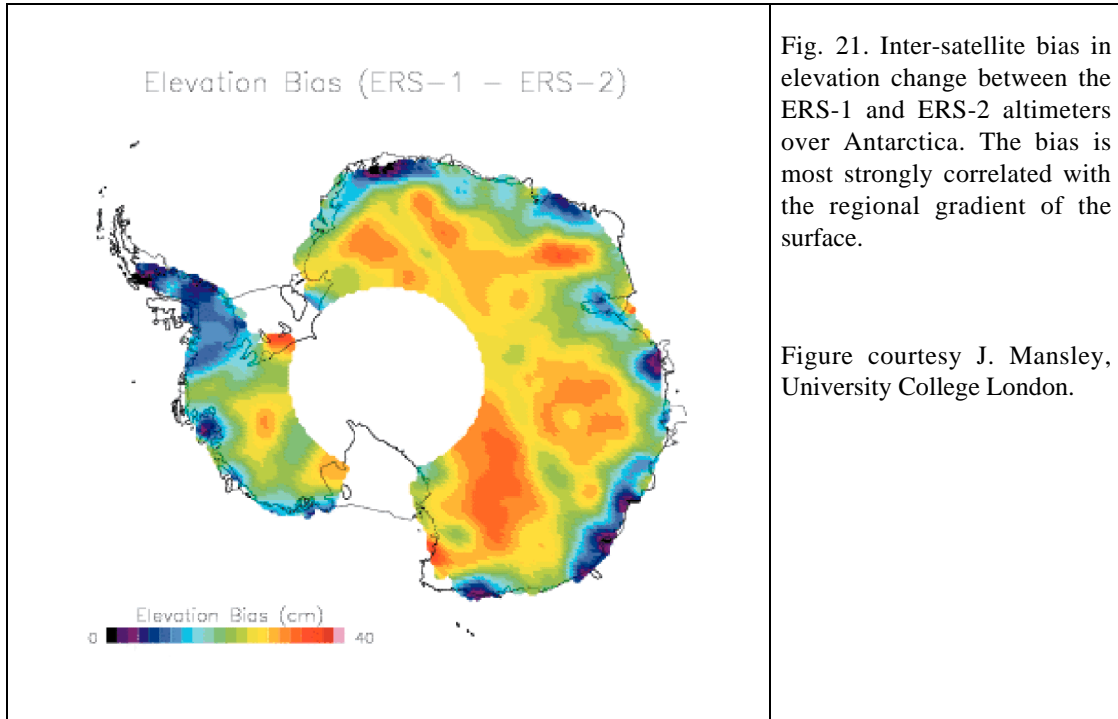
Previously, transponder experiments (Haardeng-Pedersen *et al.* 1998) have been useful to confirm that geometrical relation of surface to the pulse-limited echo in regions of significant volume scattering. An extension of these experiments that will permit a comparison of the coherent processing of the echoes with that of the ‘point target’ of the transponder may be particularly useful. Because of the complexity of the echoes, such experiments may require a careful selection of the transponder location, possibly in parallel with simulations of the likely echo shapes. Two ‘validation’ phases (Fig. 20) have been accommodated within the satellite fuel budget to allow for this type of experiment. In the ‘validation’ phase, the satellite altitude will be altered to place the satellite in a 2-day orbit repeat phase. This will allow repeated overflights of the satellite at particular locations.



3.5 Intersatellite bias

One aim of CryoSat is to extend the time-series of elevation previously measured by the ERS altimeters and, following its launch, the ENVISAT altimeter. For this purpose, an estimate of inter-satellite bias is required. The use of different instrument systems considerably complicates the trend measurement, because a number of absolute errors that cancel when a single instrument system is used will no longer do so. The change in antenna pattern, the effect of polarisation on the volume scattering (Legresy & Remy 1998, Arthern *et al.* 2001) and changes in the slope correction (Brenner *et al.* 1983, Remy *et al.* 1989) due



to orbit altitude differences, all need to be considered. While the errors arising from these effects are in principle independent of time, this may be difficult to determine when the satellite orbits pattern does not repeat regularly, as was the case with Seasat.



Some authors have stated (see *e.g.* Davis 1997) that this bias may be estimated for time-separated observations. The argument rests, essentially, on the assumption that the inter-satellite bias over the ice sheets may be estimated by comparing the measurement sets over the ocean. By comparing the inter-satellite bias of the ERS-1 and ERS-2 altimeters this argument can be tested directly. These two, nominally identical, missions overlapped for a six-month period in 1995 and the bias can be measured directly. At least in this case, the intersatellite bias is quite large and clearly dependent on the ice sheet topography. It would clearly be wise to estimate this bias by direct, temporally overlapping observations wherever possible.

3.6 Timing and location of land ice validation experiments.



A summary of the proposed approaches to the verification of the land ice measurements is given in Fig. 1. In general, the timing of the experiments depends on whether measurements contemporary with the satellites are necessary. The point worth generally

		CryoSat Calibration & Validation Concept	Doc: CS-PL-UCL-SY-0004 Issue: 1 Date: 14 November 2001
--	---	---	--

emphasising in this connection is that a great deal could be achieved independently of the satellite observations. These experiments need not be tied to the period or specific track location of the satellite, although clearly this may increase their usefulness in some cases.

With regard to the geographic location, a number of points need bearing in mind. Firstly, with regard to the mass fluctuation, all the evidence (and the very low mean accumulation) suggests that the imbalance of the East Antarctic interior is very small. On the other hand, changes are seen in the altimeter data in the Antarctic Peninsular, the Thwaites and Pine Island Glacier Basins, possibly Dronning Maud Land, and throughout Greenland. To the extent that contemporary measurements are possible, these regions deserve emphasis. Secondly, with regard to the density fluctuation, this effect is likely to be large when the accumulation is large and the firn temperature approaches or reaches the melting point. Therefore densification experiments in central and south Greenland and the Antarctic Peninsular are likely to be useful. Thirdly, the correlation of the observed elevation and power changes described in 3.4.2 has strong spatial gradients. It is not understood why the effect is absent in regions of high accumulation. Investigating the behaviour of this spatial gradient is easier in Greenland than in Antarctica, for logistic reasons.

There is a good argument for seeking to concentrate some efforts in Greenland. In the previous three sections, the three errors have been discussed separately. However, the annual cycle of the retrieval error may be correlated in regions of higher accumulation with density and possibly mass fluctuations. Because of its smaller size, relative ease of access, possibility for winter airborne surveys and relatively better coverage with ancillary measurements of meteorological parameters, performing simultaneous experiments in Greenland may provide particular benefit. In this respect, it is worth observing that the altimeter trends observed to date appear to have a similar character in Antarctica and Greenland. Finally, it is also worth noting that the aircraft payload elements required for sea ice validation (section 4.4.3) are similar to those for the land ice. Greenland offers the possibility, in relatively short distances, to perform sea- and land-ice validations in the same campaign.

		CryoSat Calibration & Validation Concept	Doc: CS-PL-UCL-SY-0004 Issue: 1 Date: 14 November 2001
--	---	---	--

4 Validation of Sea Ice Uncertainty.

4.1 Objective and general character of sea ice validation. *Equivalence of validation of thickness and thickness trend. Distinction between average ice thickness and average thickness per unit area. Ice concentration. Mass, density and freeboard errors. Sea ice thickness error covariance. The ‘omission’ error.*

4.2 The snow loading uncertainty. *Seasonal behaviour. Limited knowledge of short and intermediate scale covariability. Probable adequacy of climatology at scale of entire Arctic.*

4.3 The density uncertainty. *Observed Arctic variability at the completion of the melt season. Limited knowledge of covariability or annual cycle. Remote measurement by electromagnetic sounding and laser altimetry.*

4.4 The retrieval error. *Separation of retrieval and instrument system errors.*

4.4.1 The measurement technique and origin of the freeboard error. *Origin of the retrieval error. Timing, propagation and sea surface topography error.*

4.4.2 The character of the retrieval error. *Error from floe surface topography. Error from air-snow scattering. Error from differing character of floe and ocean echoes. Lack of present understanding and importance of investigating long-scale errors by experiment. Propagation, tide, dynamic topography and geoid errors, and the need for some investigations.*



4.4.3 The validation of the retrieval error. *The likely error covariance function. Laser measurements in the absence of snow loading. Sampling constraints imposed by ice concentration and ice motion. Complicating effects of snow loading. Usefulness of combined laser and radar observations.*

Potential importance of GLAS measurements.

4.5 Preferential sampling of large floes. *Simplification to the error in the mean. Joint statistics of thickness and ice coverage. Use of coincident imagery of the ice.*

4.6 Validation of thickness measurements. *Validation through comparison of area averages. ULS draft measurements. Under sampling of sea ice thickness distribution. Need for improved ice thickness space-time covariance function. Electromagnetic sounding measurements. Under sampling of satellite measurements.*

4.7 Timing and location of sea ice validation measurements. *Dependence or otherwise on contemporary satellite measurements. Time of year priorities. Limited evidence for geographic variation in errors. Ship-borne and submersible experiments. Aircraft platforms. Practical usefulness of Greenland as a focus for campaigns. Antarctic observations.*

		CryoSat Calibration & Validation Concept	Doc: CS-PL-UCL-SY-0004 Issue: 1 Date: 14 November 2001
---	---	---	--

4.1 Objective and general character of sea ice validation.

In this section the error in spatial averages of the sea ice thickness trend and its validation are described. As was the case with the land ice (section 3), the full problem is more complicated than simply the determination of the measurement error covariance. As with the land ice, the approach is to describe first the relationship between the measured quantity, the sea ice thickness, and the desired quantity, the spatially averaged trend in thickness imbalance. This leads in this subsection to a more complete description of the error covariance than given in section 2 that includes the contributions of snowfall and density fluctuations. In the following sub-sections, each of the contributions to the total covariance and their validation is described in detail.

On the other hand, in the case of sea ice, there is as great an interest in the short-term fluctuations of thickness as there is the longer-term trend. Unlike the case of land ice, where the short term fluctuations are something of noise that obscures the longer term dynamic behaviour, the short term fluctuations in thickness contain information concerning the interplay of the wind, the ocean and ice dynamics and thermodynamics. The thickness itself is of considerable interest. As it turns out, the sea ice measurement is anyway of the absolute thickness. Unlike the case of the ice sheets, where taking the difference of ice thicknesses at a single location removes a substantial fixed error, trends in sea ice are determined from differences in the absolute thickness. There is in addition little practical distinction between determining the uncertainty in the trend in ice thickness from that of determining the uncertainty in the thickness itself (see the comments preceding Eqn. 16, section 2.4 of the general approach). Therefore, in this section we consider the validation of the spatial average of sea ice thickness.

The spatial average estimated from the measurements is the average ice thickness in the area A :

$$\text{Eqn. 30} \quad \bar{t}_{ice} = \left(\frac{1}{A_{ice}} \right) \int_{A_{ice}} dA t_{ice}(\mathbf{x}, t)$$

Introducing a quantity η equal to unity when ice is present, and zero otherwise, the quantity

$$\text{Eqn. 31} \quad \bar{\eta} = \left(\frac{1}{A} \right) \int_A dA \eta(\mathbf{x}) = \frac{A_{ice}}{A}$$

is the ice concentration. We suppose that the area A is large enough A_{ice} may be taken as a constant, and fluctuations in ice concentration (due to a change in the area of the ice) may be ignored. The quantity $\bar{\eta} \bar{t}_{ice}$ is the average ice thickness per unit area, which is the

average thickness that is usually required in models. The average ice thickness is then given by

$$\text{Eqn. 32} \quad \bar{t}_{ice} = \left(\frac{1}{A\bar{\eta}} \right) \int_A dA \eta(\mathbf{x}) t_{ice}(\mathbf{x})$$

in terms of an average of the area A .

For sea ice in hydrostatic equilibrium,

$$\text{Eqn. 33} \quad t_{ice} = \frac{\rho_w}{(\rho_w - \rho_{ice})} f_{ice} + \frac{1}{(\rho_w - \rho_{ice})} m_{snow}$$

where ρ_w are ρ_{ice} the densities of sea water and sea ice respectively, and f_{ice} is the freeboard of the ice. The freeboard is, by definition, the distance between the water surface and the upper surface of the sea ice – see Fig. 22. m_{snow} is the mass per unit area of meteoric snow that may be lying on the surface of the ice. This is termed the snow ‘load’ for short.

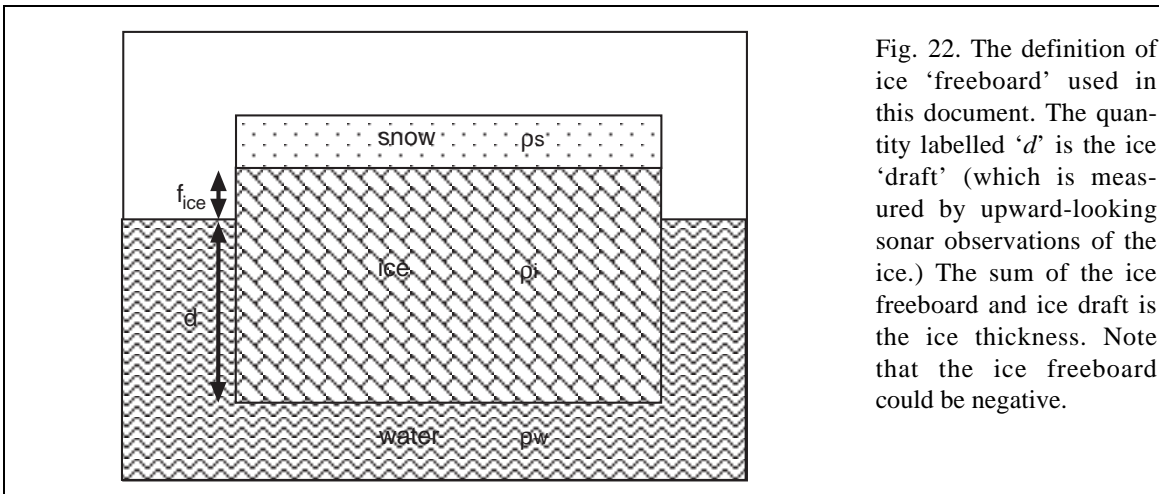


Fig. 22. The definition of ice ‘freeboard’ used in this document. The quantity labelled ‘ d ’ is the ice ‘draft’ (which is measured by upward-looking sonar observations of the ice.) The sum of the ice freeboard and ice draft is the ice thickness. Note that the ice freeboard could be negative.

The essential idea of the measurement is to use the altimeter to determine the freeboard f_{ice} of the ice, and use auxiliary measurements of the water density, ice density and snow mass to determine the thickness. To first order, the uncertainty in the thickness is given by

$$\text{Eqn. 34} \quad \varepsilon_t = \frac{1}{(\rho_w - \rho_{ice})} \varepsilon_m + \frac{f_{ice}}{(\rho_w - \rho_{ice})^2} (\rho_w \varepsilon_{pi} + \rho_{ice} \varepsilon_{pw}) + \frac{\rho_w}{(\rho_w - \rho_{ice})} \varepsilon_f$$

where ε_m , ε_{pi} , ε_{ps} and ε_f are the uncertainties in the snow load, density of sea ice, sea water and measured freeboard respectively. With the present definition of freeboard, the



snow loading error accounts for any uncertainty in the relation between the freeboard and ice thickness. On the other hand, if the radar is ranging to an elevation different from that of the snow-ice interface, this difference is accounted for by the freeboard error. The expression and categorisation of the errors (but not the total error) would change with a different definition of freeboard (*e.g.* the distance between the ocean and snow surface). The present definition of freeboard is chosen because what evidence there is suggests that over sea ice the radar is considerably more sensitive to the snow-ice interface than to the air-snow interface when snow is present.

Because the sensor resolution is finite, the radar will not sample all the ice. This is accommodated by introducing the function η_r . This function is equal to unity over ice sampled by the radar and zero otherwise. The observed ice concentration is $\bar{\eta}_r$. Like $\bar{\eta}$, we shall assume that A is large enough that $\bar{\eta}_r$ may be taken as a constant. In the measurement, it will be the observed concentration that is used to normalise the spatial average of thickness. The uncertainty in the spatial average of the thickness is then

$$\text{Eqn. 35} \quad \bar{\varepsilon}_t = \left(\frac{1}{A} \right) \left(\frac{1}{\bar{\eta}_r} \int_A dA \eta_r(\mathbf{x}) \varepsilon_t(\mathbf{x}) + \int_A dA \left(\frac{\eta(\mathbf{x})}{\bar{\eta}} - \frac{\eta_r(\mathbf{x})}{\bar{\eta}_r} \right) t_{ice}(\mathbf{x}) \right)$$

In keeping with the general approach of section 2.2, the objective of validation of the sea ice measurement is to estimate the variance of this uncertainty. We suppose that the individual contributions to point thickness uncertainty ε_t in Eqn. 34 are uncorrelated and stationary, and, further, that the function η_r may be regarded as a stationary random variable, uncorrelated with ε_t , with a covariance function denoted C_{η_r, η_r} . In this case the variance is (see section 7.3):

Eqn. 36

$$E\{\bar{\varepsilon}_t^2\} = \int_{Earth} dA W(\mathbf{s}) \times \left(\frac{1}{\bar{\eta}_r^2} (C_{\eta_r, \eta_r}(\mathbf{s}) C_{mm}(\mathbf{s}) + C_{\eta_r, \eta_r}(\mathbf{s}) C_{\rho\rho}(\mathbf{s}) + C_{\eta_r, \eta_r}(\mathbf{s}) C_{ff}(\mathbf{s})) + Cov \left[\left[\left(\frac{\eta}{\bar{\eta}} - \frac{\eta_r}{\bar{\eta}_r} \right) t_{ice} \right] (\mathbf{x}) \right] \right)$$

where C_{mm} , $C_{\rho\rho}$, C_{ff} are the covariances of the uncertainties in mass, density, and freeboard respectively. The term C_{η_r, η_r} appears in the expression for the spatial average because the extent to which the uncertainties are reduced by the spatial averaging depends on the area of ice within the area A . If there is little ice there is little opportunity to average down the errors associated with measurements of it. In similar fashion to the land ice, the point uncertainty in thickness arises from a snow mass uncertainty, a density uncertainty, and a measurement uncertainty.



The uncertainty in the spatial average of the sea ice, however, contains a new term. This term, the final term in Eqn. 36, arises because the ice coverage is not fully sampled by the radar. Physically, it accounts for the fact that the thickness distribution sampled by the radar may differ from the thickness distribution of the ice as a whole. It is an error of omission and not of commission, and for this reason it depends on the statistics of the thickness itself, rather than those of the measurement error.

In the following sections we describe what is known of the magnitude of the individual terms in the covariance function of Eqn. 36, their scales of variation, and approaches to their experimental estimation are discussed. It should be noted that very much less is known of the short and intermediate scale uncertainties in the case of sea ice than that of the land ice. Necessarily, the descriptions of these uncertainties are somewhat conjectural.

4.2 The snow load uncertainty.

The effect of snow loading on the retrieval of Arctic ice thickness from measurements of ice freeboard is illustrated in Fig. 23. It is a strong function of the time of year, increasing to a maximum in spring prior to the onset of melting. By the summer, the snow load is completely lost, before starting to increase again with the onset of freezing. It should be noted from this figure that the interval of time in which the effect of snow loading on the measurement may be ignored is very limited; generally snow will be present on the ice.

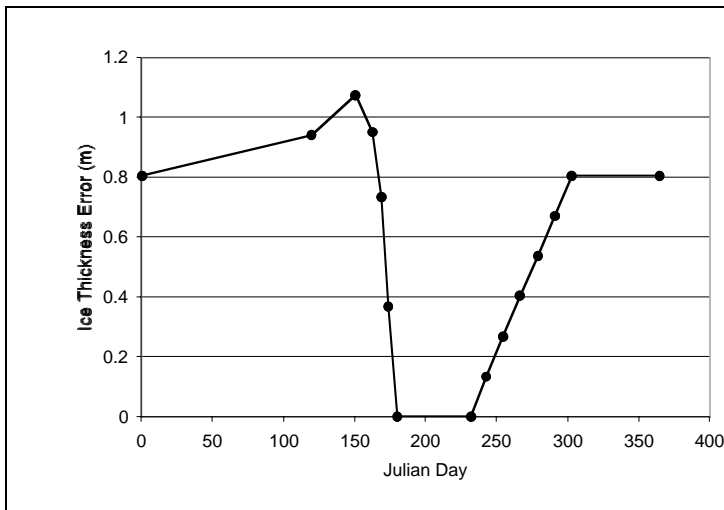


Fig. 23. The error in ice thickness arising from snow loading of the surface. The calculation is based on a climatology of Arctic snowfall of Warren *et al.* (1999) and assumes 915, 1024 and 330 - 450 kg m⁻³ for the densities of ice, sea water and snow respectively. The change in the density of snow reflects the time-variant densification that occurs during the winter. Calculation after Wadhams *et al.* (1992).

Fig. 23 shows the effect of the total loading of snow. However, because at least an Arctic climatology of snow loading exists (Gorshkov 1983, Warren *et al.* 1999), the uncertainty it

introduces into the thickness estimate arises from the departure of the actual loading from the climatology. The fluctuation of the snow load about the climatology is not well known. At the largest scales, however, the pulse-limited altimeter thickness estimates themselves show that the Arctic wide fluctuation may be small. In Fig. 24, the growth cycle of ice thickness observed by radar altimeter compares closely with that measured during the SHEBA experiment (Perovich 2001) when a correction using is made for the climatological snow loading. Also shown in the figure is the effect of making no correction. It would appear that, on an Arctic scale, the departure of the snow loading from the climatology is quite small.

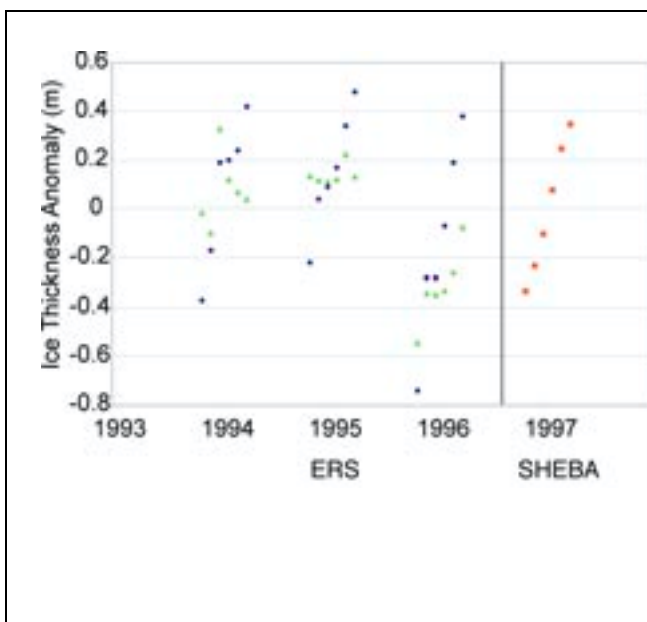
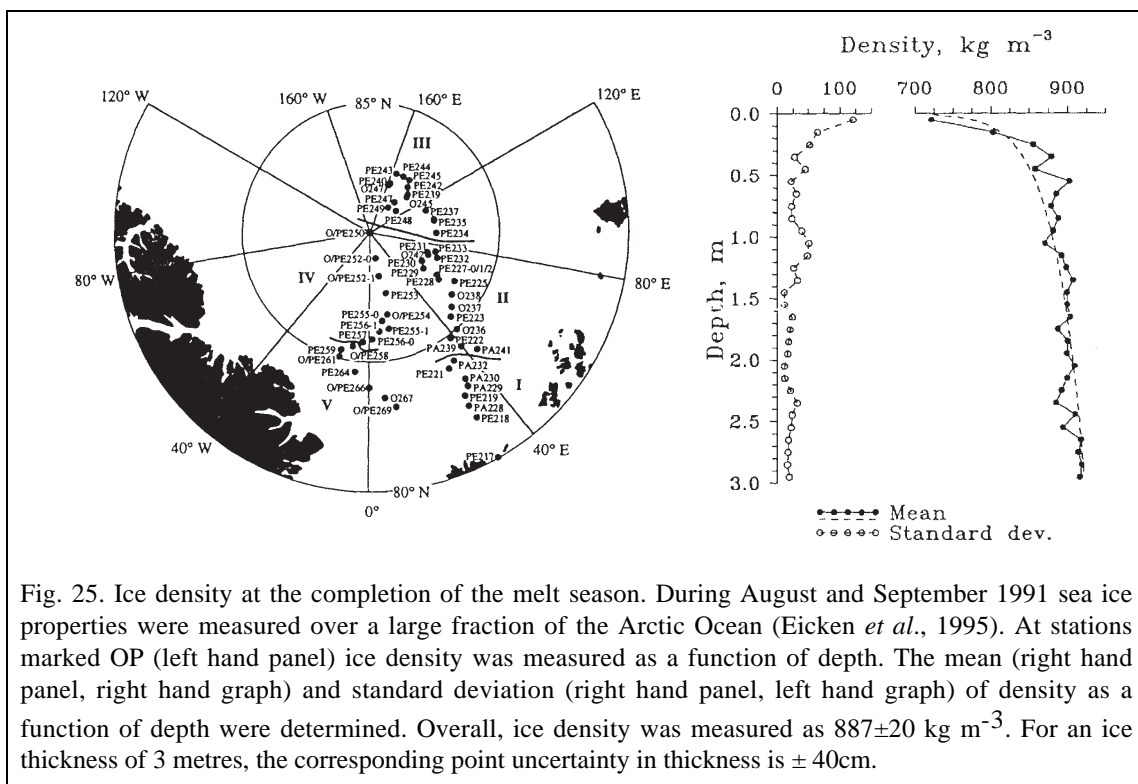


Fig. 24. The estimated winter growth of sea ice thickness determined from ERS-2 altimetry (blue circles) averaged over the entire Arctic south of 820 N from Oct 1993 - Mar 1997. Also shown is the growth cycle from direct measurements during the Sheba experiment in the Beaufort Sea between Oct 1997 and Mar 1998 (red squares). The ERS measurements have used the Warren climatology to correct for snow loading. The green triangles show ERS measurements when the correction is not made. The figure shows that, at least over large-scale averages, the climatology may be sufficient to correct the satellite observations of freeboard for snow loading.

However, unlike the case of land ice, the snow does not survive the winter and cannot be investigated after the event. Its effect at short and intermediate scales is presently a matter for conjecture. These are potentially quite large, and some attention to this possibility is needed as part of the validation activity. Clearly, this can be done by direct observation, although the effort it requires over significant distances is considerable. As is the case for the land ice, it may be possible to learn more of the fluctuations by revisiting historical surveys. Methods of achieving the measurement remotely are very similar to those concerned with the retrieval error, and are discussed in 4.4.3.

4.3 The density uncertainty

The density error contains two terms, one due to uncertainty in the density of sea water, the other due to the uncertainty in the density of ice. The density of sea water varies by only a few parts per thousand, and because of this, a standard value may be used without great impact on the thickness measurement. The density of sea ice, on the other hand, is more variable. At the end of the melt season, observations in a large section of the Arctic (Fig. 25) show a variability in net (column averaged) density of $\sim 20 \text{ kg m}^{-3}$ which would introduce a variability of 40 cm into the measurement of sea ice thickness. As is apparent from the figure, most of the variability occurs near the surface, showing that it is the effects of the atmosphere that causes the variability, rather than the ocean.



The variability shown in (Fig. 25) is on a short scale (at least in comparison with the region of data collection); whether density varies more widely is not well known. At other times of year neither the variability nor co-variability well established. During the winter the sea ice grows by a slow process of bottom freezing, and it may be that the density is largely constant, with the column density largely varying inter-annually as a result of the summer melt processes. However, this is a conjecture, and measurements are needed to investigate the matter.

As with snowfall, this can be done by direct observation, and it may be possible to learn more of the fluctuations by revisiting historical surveys. However, to provide a good idea of the spatial variability probably requires a remote technique. This has recently become possible through the development of a low-frequency, electro-magnetic sounding method (Hass & Eicken 2001, Eicken & Perovich 2001). In this method, the ice thickness is measured from a boom held several metres above the surface of the ice. Demonstrations of the technique (Fig. 26) show the ice thickness is mapped with considerable fidelity on scales of 50 metres or greater. Clearly this provides a technique to verify the thickness measurements themselves, and we return to this in 3.4.3. Here, however, we note that if the measurements are supplemented with laser altimeter measurements that can determine the ice freeboard (as in the figure), the measurements also provide a measure of the column density of the ice.

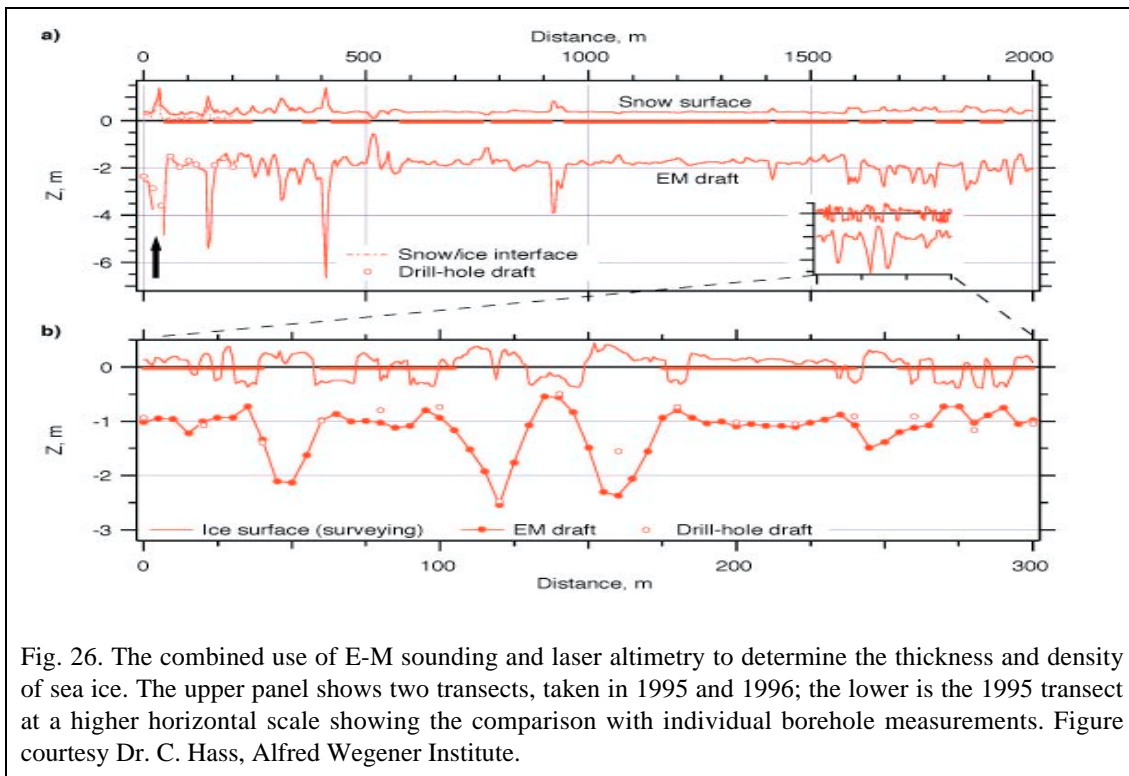




Fig. 26. The combined use of E-M sounding and laser altimetry to determine the thickness and density of sea ice. The upper panel shows two transects, taken in 1995 and 1996; the lower is the 1995 transect at a higher horizontal scale showing the comparison with individual borehole measurements. Figure courtesy Dr. C. Hass, Alfred Wegener Institute.

4.4 The retrieval error.

In the case of sea ice, the measurement is one of freeboard, and in line with the general discussion of section 2.3, the freeboard error may be separated into two components. A retrieval error arises because the reduction of the echo to an elevation depends on

		CryoSat Calibration & Validation Concept	Doc: CS-PL-UCL-SY-0004 Issue: 1 Date: 14 November 2001
--	---	---	--

simplified assumptions concerning the relation of the echo to the surface. An instrument system error arises because the measurements of echo power, phase angle, *etc.* are in error. By assumption (section 2.3) these errors are independent, and the freeboard error covariance function of Eqn. 36 may be separated into two terms:

$$\text{Eqn. 37} \quad C_{ff}(\mathbf{x}) = C_{rr}(\mathbf{x}) + C_{ss}(\mathbf{x})$$

in which C_{rr} is the retrieval error covariance and C_{ss} is the system error covariance. Although these errors both emerge at the same stage of the retrieval - the conversion of the radar echo to a distance from the satellite - they are distinct. The source of the retrieval error lies in the passage of the radar pulse through the polar atmosphere and its interaction with the ice surface, and its validation requires *in-situ* investigations. The source of the system error lies with the imperfections of the instrument, and can be determined separately. The separation of the retrieval and system errors is discussed in the following subsection, and the *in-situ* investigation of the retrieval error is the subject of the remainder this section. The system error is dealt with in section 5. (Note that approaches to the validation of the thickness error as a whole are considered separately in section 4.6.)

4.4.1 The measurement technique and origin of the freeboard error.

The concept of the measurement of ice sheet elevation over the sea is illustrated in Fig. 27. Over the sea ice, CryoSat will use synthetic aperture mode of operation. (The technical operation of this mode is described in more detail in the MDD.) In this mode the radar illuminates a narrow across-track strip of the surface. The radar transmits a thin pulse-shell, and the amplitude of the echo scattered back to the radar from the strip is recorded at an antenna as a function of the echo delay time. The same strip on the surface is illuminated many times by the radar as the satellite flies overhead, and an averaged ('multi-looked') echo is determined. The variation in the power of the echo as a function of the 'incidence angle' of the beam is also recorded. This information is used to help determine whether the echo arises from the ice or the leads between the ice.

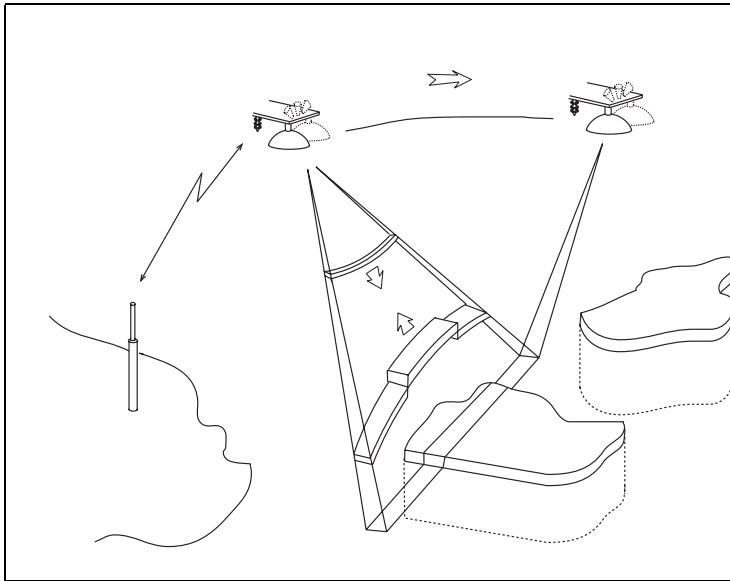


Fig. 27. The CryoSat “SAR” measurement configuration designed for use over sea ice. A single altimeter is employed. The echoes are coherently processed along-track to form very narrow (~ 250 m), across-track strips. The principle of the sea ice freeboard measurement is similar to that of pulse-limited altimetry, save that the distinction in the echo shapes from the ice and the leads is contained in the variation in power in the coherent beams, rather than echo delay.

The level *1b* data contains, essentially, the multi-looked echoes and information concerning their angular behaviour, together with the geometrical information concerning the satellite location. It amounts to the following parameters

$$\phi_{1b}(\mathbf{x}, t, \tau, k) \equiv \begin{cases} \psi(\mathbf{x}, t, \tau) \\ z(\mathbf{x}, t) \\ \Theta(\mathbf{x}, t, k) \end{cases}$$

(More details as to the actual contents of the level *1b* data may be found in the MDD). Here, \mathbf{x} is the location of a point *E* in Fig. 28 that lies on the satellite ellipsoidal ground track. z is the normal altitude of the satellite at the point *Z* normally above *E*. t is the time at which the satellite is located at the point *Z*. ψ is the power of the echo measured at one antenna located at the point *Z*; this echo is a function of the echo delay time τ from the instant of transmission. Θ is a measure of the variation of power in the echo received in each individual beam, denoted by counter k , directed at the point *Q*. (The individual beams are illustrated in Fig. 27).

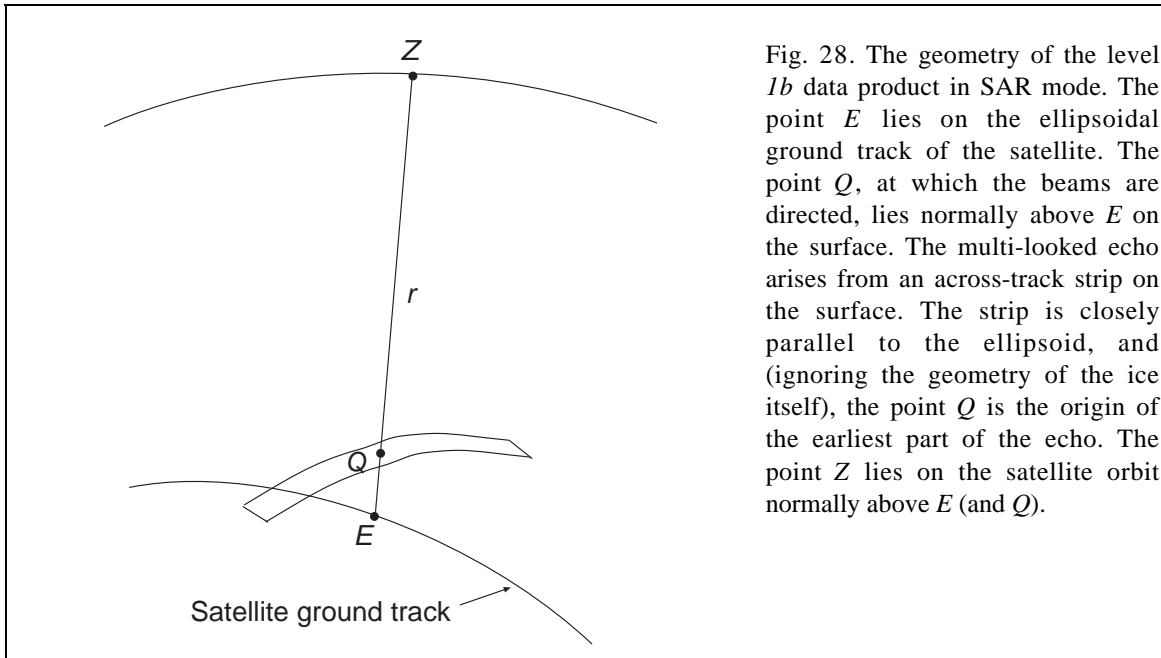


Fig. 28. The geometry of the level *1b* data product in SAR mode. The point *E* lies on the ellipsoidal ground track of the satellite. The point *Q*, at which the beams are directed, lies normally above *E* on the surface. The multi-looked echo arises from an across-track strip on the surface. The strip is closely parallel to the ellipsoid, and (ignoring the geometry of the ice itself), the point *Q* is the origin of the earliest part of the echo. The point *Z* lies on the satellite orbit normally above *E* (and *Q*).

The first step in obtaining ice freeboard estimates is the discrimination of return echoes from consolidated ice and those from open water and new ice. Fig. 29 illustrates the distinct echoes that appear with pulse-limited altimetry. By analysing return echo shape echoes originating from compact first and multi-year ice floes are distinguished from those due to leads, open water and new ice (Drinkwater 1991, Fetterer 1992, Laxon 1994).

With CryoSat, the measurements will be made with the radar in its SAR mode of operation. The purpose of this is to allow smaller ice floes to be detected relative to pulse-limited operation. That said, the distinction between the methods is small, save that the differentiation of the ocean and ice echoes will use the spread of energy across the Doppler beams, *i.e.* the parameters $\Theta(k)$, rather than the variation in power with echo delay-time seen in Fig. 29. In general, we expect the errors to behave in a similar way, although the detailed behaviour will depend on the detailed differences in the retrieval algorithms in the two cases. Echoes that originate from a mixed ice/ocean surface or those originating off-nadir are unusable and are discarded.

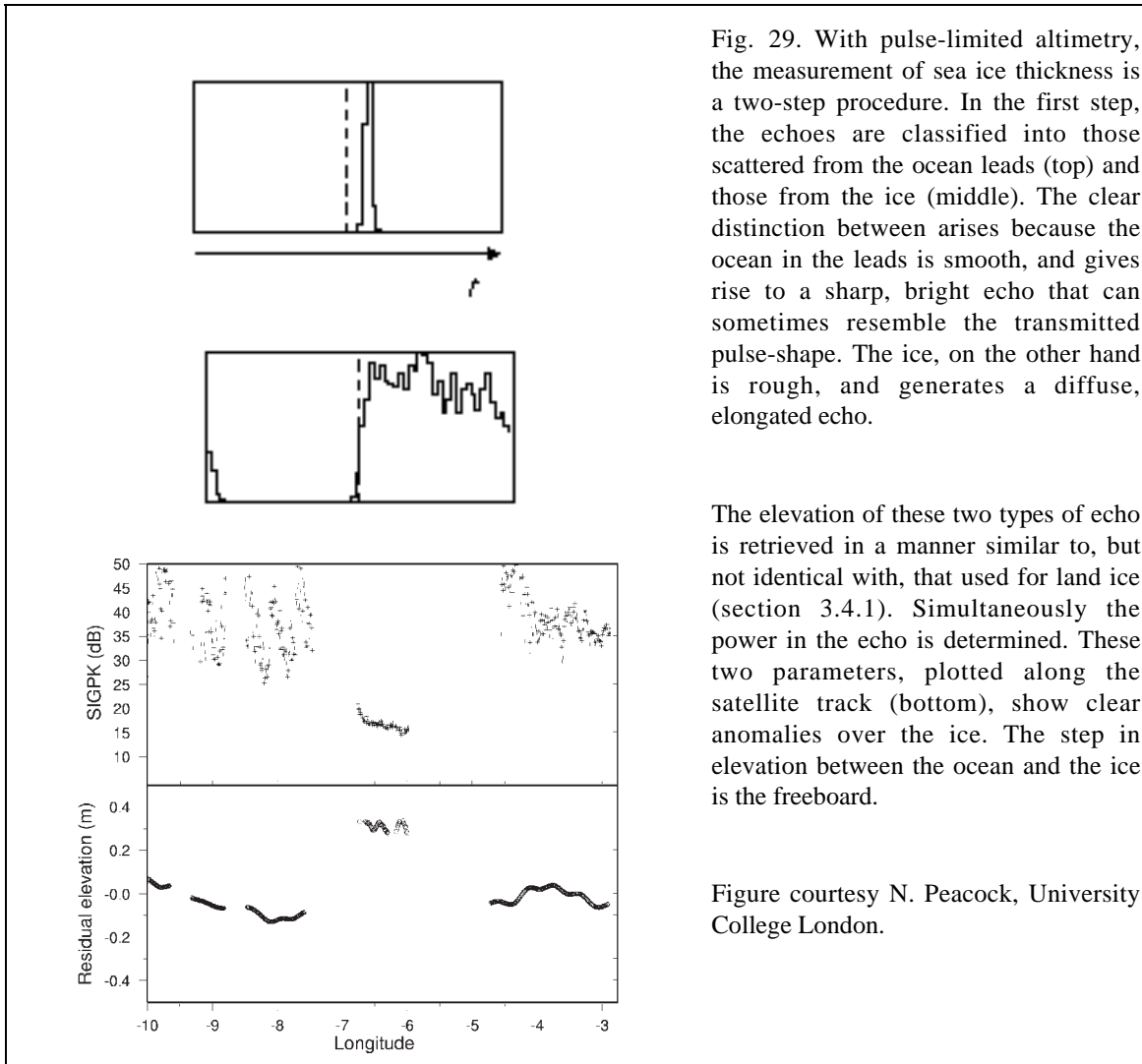


Fig. 29. With pulse-limited altimetry, the measurement of sea ice thickness is a two-step procedure. In the first step, the echoes are classified into those scattered from the ocean leads (top) and those from the ice (middle). The clear distinction between arises because the ocean in the leads is smooth, and gives rise to a sharp, bright echo that can sometimes resemble the transmitted pulse-shape. The ice, on the other hand is rough, and generates a diffuse, elongated echo.



The elevation of these two types of echo is retrieved in a manner similar to, but not identical with, that used for land ice (section 3.4.1). Simultaneously the power in the echo is determined. These two parameters, plotted along the satellite track (bottom), show clear anomalies over the ice. The step in elevation between the ocean and the ice is the freeboard.

Figure courtesy N. Peacock, University College London.

The elevation of sea ice or lead is determined from these data by determining the value of earliest echo delay time, $\tau_r^{(ice)}$ or $\tau_r^{(lead)}$, from the shape of the average echo $\psi(\tau)$ received at the point Z from the surface at the point Q in Fig. 30. These echo delays are used to determine the elevations $g^{(ice)}$ or $g^{(lead)}$ using the velocity of light c according to, for example,

$$\text{Eqn. 38} \quad g^{(ice)} = z - c\tau_r^{(ice)} / 2$$

An individual freeboard measurement is then determined by differencing an ice elevation from some local average of the ocean elevation measurements

		CryoSat Calibration & Validation Concept	Doc: CS-PL-UCL-SY-0004 Issue: 1 Date: 14 November 2001
---	---	---	--

$$\begin{aligned}
\text{Eqn. 39} \quad f(\mathbf{x}, t) &= g^{(ice)}(\mathbf{x}, t) - \Delta g^{(ice)}(\mathbf{x}, t) - \sum_j y_j(\mathbf{x}, t) \left(g^{(lead)}(\mathbf{x}_j, t_j) + \Delta g^{(lead)}(\mathbf{x}_j, t_j) \right) \\
&\equiv g^{(ice)}(\mathbf{x}, t) - \tilde{g}^{(lead)}(\mathbf{x}, t)
\end{aligned}$$

Here, $\tilde{g}^{(lead)}$ is the estimate of where the surface of the lead would have been, were the floe not present. $\Delta g^{(lead)}$ is a correction that accounts for differences in tides and ocean topography at the times and locations of measurement between the ice and lead observations. To highest order, the expression for the error in the freeboard is

$$\begin{aligned}
\text{Eqn. 40} \quad \epsilon_f(\mathbf{x}, t) &= c \left(\epsilon_\tau^{(ice)}(\mathbf{x}, t) - \tilde{\epsilon}_\tau^{(lead)}(\mathbf{x}, t) \right) / 2 \\
&+ \tau_r \left(\epsilon_c(\mathbf{x}, t) - \tilde{\epsilon}_c(\mathbf{x}, t) \right) / 2 + \epsilon_z(\mathbf{x}, t) - \tilde{\epsilon}_z(\mathbf{x}, t) + \epsilon_r(\mathbf{x}, t) - \tilde{\epsilon}_r(\mathbf{x}, t)
\end{aligned}$$

where the notation is similar to that used to describe the land ice measurement errors (Eqn. 28). The new error ϵ_r , which does not occur in the case of the land ice, is the error in the ocean tide and topography models. In a similar fashion to the land ice, it is the errors ϵ_τ , ϵ_c and ϵ_r that give rise to the retrieval error.

The ‘first-arrival time’ τ_r is determined by examining in detail the shape of the ice and lead echoes in a fashion that is similar to, but not identical with, that of the land ice. Essentially, the retrieval assumes the surface to be locally plane. As this assumption will generally not describe in detail the actual situation, a retrieval error ϵ_r will result in τ_r . There is in addition an instrument contribution to the error in the travel time τ_r and generally, for example,

$$\text{Eqn. 41} \quad \epsilon_\tau^{(ice)}(\mathbf{x}, t) = \epsilon_r^{(ice)}(\mathbf{x}, t) + \epsilon_i^{(ice)}(\mathbf{x}, t)$$

In the remainder of this section the character and validation of the errors ϵ_r , ϵ_c and ϵ_r are discussed. The contribution of ϵ_i in Eqn. 41 and the remaining terms in Eqn. 40 are the subject of section 5.

4.4.2 The character of the retrieval error.

There are no point-by-point comparisons of altimeter thickness observations with independent observations, and a discussion of the retrieval error is necessarily somewhat speculative. Nonetheless, experience with pulse-limited observations over land ice suggests that three errors are foreseeable. Firstly, the ice surface is not smooth but contains corrugations (Fig. 31). This will cause a perturbation in the shape of the leading edge of the echo. How this effects the retrieval of ice elevation depends considerably on the scale of the corrugation. If there are many corrugations within the area of $\sim 1 \text{ km}^2$ illuminated by

the radar, the echo will be sensitive only to their average properties. This situation would be similar to the way that the pulse-limited echo from the open ocean is only sensitive to the average properties of the waves (see *e.g.* Brown 1977). On the other hand, if the corrugation structure is larger, or if it has particular orientations (as pressure ridges may well do), the effect on the echo may be complicated, and the elevation biased as a result. (This topographic bias is well known in ice sheet altimetry, but is irrelevant to trend measurements because- as discussed in section 3.4 - it cancels out.)

It is not easy without detailed simulations to determine the likely magnitude of the bias. However, because it is related to the illumination of the beam, and because this has an extent of ~ 200 m along the track, this bias will be a short scale fluctuation. In practise it may be difficult to distinguish from the short-scale, instrument system error fluctuation.

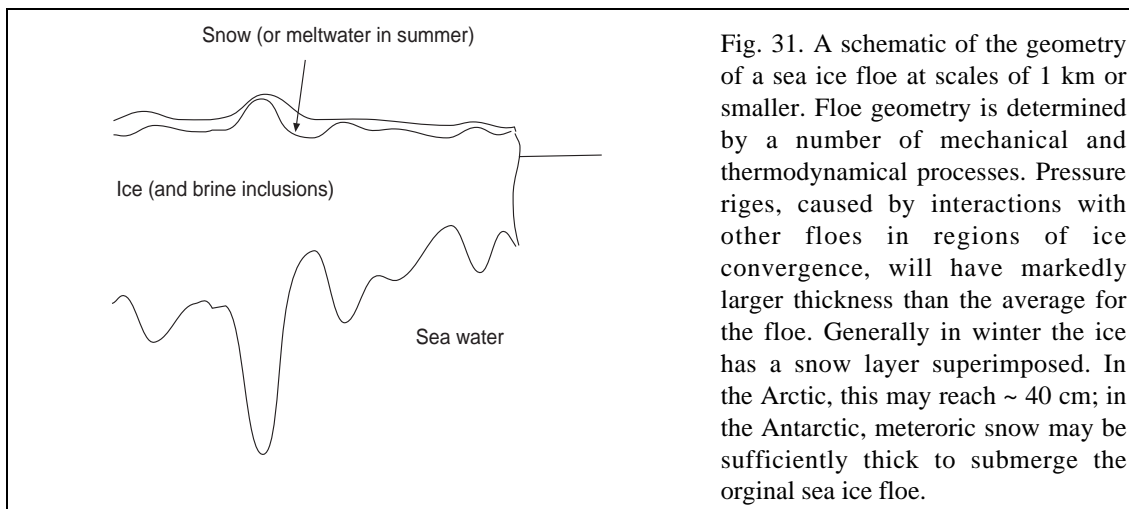


Fig. 31. A schematic of the geometry of a sea ice floe at scales of 1 km or smaller. Floe geometry is determined by a number of mechanical and thermodynamical processes. Pressure ridges, caused by interactions with other floes in regions of ice convergence, will have markedly larger thickness than the average for the floe. Generally in winter the ice has a snow layer superimposed. In the Arctic, this may reach ~ 40 cm; in the Antarctic, meteoric snow may be sufficiently thick to submerge the original sea ice floe.

The second retrieval error that may be foreseen arises because the radar may be sensitive to the air-snow interface when snow is present. Evidence from the laboratory (Beaven *et al.* 1995, Lytle *et al.* 1993), suggest that the snow-ice interface will be the dominant scatterer at 13.8 GHz. This is also supported at large scales by the observed area average of growth curves deduced from altimetry freeboard when converted to thickness on the assumption that this is the case (Fig. 24). However, there are no direct observations to confirm this assumption, and these measurements need to be made. On short and intermediate scales the situation may be complicated.

The third retrieval error that may be foreseen lies in the observed floe height relative to that of the surrounding water. It is the difference (Eqn.) between these two observations that

forms the freeboard estimate. Because the shape and character of the echo from the two surfaces is very different, the effect of the finite radar bandwidth on the echoes will be different. This will only be correctable to some degree, and it is almost inevitable that a bias will result in the difference. This bias may have large scales, and is potentially an important source of error in the spatial average.

Evidence that a long-scale bias exists is shown in Fig. 32 which shows a comparison between altimeter thickness and that deduced from upward looking sonar from submarine. There is clear evidence of a bias between the two measurements. (A similar bias is apparent in the comparison shown Fig. 36). Because the measurements were made in October, snow loading may also contribute to the bias. Although the sonar observations themselves may contain biases (see *e.g.* Vinje *et al.* 1998), it seems likely that some at least lies with the altimetry.

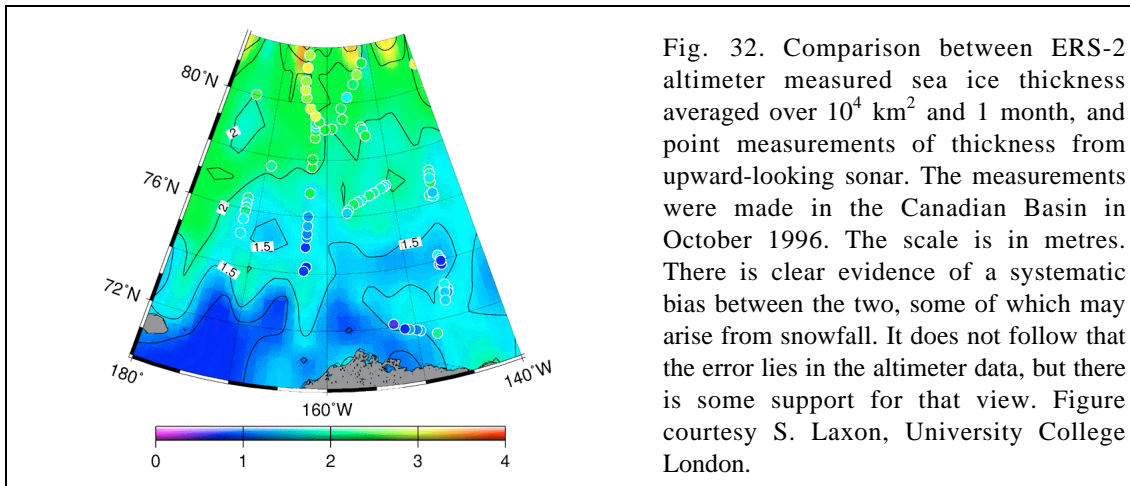




Fig. 32. Comparison between ERS-2 altimeter measured sea ice thickness averaged over 10^4 km² and 1 month, and point measurements of thickness from upward-looking sonar. The measurements were made in the Canadian Basin in October 1996. The scale is in metres. There is clear evidence of a systematic bias between the two, some of which may arise from snowfall. It does not follow that the error lies in the altimeter data, but there is some support for that view. Figure courtesy S. Laxon, University College London.

It is possible that the retrieval error arising from scattering from the air-snow interface, as well as that from floe-ocean differences, will also have large spatial scales. Very little is known today. Because of their large spatial coherence, it is important that these errors are investigated by validation experiments.

The importance of the propagation and tidal errors depends to a large extent on how the difference of ice elevation and ocean elevation (Eqn.) is performed. One extreme is to form an estimate of the mean sea surface from all of the ocean observations, and to determine the ice freeboard as an anomaly from this sea surface. In this case, the retrieval error (Eqn. 40) from this source is, essentially, that due to the ice elevation measurement, that is

$$\text{Eqn. 42} \quad \epsilon_c(\mathbf{x}, t) - \tilde{\epsilon}_c(\mathbf{x}, t) \sim \epsilon_c(\mathbf{x}, t) \quad \epsilon_t(\mathbf{x}, t) - \tilde{\epsilon}_t(\mathbf{x}, t) \sim \epsilon_t(\mathbf{x}, t)$$

		CryoSat Calibration & Validation Concept	Doc: CS-PL-UCL-SY-0004 Issue: 1 Date: 14 November 2001
--	---	---	--

This method is essential with some pulse-limited observations because the density of along-track measurements of ice is low.



With CryoSat, however, the along-track density of measurements is expected to be much higher. On this assumption, another extreme case is to extrapolate the ocean surface along the satellite track, forming an ‘instantaneous’ estimate of the mean sea surface. In this case, because the propagation and tide errors have length scales larger than that of the floes, the errors largely cancel in Eqn. 40 and

$$\text{Eqn. 43} \quad \epsilon_c(\mathbf{x}, t) - \tilde{\epsilon}_c(\mathbf{x}, t) \sim 0 \quad \epsilon_t(\mathbf{x}, t) - \tilde{\epsilon}_t(\mathbf{x}, t) \sim \tilde{\epsilon}_t(\mathbf{x}, t)$$

where $\tilde{\epsilon}_t$ will not include tidal or dynamic topography components, but only short-scale geoid errors. On the other hand, in this second case the effect of instrument system errors on the estimate of the sea surface will be increased, possibly considerably.

In between these two end cases lies a range of possibilities, depending on how much temporal variability is included in the model of the sea surface. Considering first the error in the sea surface $\tilde{\epsilon}_t$, this will in all cases contain the short-scale geoid error. Experience shows with pulse-limited altimetry that the ocean observations, averaged over several years, provide an accurate representation of the gravity field (Laxon & McAdoo 1994). Calculations presented in MRD (1999) based on ERS-1 experience estimated point errors of 14 cm, reducing to 1.6 cm at scales of 10^5 km^2 . This is almost certainly an over estimate. CryoSat will provide considerably higher sampling density than the ERS missions at high latitudes. In addition CryoSat will benefit in the improvements in high latitude gravity that will arrive from the CHAMP and GRACE satellite missions (see <http://op.gfz-potsdam.de/champ/> and <http://www.csr.utexas.edu/grace/> respectively). High resolution, accurate ground surveys of marine gravity do exist in the Canadian Basin, and may be used for validating the gravity field used in the CryoSat measurement.

The time-variant component of $\epsilon_t - \tilde{\epsilon}_t$ consists of unmodelled dynamic topography and errors in the tidal corrections. The dynamic topography of the Arctic is very small (of the order of 2 cm), and its variability may be ignored except in the case of the Fram Strait, where variability associated with the East Greenland Current may be of the order of 4 cm (Reference). Tide model errors may be significant in the Arctic, where there are comparatively few records to constrain the models and the bathymetry is not well known. In detail, the effect of tide-model errors is complicated by the space-time sampling of the satellite, and it has not been much studied for the inclination and repeat-cycle used by CryoSat. Detailed investigations require simulation. On the other hand, a good deal of the tidal error is apparent in the altimeter observations themselves, and the models may be

		CryoSat Calibration & Validation Concept	Doc: CS-PL-UCL-SY-0004 Issue: 1 Date: 14 November 2001
--	---	---	--

improved by using the observations (Peacock 2001). In summary, the matter could do with some investigation.

Of the atmospheric refraction errors, the ionosphere will be measured by the DORIS system. This, coupled with the low total electron content of the polar ionosphere, makes significant errors from this source unlikely, although some investigation to confirm this is worthwhile. Atmospheric pressure (*i.e.* dry atmospheric mass) is well modelled, and this error may be ignored. The wet atmospheric correction over the Arctic Ocean deserves some attention. CryoSat depends on atmospheric forecast models for this correction. Although at high latitudes the error in this correction is expected to have negligible effect in a trend measurement (see Fig. 17), this may not be the case in, for example, a monthly mean over 10^5 km^2 . Further investigation of an error from this source deserves attention. It may need a validation activity.

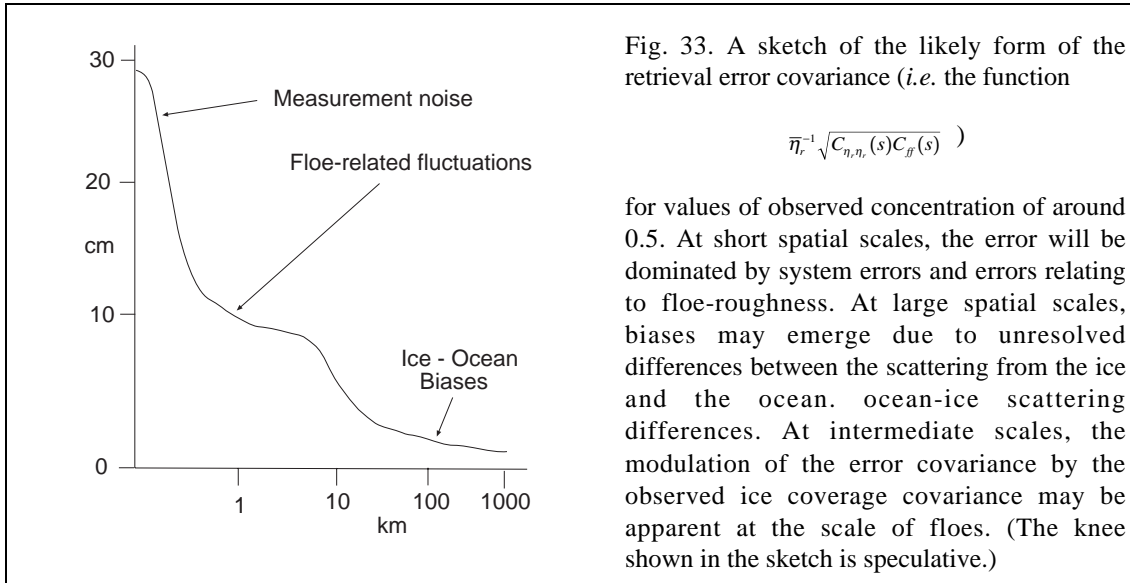
4.4.3 Validation of the retrieval error.

It has already been noted that there are no measurements that compare coincident satellite and ground observations of freeboard, and in distinction to the case of land ice there is little empirical experience that may illuminate the behaviour of retrieval error covariance $\bar{\eta}_r^{-2} C_{\eta_r, \eta_r}(s) C_{rr}(s)$. On the other hand, it is important to have some idea of this function to inform sampling strategies for its independent measurement. On the basis of the discussion of sections 4.4.2, a sketch of a likely form for this function is provided in Fig. 33.

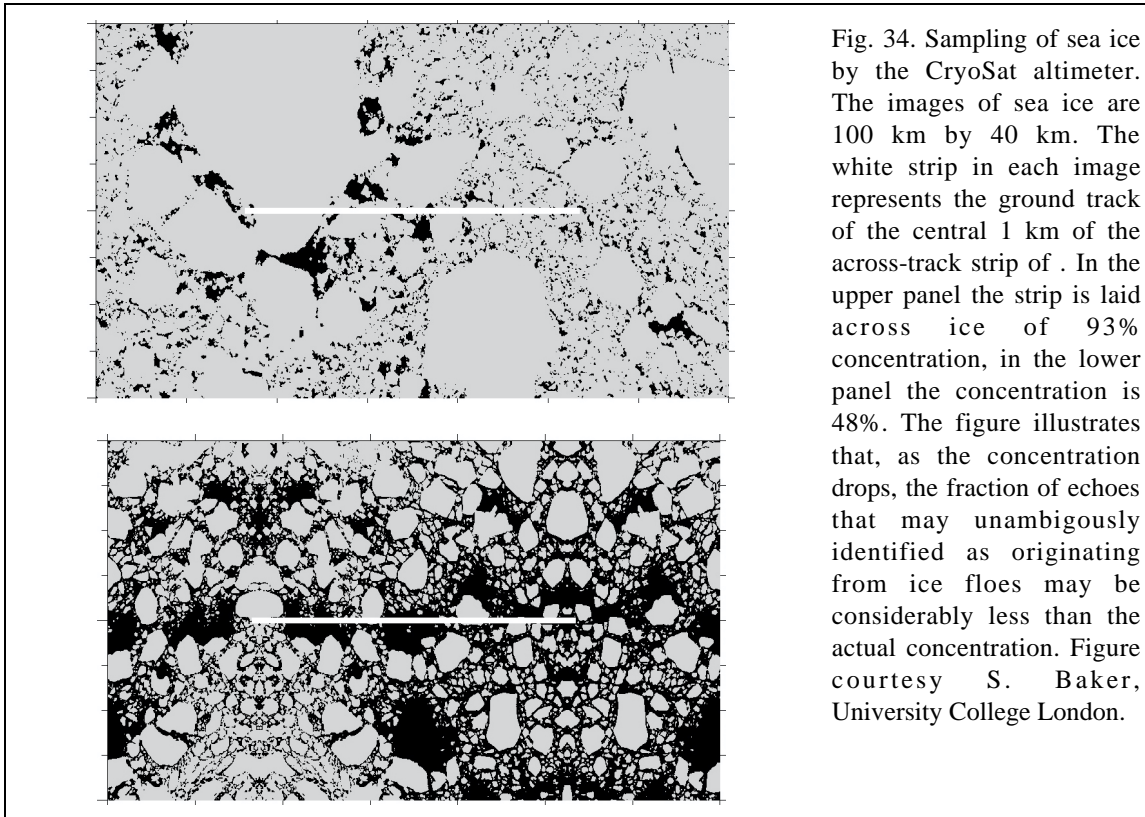
At the shortest scales, the error is likely to be dominated by the speckle contribution of the instrument system error (section 5.2.1) and the fluctuations introduced by uncertain floe roughness (section 4.4.2). These have, respectively, length scales of the instrument resolution and the floe roughness length. In practise, these are likely to be difficult to distinguish. The magnitude of this error depends on the detailed form of the retrieval algorithm; the figure of $\sim 30 \text{ cm}$ is a first guess at this value. At very large scales, there is evidence of biases as discussed in section 4.4.2. These appear to have values of around a few cm.

The covariance $C_{ff}(s)$ is modulated by the covariance function $C_{\eta_r, \eta_r}(s)$ in the total error covariance. The form of this function is also not well known, but it is reasonable to suppose that it will have a length scale that is loosely that of a ‘floe radius’, perhaps around 10 km. This is shown as a knee in the curve in Fig. 33, although it is to be emphasised that this speculative. It is also possible that when snow is present (the normal case), intermediate-

scale retrieval errors will arise from confusion between the air-snow and snow-ice interfaces.





An estimate of the retrieval error may be provided with measurements that are spatially and temporally co-incident with those of the satellite. In the absence of snow, direct measurement of freeboard and floe surface geometry is possible with laser altimetry, illustrated in Fig. 26. In planning such measurements, however, the likely form of the freeboard error covariance needs careful consideration. For averages over large areas, it is the longer-scale errors that are of greater importance. On the other hand, individual satellite measurements will be dominated by the short and intermediate scale error (as discussed generally in section 2.4). A sufficient number of observations is needed to illuminate the longer scale errors, which in turn implies a minimum length L of coincident observations. At its simplest, the satellite spatial resolution r_0 , a mean floe 'radius' f_0 and the apparent concentration $\bar{\eta}_r$, determine the length of track required on average: the effective number of samples of the short-scale error is $\bar{\eta}_r L / r_0$; the effective number of independent floes is $\bar{\eta}_r L / f_0$.



The second complexity connected with direct comparison with the satellite measurements is that the floes are moving. Generally the spatial distribution of the floes will translate with the mean ocean current, and in addition decorrelate as a result of the unsteady action of the wind, the ocean and other ice. Little information may be available on the motion of the ice. Floe drift speeds are ~ 3 cm/s to 30 cm/s, and the ice distribution will move a distance larger than the instrument resolution in ~ 15 minutes to ~ 2.5 hours. The time window available for measurements of any given satellite track is somewhat less than this.

When snow is present, the situation is more complicated for two reasons. First, an additional retrieval error may arise through air-snow and snow-ice confusion in the radar signal. (In this respect, the assumed independence in Eqn. 36 of the snow-loading and measurement error may over simplify the actual situation). Second, laser altimetry will not of itself be sufficient to determine the retrieval error. The laser measurements will determine the snow plus ice, rather than the ice, freeboard. At present, there is no remote instrument system that may address these problems.

		CryoSat Calibration & Validation Concept	Doc: CS-PL-UCL-SY-0004 Issue: 1 Date: 14 November 2001
--	---	---	--



In principle, to make direct comparisons with the satellite measurements on any significant length scale requires two simultaneous, remote measurements: the 13.8 GHz scattering cross-section as a function of depth, and the snow loading. However, it is possible that a great deal may be learnt by experiments that are not (necessarily) contemporary with the satellite and do not (necessarily) deal with the problems simultaneously.

Firstly, careful experiments that compare the scattering cross section with depth in conditions of known snow loading would be extremely useful – they could establish directly the extent to which the snow is responsible for backscattered energy in the echo. To achieve this, a wide bandwidth (2 GHz, for example) 13.8 GHz radar system is required. The bandwidth is important because the bandwidth of the satellite radar (320 MHz) is too small to resolve in echo delay time the difference between the air-snow and snow-ice interface. The carrier frequency is important because the scattering may be expected on general grounds to be a strong function of wavelength. In an airborne system, a laser altimeter would provide the location of the air-snow interface. Careful attention will be needed to cross calibrate in range the laser and radar echoes.

Second, in principle a separate problem, is the development of a system that may determine the snow load directly, or at least the snow thickness. (By the definition of section 3.1 snow load is a mass per unit area, not a thickness). Again, a very-high-bandwidth radar would appear to offer a solution. Such a system would need to maintain a small illuminated area on the floe (a few metres for example) or confusion will result between the echo from the variable topography of the snow-air interface and the echo from depth. It is of course entirely possible that the two problems could be solved with the same radar system, although an optimal ‘snow load’ radar may have carrier frequency different from 13.8 GHz. It is also worth noting the close similarity between the kind of instrumentation needed to understand these problems and those required for the land ice validation (see sections 3.2 and 3.4.3).

The situation that occurs when snow loading is present is important to understand, because a snow load will be the general case. There is no well-established solution at present. As observed in section 4.2, it is anyway important to determine the behaviour of departures of the snow-load from the climatology at short and intermediate scales.

The potential of the GLAS instrument on ICESAT (Zwally *et al.* 2001) for ice freeboard estimation has yet to be explored but a significant gain may be possible by combining the measurements from the two missions. In particular, independent estimates of the snow and ice thickness may eventually become possible. Combining GLAS and the ENVISAT RA-2

		CryoSat Calibration & Validation Concept	Doc: CS-PL-UCL-SY-0004 Issue: 1 Date: 14 November 2001
---	---	---	--

altimeter measurements will also provide valuable insights once these two missions are operational prior to the launch of CryoSat.

4.5 Preferential sampling of large floes.

In the development of the sea ice thickness error covariance in section 4.1 a term arose which resulted from the fact that the ice coverage seen by the radar will generally differ from the coverage as a whole. In practise, as is illustrated below, this arises because the radar may miss small floes. If the statistics of the sampled ice differs significantly from the ice as a whole, an error will result in the estimate of spatial average of the thickness. This section is concerned with the estimate of this error.

In general, the omission error that results from undersampling the ice cover is

$$\text{Eqn. 44} \quad \frac{1}{\bar{\eta}^2} \int_{Earth} dA W(\mathbf{s}) Cov \left[\left[\left(\frac{\eta}{\bar{\eta}} - \frac{\eta_r}{\bar{\eta}_r} \right) t_{ice} \right] (\mathbf{x}) \right]$$

(see Eqn. 36). In general this is a rather complicated object. To make it the subject of practical experimental investigation, it needs some simplification. First, one may distinguish in it two contributions: a contribution in the mean, and a fluctuation about the mean. This second fluctuation arises because, as a result of spatial fluctuations in thickness, the thickness averaged over the area covered by $\eta_r(\mathbf{x})$ will generally differ from that over $\eta(\mathbf{x})$. However, by assumption we take the observed area to be large enough that these fluctuations may be ignored (see, however, the comments on sampling density in the next section). This leaves the contribution in the mean, namely

$$\text{Eqn. 45} \quad \left(E \left\{ \int_A dA \frac{1}{A} \left(\frac{\eta(\mathbf{x})}{\bar{\eta}} - \frac{\eta_r(\mathbf{x})}{\bar{\eta}_r} \right) t_{ice}(\mathbf{x}) \right\} \right)^2$$

If the ice thickness fluctuation is independent of the way the radar selects the observed area, one would not expect an error to result from the reduction in the observed region from $\eta(\mathbf{x})$ to $\eta_r(\mathbf{x})$ because the average properties of the ice in the region $\eta_r(\mathbf{x})$ will be the same as those of $\eta(\mathbf{x})$. In fact, treating the thickness as a stationary random variable, one has

$$\text{Eqn. 46} \quad \left(E \left\{ \int_A dA \frac{1}{A} \left(\frac{\eta(\mathbf{x})}{\bar{\eta}} - \frac{\eta_r(\mathbf{x})}{\bar{\eta}_r} \right) t_{ice}(\mathbf{x}) \right\} \right)^2 = (E \{ t_{ice}(\mathbf{x}) \})^2 \left(E \left\{ \int_A dA \frac{1}{A} \left(\frac{\eta(\mathbf{x})}{\bar{\eta}} - \frac{\eta_r(\mathbf{x})}{\bar{\eta}_r} \right) \right\} \right)^2 = 0$$

when the thickness is an independent variable, in keeping with this argument. (The result follows because the integral in the second expression is zero by definition.) The error will only arise if the statistics of the thickness are correlated with those of the coverage.

Physically, $\eta_r(\mathbf{x})$ differs $\eta(\mathbf{x})$ from because the radar has a finite resolution. Small floes will be ignored by the radar – as illustrated in Fig. 34 and again in Fig. 35. If the small floes have a distinctly different thickness distribution than the larger floes observed by the radar, an omission error will result.

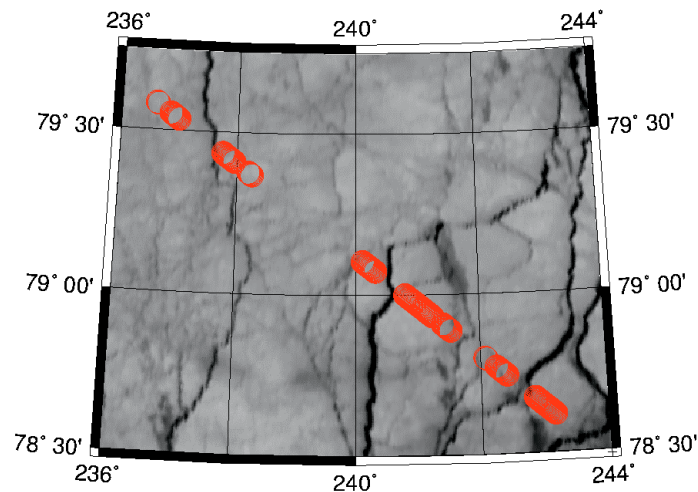




Fig. 35. The figure shows a thermal ATSR image of large ice floes in the Fram Strait (77°N), with the location of detections of ice floes by coincident ERS radar altimetry. The red rings are drawn to the scale of the radar resolution, and it can be seen that only the large floes are detected. The CryoSat radar resolution is a ten-fold improvement; nonetheless, small floes will be missed. Figure courtesy S. Laxon, University College London.

There appears to be very little information in the literature that examines the joint statistics of floe thickness and area. For this error to be estimated, some experiments will need to be done. The problem has, essentially, two components: what is the joint probability function of ice thickness and floe area, and what is the probability of a floe of a given area resulting in an unambiguous measurement of ice thickness. The first of these requires a comparison of the thickness, measured for example by laser altimetry (section 4.4.3) or electromagnetic sounding (sections 4.3 and 4.6), co-located with imagery of some kind; the second by superimposing the successful detections made from the satellite with coincident imagery. This second step is illustrated in Fig. 35.

		CryoSat Calibration & Validation Concept	Doc: CS-PL-UCL-SY-0004 Issue: 1 Date: 14 November 2001
--	---	---	--

As Fig. 34 implies, it is likely that the omission error may be a function of ice concentration. It is also to be noted that this kind of experiment may also supply information on the ice thickness covariance itself. This is of importance to the validation of ice thickness measurements described in the next section.

4.6 Validation of thickness measurements

In the previous sections, the contributions to the total thickness error covariance have been considered separately. The alternative approach is to validate the thickness measurements directly. In the main, the methods for doing this do not use platforms that meet the sampling requirements discussed in section 4.4.3 for direct comparison with the satellite measurements. The alternative approach is to compare spatial and temporal averages of the satellite and ground measurements. In this section, we assume this is the approach that will be taken. In making the comparison this way, it should be appreciated that all of the errors in the satellite measurements will be present (Fig. 2 provides a quick summary). An understanding of the satellite thickness error covariance as a whole, that of the ground observations, *and* that of the ice thickness itself (see Wadhams 2000, p. 157), is generally needed in order to draw conclusions from the comparison.

The most useful source of data to date for the validation of satellite ice thickness measurements have been provided by upward looking sonar (ULS) instruments mounted on submarines (see *e.g.* Rothrock *et al.* 1999, Tucker *et al.* 2001, Wadhams & Davis 2000, Wadhams 2000, p 158). These provide estimates of ice draft over wide areas and on time-scales of one or two months. The conversion of draft to thickness uses the same principle of hydrostatic equilibrium as that used to convert freeboard (Eqn. 33) and is subject to errors from snow-loading and density in similar fashion. The similarity of the density of water and ice means, however, that the error arising from these sources is considerably smaller. There are also corrections required for the velocity of sound in sea-water that are analogous to the refraction correction of altimetry (section 4.4.1). In general, however, point observations from ULS are expected to be considerably more accurate than those of the satellite. Measurements of thickness from boreholes may also be used for comparison.

Comparisons of measurements of thickness from satellite and ULS are shown in Fig. 36 and Fig. 37.

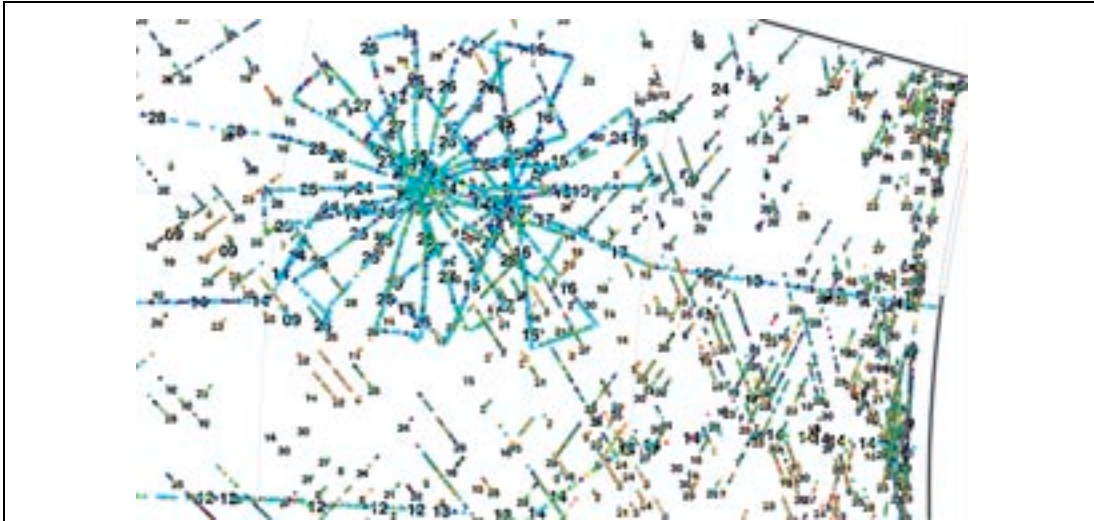
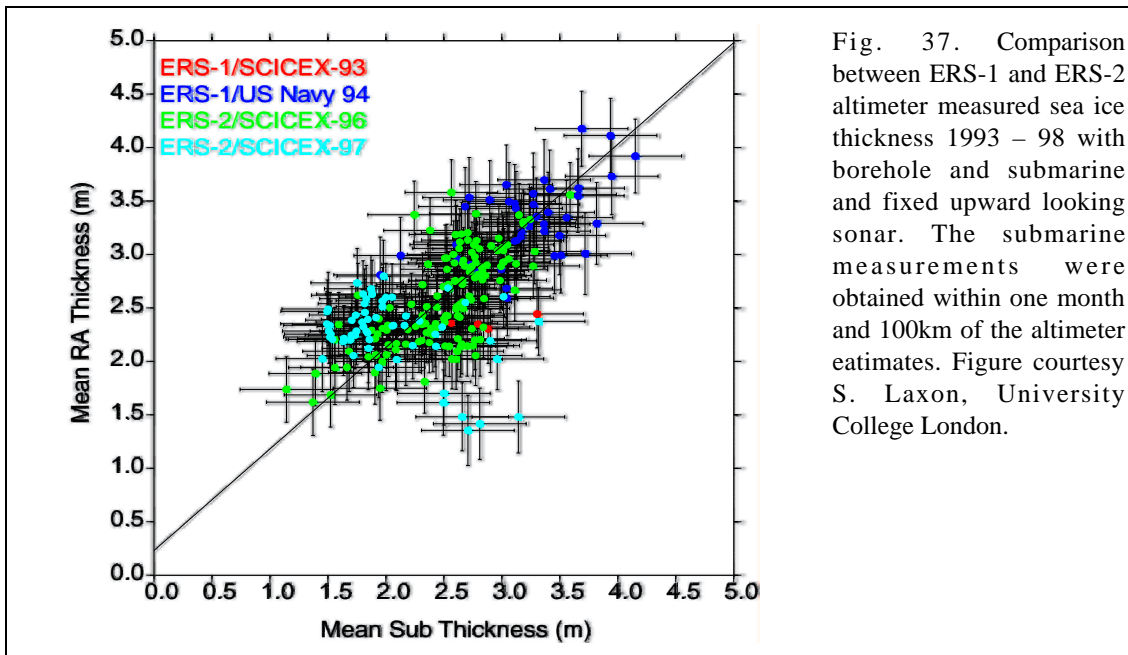


Fig. 36. A comparison of ERS-2 and submarine estimates of sea ice thickness during October 1996 in the Beaufort Sea. The submarine data are represented by triangles; the ERS data by smaller circles. (The satellite data lies on the straight lines of the ascending and descending satellite tracks; the submarine data on the 'rose' and more wavy lines). The area shown in the figure is approximately 400 km across. Figure courtesy Dr. Seymour Laxon, University College London.

Important as these ULS measurements are, the sampling density they provide is, nonetheless, sparse. An illustration of the sampling situation in practise is shown in Fig. 36. In this situation it is not longer possible to ignore the quadrature error that results when spatial averages of the ice thickness are compared. This error will depend on the spatial scale of the fluctuation of ice thickness itself. In the case shown in Fig. 36 for example it is clear that if the ice thickness has a scale of variation somewhat larger than the sampling 'rose' of the submarine, the spatial average obtained from it will be biased in comparison with that of the altimeter.

While it is beyond the scope of this document to provide a more quantitative discussion of this error, it is perhaps worth remarking that a quadrature error is a form of omission error. Theoretically it can be dealt with a similar framework to that used to deal with the preferential sampling error discussed in section 4.5. In any practical situation, estimating the error invariably needs Monte-Carlo methods because the irregularity of the sampling precludes much in the way of analytic simplification. It is also worth observing that the absence of this kind of calculation bedevils attempts to determine long term trends in sea ice thickness from sparse submarine observations.



Another illustration of the complexity of directly comparing thickness estimates is illustrated in Fig. 37. This shows a point-wise comparison of ERS altimeter and ULS observations. The regression line has a gradient that is very close to unity, and a bias (intercept) is also present that is similar in magnitude to the bias apparent in Fig. 32. In making this comparison, point data have been compared that are within 50 km and 1 month of each other. Before one can interpret the degree to which scatter in the plot is the result of the error in the satellite observations, one has first to account for the expected variability resulting from the displacement in time and space of the samples. This again requires an estimate of the covariance function of the thickness itself. In fact (Laxon, personal communication) the scatter in the plot can be accounted for by the combination of this variability and the short-scale instrument system error described in section 5.

These results illustrate that other methods that may increase the areal coverage of thickness measurements would be extremely useful. For this reason, estimates of ice thickness through electromagnetic sounding (Fig. 26) may be of considerable importance (Haas & Eiken 2001). These measurements may be made from helicopter platforms operating from ships. While meeting the sampling requirements for direct comparison with the satellite data may be difficult (although of great value if possible), a great deal may also be achieved using this technique to provide dense observations of thickness over (say) 10^6 km² and 1 month. An important new platform that may be of considerable use to the CryoSat validation is the autonomous underwater vehicle (AUV). Trials of the UK AUV ‘Autosub’

are presently underway (see, for example, the description of <http://www.soc.soton.ac.uk/SOES/MSC/OC/CEO/aii/aii.html>).

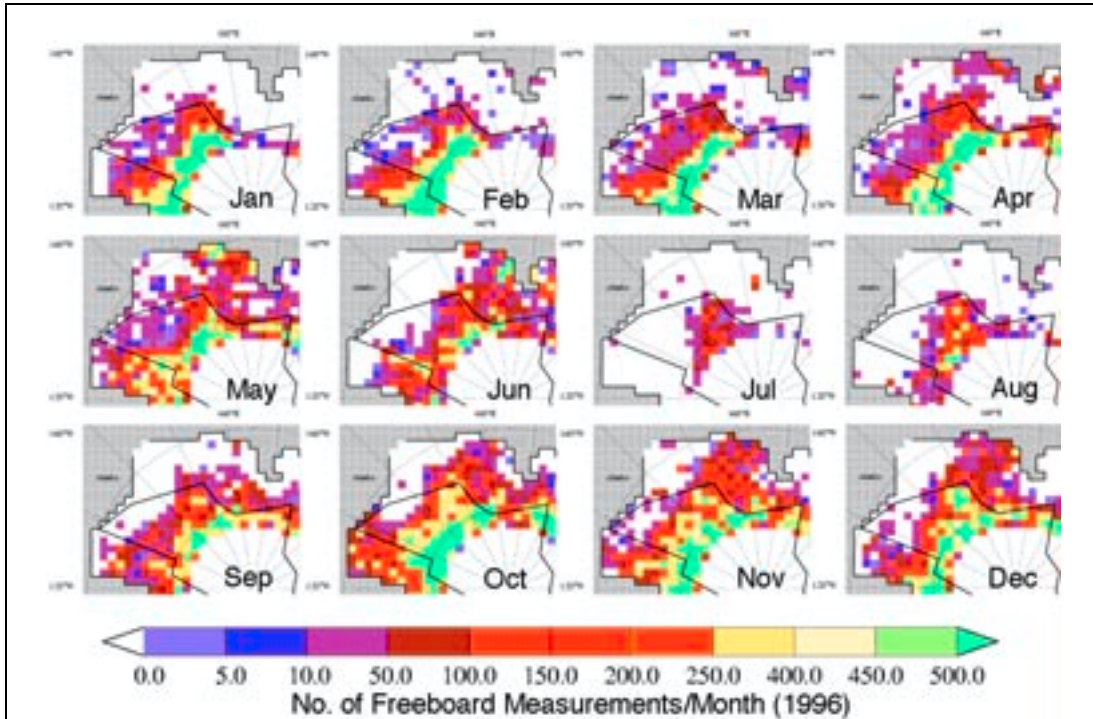




Fig. 38. Sampling density of ERS radar altimeter measurements of sea ice during 1996. The highest density of measurements occurs during the winter months and close to the latitudinal limit. Figure courtesy S. Laxon, University College London.

Under sampling may also effect the satellite observations. Fig. 38 shows the sampling density of successful ice detections obtained using the ERS altimeters. CryoSat has greatly improved resolution, and has an orbit more suited to sampling the polar regions that that of ERS. An objective of the mission is to improve on this sampling pattern. On the other hand, the actual sampling density will only be determined post-launch. This figure emphasises the importance of understanding better the space-time covariance of ice thickness itself. It also suggests that, if resources are limited, it may be better to plan campaigns in regions of high ice concentration, and at higher latitudes which have a higher spatial sampling density.

		CryoSat Calibration & Validation Concept	Doc: CS-PL-UCL-SY-0004 Issue: 1 Date: 14 November 2001
--	---	---	--



4.7 Timing and geographical emphasis of the sea ice validation experiments.

A summary of the proposed approaches to the verification of the sea ice measurements is given in Fig. 2. As was the case for land ice validation experiments, the point worth emphasising is that many useful experiments may be done independently of the satellite observations. These experiments need not be tied to the period or specific track location of the satellite, although clearly this may increase their usefulness in some cases.

With regard to the time of year, it is obviously desirable to investigate the error at any time of year. The interannual variability is important. On the other hand, as observed in section 2.4, this may only be examined by repeated measurements at the same time of year. If resources are limited, it would be sensible to concentrate on the times at which the maximum and minimum of the snow loading occur: late spring just prior to the onset of melt, and early autumn, just following the onset of freeze up.

The selection of ship cruise locations are subject to strong resource limitations which make any one cruise the subject of a compromise between a wide range of scientific experiments. A similar situation exists in the case of submarines. While dedicated submarine cruises are unlikely, submarines continue to collect ice draft observations. The opportunity to make measurements should be exploited wherever possible. For a ship equipped with helicopters, direct comparison with the satellite observations may be possible. Even if this is not the case ship-borne measurements (whether by boreholes, autonomous submersibles or by electromagnetic methods) of thickness and density over a region of order 10^6 km^2 and an interval of 1 month may be extremely valuable to investigate intermediate scale errors. Moored ULS deployments (such as those presently operating in Fram Strait) that are contemporary with the mission may be particularly useful in validating estimates of the seasonal cycle, and the effects of seasonally varying errors.



At present, the sparseness of independent observations of sea ice thickness provides little basis to suggest a geographical distribution in the error in the measured thickness. This is in contrast to the case of the land ice, where historical measurements and independent validation of the ERS altimeter measurements (section 3) provide a basis for the geographical focus of experiments. This means that in the case of sea ice there are not strong arguments based on the behaviour of the errors for selecting a particular region. Careful experiments in any region of the Arctic containing multi-year ice will be of considerable value.

		CryoSat Calibration & Validation Concept	Doc: CS-PL-UCL-SY-0004 Issue: 1 Date: 14 November 2001
--	---	---	--

On the other hand, the experience of ERS suggests that sampling will degrade at lower latitudes and at low ice concentrations. If resources are limited it would be better to concentrate them at higher latitudes.

One may also suppose that the errors may vary with ice concentration. Strong east-west spatial gradients in ice concentration occur in the Arctic Ocean north Greenland, varying from essentially free-drift conditions in the Fram Strait to high concentration, thick ice north and west of Greenland. For aircraft experiments, which can access scales of 1000 km, this is a sensible region to conduct experiments. As noted in section 4.4.3, this may also allow essentially the same payload to perform sea- and land-ice validation experiments in the same campaign, and it also permits relatively easier winter operations.

Finally, although CryoSat is principally aimed at the measurement of multi-year, Arctic ice thickness, observations will be collected over Antarctic sea-ice. It is not clear that the measurement technique will work over the seasonal Antarctic sea ice cover, the majority of which is meteoric in origin. Nonetheless, the Weddell Sea in particular contains multi-year ice. Validation measurements in the Weddell Sea, from ship or aircraft platforms may be very valuable, particularly if they fall outside the melt season.

		CryoSat Calibration & Validation Concept	Doc: CS-PL-UCL-SY-0004 Issue: 1 Date: 14 November 2001
--	---	---	--

5 Calibration of the satellite measurements.

5.1 Objective and general character of calibration. *Instrument systems errors as they appear in the level 1b data: Timing, angle, orbit and datation errors. Characteristic behaviour along track. Temporal correlation function: short-scale errors, orbit period errors; drift errors. The effect of system errors on the spatial covariance functions. The complexity of orbit errors and the need to simulate them. Distinct behaviours of the system errors in the land ice and sea ice cases.*

5.2 Source and scales of fluctuation of instrument system errors. *Relationship of errors in level 1b data to hardware imperfections.*

5.2.1 The error in echo delay timing ϵ_i . *Clock errors. RF path length errors. Signal distortions. IF filter errors. Speckle errors.*

5.2.2 The error in echo direction ϵ_θ . *RF path length differences. IF filter differences. Speckle errors. Baseline length error. Baseline orientation error. Attitude errors.*

5.2.3 The error in radial component of the orbit ϵ_z . *Measurement and forcing errors. Potential important of tidal forcing errors.*



5.2.4 The along-track position error ϵ_x . *Position and datation errors. Transmission timing. Need to foresee datation correction.*

5.3 Internal and external calibration. *Internal and external calibration paths. Internal calibration modes. Frequency of internal calibrations. External calibration modes and experiments. Frequency of measurements. Laser observations. Advantages and limitations of transponder experiments. Cross-calibration with ENVISAT and JASON altimeter missions.*

5.1 Objective and general character of calibration.

In line the general approach of section 2.2, sections 3.4 and 4.4 divided the task of determining the land ice and sea ice measurement error covariance into a contribution of the elevation retrieval and a contribution of the instrument system. The instrument system contributions were described respectively by the covariance functions Γ_{ss} and C_{ss} in the case of land ice and sea ice respectively. In general terms, the objective of instrument system calibration is to estimate these covariance functions. As noted in section 2.4, the instrument system errors differ from the retrieval and other errors in that they do not need to be determined *in-situ*. It is true that the manner in which they separately manifest themselves over sea ice and land is dependent on the retrieval algorithms and on the way that local and larger scale averages are formed, but this may be calculated once the instrument system errors themselves have been estimated or measured.

The contributions to the instrument system error as they appear in the level 1b data in the case of the land ice were introduced in section 3.4.1 (Eqn. 28 and Eqn. 29), and may be collected into the form

		CryoSat Calibration & Validation Concept	Doc: CS-PL-UCL-SY-0004 Issue: 1 Date: 14 November 2001
---	---	---	--

$$\text{Eqn. 47} \quad \epsilon_s(\mathbf{x}, t) = c \epsilon_i(\mathbf{x}, t) / 2 + c \tau_r \epsilon_\theta^2(\mathbf{x}, t) / 4 + \epsilon_z(\mathbf{x}, t) + \gamma \epsilon_x(\mathbf{x}, t)$$

where ϵ_i is the instrument contribution to the echo delay-time error, ϵ_θ the error in the angle of approach of the echo, ϵ_z the error in the radial component of the satellite position – the ‘orbit’ error, and ϵ_x the error in position arising from an error in t – the ‘datation’ error. In the case of sea ice, the corresponding instrument system error, introduced in section 4.4.1 (Eqn. 40 and Eqn. 41), may be collected as

$$\text{Eqn. 48} \quad \epsilon_s(\mathbf{x}, t) = c(\epsilon_i^{(ice)}(\mathbf{x}, t) - \tilde{\epsilon}_i^{(lead)}(\mathbf{x}, t)) / 2 + \epsilon_z(\mathbf{x}, t) - \tilde{\epsilon}_z(\mathbf{x}, t)$$

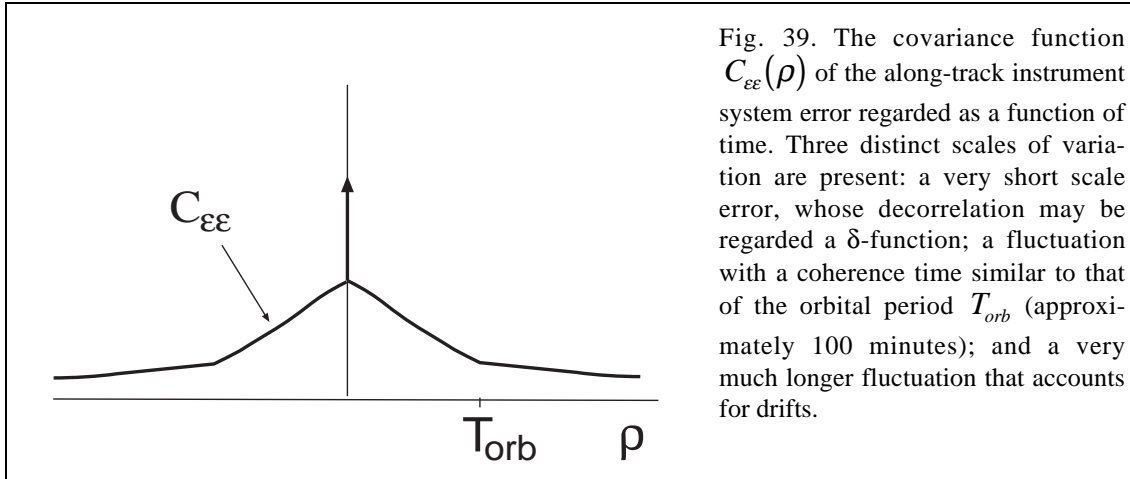
This has no contribution from the angle of approach, and the datation error is likely to be negligible (as far as determining ice freeboard is concerned). On the other hand, the timing and orbit error appear twice, with a contribution ϵ from an ice elevation and $\tilde{\epsilon}$ from a smoothed ocean elevation.

To establish a calibration concept, these errors, which are described as they appear in the level Ib data, need to be related to their actual source in the instrument hardware (or related software). This is done in the next section. The system errors do, however, have general timescales of fluctuation that largely determine their contribution to the covariance functions Γ_{ss} and C_{ss} and it is useful to describe at these outset. Firstly, as noted in section 3.4.1, the location of the satellite is determined by its orbit and the ellipsoidal location \mathbf{x} may be parameterised in terms of time as $\mathbf{x}(t)$. This is true too of the instrument system errors, and it is common to consider the instrument system errors as functions of time in the same way. The fluctuations of the error as the satellite passes along its orbit are then characterised by the temporal covariance of this error (see *e.g.* Chelton *et al.* 1993). By assumption, this error may be regarded as stationary, so that

$$\text{Eqn. 49} \quad E\{\epsilon_s(\mathbf{x}(t)) \epsilon_s(\mathbf{x}(t + \rho))\} \equiv C_{\epsilon\epsilon}(\rho)$$

In general, this covariance function has the structure illustrated in Fig. 39. There are three scales of variation. The shortest scale, illustrated as a δ -function in the figure, arise from errors that completely decorrelate from observation to observation. Their source is noise in the sensors. These errors are not measured or estimated by the instrument system. Instead, the sensors are designed to achieve a level of noise performance that the measurement goals require. The second scale, which decorrelates on timescales similar to that of the orbit period, arise either from the orbit error itself, or mechanical or electronic fluctuations that are driven mainly by the solar illumination, which varies most strongly on orbit period. The satellite is equipped with some capability to monitor and correct for these errors. Finally, there are errors that vary on long timescales – drifts – which are due to, for example, ageing



effects. The timescales involved here could range over months or years. The satellite also has some capability to monitor and correct for drifts.



The way these errors effect the land ice instrument error covariance Γ_{ss} depends on their scale of variation. The contribution of the point-to-point independent errors to the variability of a local spatial and temporal average (Eqn. 4) is simply their point variability divided by the number of observations; in larger area averages, their contribution to the local averages may also be regarded as independent one from another. These errors usually dominate the local area averages, as is clearly seen in the measured covariance of Fig. 5.

The contribution of errors with orbital frequencies can be quite subtle: while on the one hand their duration is short (~ 1 hour), their spatial scale is large, usually far larger than the area over which the average is formed. On the other hand, it is not difficult to compute an estimate of the effect of orbit errors in any given situation; again Fig. 5. provides a particular illustration. In that case, the orbit error was estimated by calculating the covariance function of two, independently calculated orbits. At much longer time-scales, the situation simplifies again because the spatial averaging has little effect on these errors (*cf* eqn. Eqn. 12), and the drifts map more or less directly into the spatially averaged trend.

As with the tidal and other retrieval errors discussed in section 4.4.2, the manner in which system errors effect the covariance function C_{ss} depends a good deal on how the ocean observations are averaged in Eqn. . As noted in section 4.4.2, the one extreme is to form an estimate from all of the ocean observations of the mean sea surface, and to determine the ice freeboard as an anomaly from this sea surface. In this case, the retrieval error (Eqn. 48) from this source is, essentially, that from the ice elevation measurement, that is

		CryoSat Calibration & Validation Concept	Doc: CS-PL-UCL-SY-0004 Issue: 1 Date: 14 November 2001
---	---	---	--

$$\text{Eqn. 50} \quad \epsilon_s(\mathbf{x}, t) \sim c \epsilon_i^{(ice)}(\mathbf{x}, t) / 2 + \epsilon_z(\mathbf{x}, t)$$

As was the case with the land ice, the short-scale contribution to the variance of a spatial average simply reduces as the number of observation and is independent from average-to-average; the effect of orbit errors will generally be complex and require simulation, while the drift errors will be more-or-less unaffected by the averaging.

The other extreme case is to extrapolate the ocean surface along the satellite track, forming an ‘instantaneous’ estimate of the mean sea surface. In this case, because the orbital scale errors and drifts have length scales larger than that of the floes, these errors largely cancel in Eqn. 48 and the instrument system error is dominated by the short-scale, rapidly-decorrelated error, that is

$$\text{Eqn. 51} \quad \epsilon_s(\mathbf{x}, t) \sim c(\epsilon_i^{(ice)}(\mathbf{x}, t) - \tilde{\epsilon}_i^{(lead)}(\mathbf{x}, t)) / 2$$



In a spatial average, the first term $\tilde{\epsilon}_i^{(ice)}$ will reduce as the number of observations. If the area of a spatial average is large compared with that used to estimate the sea surface elevation, this will be true too of the term $\tilde{\epsilon}_i^{(lead)}$, which may be appreciable in this case.

5.2 Source and scales of fluctuation of instrument system errors.

The description of the instrument system errors above are in terms of how these errors appear in the parameters of the level *1b* data. Their source, however, lies in the instrument hardware, and a complete error analysis would provide a description of how imperfections in the hardware system map into the data parameters. Such a description is beyond the scope of this concept document; in detail it is a complicated matter. Nonetheless, it is useful to have at least a qualitative description of how the errors in the data arise in the hardware, and how this leads to the calibration concept. A fuller description of the hardware may be found in the MDD.

5.2.1 The error in echo delay timing ϵ_i .

There are a number of sources of the error in echo delay timing. These are the error in the clock that measures the timing, errors in the path length of the radio-frequency (RF) sections of the instrument and errors that arise due to distortions in the shape of the echo. On CryoSat the first two of these are expected to be small. Clock errors in altimetry typically arise from drifts in the oscillators used to generate the clock pulses that time the echo flight. CryoSat uses the DORIS system for orbit reconstruction, which makes the comparison of the on-board timing of the echo with an absolute time (TAI) a relatively

		CryoSat Calibration & Validation Concept	Doc: CS-PL-UCL-SY-0004 Issue: 1 Date: 14 November 2001
--	---	---	--

simple matter. Time-of-flight errors from this source are expected to be negligible. Barring mistakes, the absolute length of the RF sections is well-determined pre-launch, and its variation is expected to be negligible. This is particularly true on CryoSat, where the demands of interferometry have led to thermally stable waveguides especially constructed from carbon fibre.



On the other hand, variations in shape of the echo will lead directly to variations in echo timing because, as explained in sections 3.4.1 and 4.4.1, the timing of the echo is determined in detail from its shape. Because the precision demanded of the measurement is very small, and in particular very much smaller than the instrument resolution, very subtle variations in echo shape can give rise to apparent changes in measured time-of-flight. In detail, there are many instrument sources of such an error. Two in particular are important.

Firstly, all radar echoes suffer from a signal distortion termed ‘speckle’. This fluctuation arises because the echoes are the incoherent summation of many small, randomly phased echoes from small scattering regions of the surface. In consequence the echo power of an individual echo is exponentially distributed. The main purpose of multi-looking is to reduce this fluctuation through summing statistically independent ‘looks’ at any given surface location. Nonetheless a fluctuation remains – it can be clearly seen in the echoes seen in Fig. 12 and Fig. 29. This fluctuation is minimised by instrument design; it is nonetheless the largest single source of error in a point measurement. On the other hand, by design, speckle errors decorrelate completely from observation to observation; they are δ -correlated errors in this sense.

The second source of signal distortion that is important arises from the intermediate-frequency (IF) sections of the instrument. These contain signal filters that precede the digitisation of the signals. The response of these filters may vary with temperature and with age, giving rise to timing errors that may occur at orbital frequencies or longer-term drifts.

5.2.2 The error in echo direction ϵ_{θ} .

Errors in the echo direction arise through errors in the interferometer phase difference, errors in the interferometer baseline and errors in baseline orientation. Errors in the interferometer phase difference has some similarity to that of timing, in that their source lies in the RF path length, the IF filter responses and the echo speckle, except that it is the difference in these effects between the two interferometer receivers that is important. The CryoSat SIRAL radar is carefully designed to minimise RF pathlength differences (see the MDD) and it is expected that variations from this source will be small.

		CryoSat Calibration & Validation Concept	Doc: CS-PL-UCL-SY-0004 Issue: 1 Date: 14 November 2001
--	---	---	--

On the other hand, as with all interferometers, radar speckle will cause a phase noise on the interferometer measurement. In fact, the design is such as to make this contribution small in comparison with the timing error arising from the speckle. In any event, it is δ -correlated, and will be independent from point measurement to point measurement. On the other hand, phase differences arising from differences in the two IF sections of the receivers may give rise to fluctuations at orbit and drift time-scales.



Errors in the baseline length are also expected to be negligible by design. The baseline orientation is measured by star-trackers that are attached to the rigid carbon fibre bench. These may be expected to introduce some δ -correlated attitude noise, and it is at least possible that ageing effects may occur that gives rise to drift errors in the measured attitude.

5.2.3 The error in radial component of the orbit ϵ_z .

The orbit of CryoSat will be determined from the measurements of the DORIS RF tracking system. These measurements are combined with models of the forcing of the satellite to calculate the best estimate of the location of the satellite. In detail this procedure is complicated. Because of its general importance, a considerable literature exists on the subject of its errors (see, for example, Scharroo & Visser 1998). For our purposes, here, however, the most important feature of orbit errors is that they are dominated by fluctuations near the orbital period; they do not have a short-scale component. On the other hand, it is possible that longer time-scale errors will arise, and these may have equally to do with uncertainties in the position of the Earth-fixed reference frame in which the DORIS measurements are made than the orbit itself. It is worth noting here that experience is limited of the orbit error of very high inclination, long repeat satellites such as CryoSat. Some forcing terms, such as the tidal forcing of the satellite, may need closer attention when account is taken of the effect of aliasing in the spatial averaging of the data. The matter deserves closer study. It is also worth noting that, even for a given satellite, the orbit error often improves with time as the force modelling of the satellite improves.

5.2.4 The along-track position error ϵ_x .

As has been noted previously in section 3.4.1, the along-track position error arises through orbit errors (*i.e.* errors in \mathbf{x} for known t) and through errors in the timing of the echo transmissions (*i.e.* errors in $\mathbf{x}(t)$ arising from errors in t). The datation is performed by marking the data, in some fashion, with an on-board clock that gives the time of transmission, and then registering the on-board clock with an absolute time reference. In

		CryoSat Calibration & Validation Concept	Doc: CS-PL-UCL-SY-0004 Issue: 1 Date: 14 November 2001
--	---	---	--

principal, datation errors on altimeters should be negligible by design. With CryoSat, which has absolute TAI available to the spacecraft through the DORIS system, this should be the case. Nonetheless it is a fact that in many altimeter mission datation errors are known to occur. They can be important, because as Eqn. 47 implies, elevation errors occur in proportion to the local surface gradient. They tend to be static offsets, and therefore of less importance to the measurement of trends. Nonetheless, they should be minimised as a matter of good practice.

5.3 Internal and External Calibration.

The satellite system is provided with a number of ancillary measurement modes and equipment whose purpose is to provide an independent measurement of the system errors. In some cases, these also provide on-going measurements that are then used to make corrections to the raw data. These measurements separate into two approaches, depending on which part of the instrument system is being investigated. The radar contains a calibration path (see MDD 2001) which injects the transmitted signal directly into the receiver chain immediately downstream of the antenna. All instrument time and phase paths within this internal loop may be measured in this way – so-called ‘internal’ calibration modes. On the other hand, an important element of the radar system cannot be measured this way - the antennas. In addition, it is not possible from internal measurements to establish the error in position and attitude with respect to an Earth-fixed reference frame. Both these system elements require an externally generated signal incident on the antenna – so-called ‘external calibration’.

A summary of the breakdown of internal and external calibration requirements is given in Table 1. Also included are those elements that will be the subject of pre-launch measurements and characterisation. In general, pre-launch measurements will determine absolute offsets (*e.g.* that between the nominal and actual star tracker axes). Internal calibration measurements are instructed under ground command. These can therefore sample a wide range of time scales. Typically, a high temporal density of internal calibrations is used early in the mission to establish the behaviour on, for example, orbital timescales, and a lower number is used thereafter.

A summary of the planned approach to external calibration is given in Table 2. These may be divided, from a temporal sampling point-of-view, into two cases. External calibration of the echo direction will be performed using a specific measurement mode over the ocean surface. So long as the satellite is over the ocean, this measurement mode can be instructed from ground command. Like internal calibration, it too can span a wide range of timescales.



Table 1. Internal and External Calibration of Level 1b Data.			
Error	Pre-launch testing	Internal Calibration	External Calibration
Echo timing	Yes.	Yes.	No.
Echo Datation	No	No	Yes
Satellite Altitude	No	No	Yes
Total Echo Power	Yes	In part	Yes
Echo Shape	Yes	Yes	No
Baseline Vector	In part	No	Yes
Interferometer Phase	In part	In part	Yes

Note that it will not be possible to separately calibrate the baseline attitude and the interferometer phase error, but only the combined effect of these on the echo direction measurement.

The ‘calibration’ of the satellite altitude is performed through laser retro-reflector measurements. These depend to some extent on the availability of the laser measurements. At the time of writing, this is not well established. The term ‘calibration’ is put in inverted commas because there is an inevitable tendency to use the laser measurements within the orbit computation once they become available. Nonetheless, they do provide an accurate and independent check on the point variability of the orbit deduced from the RF DORIS measurement system.

Finally, there are measurements that require transponders. (In principle these could use corner reflectors, but simple calculations suggest these will not generate sufficiently powerful reflections.) These cannot provide such dense temporal sampling, because the satellite must overfly the transponder locations. It is expected that such measurements will be performed in the validation phase. Transponder measurements also offer a very effective way of checking out the lower level processing of the data such as, for example, the directional accuracy of individual beams prior to multi-looking.





Table 2. External calibration approach and estimated magnitudes.

Error	Technical Approach	Mission Variability Requirement	Mission Bias Requirement*
Echo datation	Transponder	2 m	None
Satellite Altitude	Laser Retroreflector	3 cm	0.17 cm/yr
Total Echo Power	Transponder	3 dB	0.05 dB/yr
Baseline Vector	Ocean surface	10''	None
Interferometer Phase	Transponder	6°	None

*None = No specification on this parameter in system design requirements.



Taken together, this set of measurements can build up a good picture of the residual (*i.e.* after correction) along-track temporal behaviour of the errors. Nonetheless, because the measurements of interest are formed from spatial averages of many individual data, the accuracy required of the instrument system is difficult to calibrate by this set of measurements. To illustrate the point, individual laser measurements may be accurate to a few cm. From a set of such measurements it may be difficult to establish whether there is a slow, small drift of a few mm each year. Such drifts could also arise from trends in the atmospheric corrections, particularly the wet troposphere correction, which will depend on forecast models.

Drifts of this kind are more-or-less impossible to observe directly. However, CryoSat will be contemporary to the ENVISAT and Jason altimeter missions, and will make pulse-limited observations of the world's oceans. Jason in particular is expected to provide highly precise measurements of the elevation of the Southern Ocean. Crossover comparisons between the CryoSat ocean measurements and those of Jason and ENVISAT are of particular importance in identifying slow drifts in the instrument system.



		CryoSat Calibration & Validation Concept	Doc: CS-PL-UCL-SY-0004 Issue: 1 Date: 14 November 2001
--	---	---	--

6 References.



- Arthern, R.J. & D.J. Wingham, 1998, 'The natural fluctuations of firn densification and their effect on the geodetic determination of ice sheet mass balance', *Climatic Change*, **40**, 605-624.
- Arthern, R.J., D.J. Wingham & A.J. Ridout, 2001, 'Controls on ERS altimeter measurements over ice sheets: footprint-scale topography, backscatter fluctuations, and the dependence of microwave penetration depth upon satellite orientation', *J. Geophys. Res.*, in press.
- Bamber, J.L, 1994, 'Ice sheet altimeter processing scheme', *Int. J. Remote Sensing*, **15**, 925 – 938.
- Beaven, S. G., G. L. Lockhart, S. P. Gogineni, A. R. Hosseinmostafa, K. Jezek, A. J. Gow, D. K. Perovich, A. K. Fung & S. Tjuatja, 1995, 'Laboratory measurements of radar backscatter from bare and snow-covered saline ice sheets', *Int. J. Remote Sensing*, **16**(5), 851-876.
- Bentley, C.R., and J.M. Wahr, 1998, 'Satellite gravity and mass balance of the Antarctic ice sheet', *J. Glaciology*, **44**, 207-213.
- Braithwaite, R.J., 1994, 'Thoughts on monitoring the effects of the climate change on the surface elevation of the Greenland ice sheet', *Global and Planetary Change*, **9**, 251 – 261.
- Brenner, A.C., R.A. Bindschadler, R.H. Thomas, & H.J. Zwally, 1983, 'Slope-induced errors in radar altimetry over continental ice sheets', *J. Geophys. Res.*, **88**, 1617 – 1623.
- Brown, G.S., 1977, 'The average impulse response of a rough surface and its implications', *IEEE Trans. Antennas Propagation.*, **25**, 67 – 74.
- Chelton, D.B., & M.G. Schlax, 1993, Spectral characteristics of the time dependent orbit errors in altimeter height measurements, *J. Geophys. Res.*, **98**, 12579 – 12600.
- Davis, C.H., 1995, 'Growth of the Greenland Ice Sheet: a performance assessment of altimeter retracking algorithms', *IEEE Trans. Geoscience Remote Sensing*, **33**, 1108-1115.
- Davis, C.H., 1997, 'A robust threshold retracking algorithm for measuring ice sheet surface elevation changes from satellite radar altimeters', *IEEE Trans. Geoscience Remote Sensing*, **35**, 974 – 979.
- Drinkwater, M. R., 1991. 'Ku Band Airborne Radar Altimeter Observations of Marginal Sea Ice During the 1984 Marginal Ice Zone Experiment', *J. Geophys. Res.*, **96**(c3), 4555-4572.
- Eicken, H., M. Lensu, M. Lepparanta, W.B.Tucker III, A.J. Gow and O. Salmela, 1995 'Thickness, structure and properties of level summer multi-year ice in the Eurasian sector of the Arctic Ocean', *J. Geophys. Res.*, **100**, 22697-22710.

		CryoSat Calibration & Validation Concept	Doc: CS-PL-UCL-SY-0004 Issue: 1 Date: 14 November 2001
--	---	---	--

- Enomoto, H., 1991, 'Fluctuations of snow accumulation in the Antarctic and sea level pressure in the Southern Hemisphere in the last 100 years', *Climatic Change*, **18**, 67 - 87.
- Femenias, P., F. Remy, P. Raizonville & J-F Minster, 1993, Analysis of satellite altimeter height measurements above ice sheets', *J. Glaciology*, **133**, 591 – 600.
- Fetterer, F., M. Drinkwater, K. Jezek, S. Laxon, R. Onstott & L. Ulander, 1992, 'Altimeter backscatter microwave remote sensing of sea ice'. In *Microwave Remote Sensing of Sea Ice*, AGU Monograph Series, Vol. **68**, 111-132.
- Fu, L-L., & A. Cazenave (eds.), 'Satellite Altimetry and Earth Sciences: A Handbook of Techniques and Applications', Academic Press, 2001.
- Gorshkov, S.G., 1983, *World Ocean Atlas*, Vol. 3, Arctic Ocean, Pergamon, New York.
- Gundestrup, N.S., Bindschadler, R.A. & Zwally, H.Z., 1986, 'Seasat range measurements verified on a 3-D ice sheet', *Ann. Glaciology*, **8**, 69 – 72.
- Haardeng-Pedersen, G., K. Keller, C.C. Tscherning & N. Gundestrup, 1998, 'Modelling the signature of a transponder in altimeter return data and determination of the reflection surface of the ice cap near the GRIP camp, Greenland', *J. Glaciology*, **44**, 625 – 633.
- Hamilton, G.S. & I.M. Whillans, 2000, 'Point measurements of mass balance of the Greenland ice sheet using precision vertical global positioning system', *J. Geophys. Res.*, **105**, 16259 – 16301.
- Hanna, E., & P.J. Valdes, 2001, 'Validation of ECMWF (re) analysis surface climate data, 1979 – 1998, for Greenland and implications for mass balance modelling of the Ice Sheet', *Int. J. Climatology*, **21**, 171-195.
- Haas, C. and H. Eicken, 2001, 'Interannual variability of summer sea ice thickness in the Siberian and central Arctic under different atmospheric regimes', *J. Geophys. Res.*, **106**(C3), 4449-4462.
- Jacka, T.H. & Li Jun, 1994, 'The steady-state crystal size of deforming ice', *Ann. Glaciology*, **20**, 13 – 18.
- Laxon, S.W., 1994. 'Sea ice altimeter processing scheme at the EODC', *Int. J. Remote Sensing*, **15**(4), 915-924.
- Laxon, S.W., & D. McAdoo, 1994, "Arctic Ocean gravity field derived from ERS-1 satellite altimetry", *Science*, **256**, 621 - 624, 1994.
- Legresy, B., & F. Remy, 1998, "Using the temporal variability of radar altimetric observations to map the surface characteristics of the Antarctic ice sheet", *J. Glaciology*, **44**, 197 – 206.
- Legresy, B. & F. Remy, 1999, 'Different ERS altimeter measurements between ascending and descending tracks caused by wind-induced features over ice sheets', *Geophys. Res. Lett.*, **26**, 2231 – 2234.

		CryoSat Calibration & Validation Concept	Doc: CS-PL-UCL-SY-0004 Issue: 1 Date: 14 November 2001
--	---	---	--

- Lytle, V. I., K. C. Jezek, A. R. Hosseinmostafa & S. P. Gogineni, 1993, 'Laboratory backscatter measurements over sea ice with a snow cover at Ku band' *IEEE Trans. Geoscience Remote Sensing*, **31**(5), 1009-1016.
- Kanagaratnam, P, S.P. Gogineni, N. Gundstrup & L. Larsen, 2001, 'High-resolution mapping of internal layers at NGRIP', *J. Geophys. Res.*, in press.
- Martin, T.V., H.J. Zwally, A.C. Brenner & R.A. Bindshadler, 1983, 'Analysis and retracking of continental ice sheet radar altimeter waveforms', *J. Geophys. Res.*, **88**, 1608 – 1616.
- Mayewski, P.A. & I.D. Goodwin, 1996, '200 years of past Antarctic climate and environmental change: Science and implementation plan', PAGES Workshop Report, Series 97-1, <http://www.ume.maine.edu/itase/toc.html>.
- McConnell, J.R., R.J. Arthern, E.Mosley-Thompson, C.H. Davis, R.C. Bales, R. Thomas, J.F. Burkhart & J.D. Kyne, 2000, 'Changes in Greenland ice sheet elevation attributed primarily to snow accumulation', *Nature*, **406**, 877879.
- Oerlemans, J., 1981, 'Effect of irregular fluctuations in Antarctic precipitation on global sea level', *Nature*, **290**, 770 – 772.
- Oerter, H., W.Graf, F. Wilhelms, A. Minikin & H. Miller, 1999, 'Accumulation studies on Amundsensien, Dronning Maud Land, Antarctica', *Ann. Glaciology*, **29**, 1-9.
- Ohmura, A., & N. Reeh, 1991, 'New precipitation and accumulation maps for Greenland', *J. Glaciology*, **27**, 140 – 148.
- Papoulis, A., 1965, 'Probability, Random Variables and Stochastic Processes', International Student Edition, McGraw-Hill, Kogakusha.
- Paterson, W.S.B, & N. Reeh, 2001, 'Thinning of the ice sheet in northwest Greenland over the past forty years', *Nature*, **414**, 60 – 62.
- Perovich, D. K. and B. C. Elder, 2001, 'Temporal evolution of Arctic Sea Ice Temperature', *Ann. Glaciology*, *In press*.
- Petit, J.R., J. Jouzel, M. Pourchet & L. Merlivat, 1982, 'Detailed study of snow accumulation and stable isotope content in Dome C (Antarctica)', *J. Geophys. Res.*, **87**, 4301-4308.
- Phillips, H.A., I. Allison, R. Coleman, G. Hyland, P.J. Morgan & N.W. Young, 1998, "Comparison of ERS satellite altimeter heights with GPS-derived heights on the Amery Ice Shelf, East Antarctica', *Ann. Glaciology*, **27**, 19 – 24.
- Remy, F., P. Mazzege, S. Houry, C. Brossier & J.-F. Minster, 1989, 'Mapping of the topography of continental ice by inversion of satellite altimeter data', *J. Glaciology*, **35**, 98 – 107.
- Rothrock, D. A., Y. Yu and G. A. Maykut. 1999. Thinning of the Arctic sea-ice cover. *Geophys. Res. Lett.*, **26**(23), 3469-3472.

		CryoSat Calibration & Validation Concept	Doc: CS-PL-UCL-SY-0004 Issue: 1 Date: 14 November 2001
--	---	---	--

- Scharroo, R., & P. N. A. M. Visser, 1998, Precise orbit determination and gravity field improvement for the ERS satellite, *J. Geophys. Res.*, **103**, 8113-8127.
- Shepherd, A.P., D.J. Wingham, J.A.D.Mansley & H.Corr, 2000, 'Inland Thinning of Pine Island Glacier, West Antarctica', *Science*, **291**, 862 – 864.
- Shepherd, A.P., D.J. Wingham, J.A.D.Mansley, 2001, 'Inland thinning of Thwaites Glacier Basin, West Antarctica', *Geophys. Res. Lett.*, **291**, submitted.
- Tucker, W. B., J. W. Weatherly, D. T. Eppler, L. D. Farmer & D. L. Bentley, 2001, 'Evidence for the rapid thinning of sea ice in the western Arctic Ocean at the end of the 1980's', *Geophys. Res. Lett.*, **28**(14), 2851-2854.
- van der Veen, C.J., and J.F. Bolzan, 1999, 'Interannual variability in net accumulation on the Greenland ice sheet: observations and implications for mass balance measurements', *J. Geophys. Res.*, **104**, 2009 – 2014.
- Vinje, T., N. Nordlund & A. Kvambekk, 1998, 'Monitoring ice thickness in the Fram Strait', *J. Geophys. Res.*, **103**(C5), 10437-10449.
- Wadhams, P., W.B.Tucker III, W.B. Krabill, R.N. Swift, J.C. Comiso and N.R. Davis, 1992, 'Relationship Between Sea Ice Freeboard and Draft in the Arctic Basin, and Implications for Ice Thickness monitoring', *J. Geophys. Res.*, **97**, 20325-20334
- Wadhams, P., 2000, 'Ice in the Ocean', Gordon and Breach, Amsterdam.
- Wadhams, P. & N. R. Davis, 2000, 'Further evidence for ice thinning in the Arctic Ocean', *Geophys. Res. Lett.*, **27**(24), 3973-3975.
- Warren, S. G., I. G. Rigor, N. Untersteiner, V. F. Radionov, N. N. Bryazgin, Y. I. Aleksandrov & R. Colony, 1999, 'Snow depth on Arctic sea ice', *J. Climate*, **12**(6), 1814-1829.
- Wingham, D.J., 1995, 'A method for determining the average height of a large topographic ice sheet from observations of the echo received by a radar altimeter', *J. Glaciology*, **41**, 125-141.
- Wingham, D.J., 2000, 'Small fluctuations in the density and thickness of a dry firn column', 2000, *J. Glaciology*, **46**, 399 – 411.
- Wingham, D.J., A.J. Ridout, R. Scharroo, R.J. Arthern & C.K. Shum, 1998, 'Antarctic Elevation Change from 1992 to 1996', *Science*, **282**, 456 – 458.
- Zwally, H.J. & Li Jun, 2001, 'Seasonal and Interannual variations of ice sheet surface elevation at the Summit of Greenland: Observed and Modelled', *Ann. Glaciology*, *in press*.
- Zwally, H.J., B. Schutz, W. Abdalati, J. Abshire, C. Bentley, A. Brenner, J. Bufton, J. Dezio, D. Hancock, D. Harding, T. Herring, B. Minster¹, K. Quinn, S. Palm, J. Spinhirne, and R. Thomas, 2001, 'ICESat's Laser Measurements of Polar Ice, Atmosphere, Ocean, and Land', *J. Geodynamics, Special Issue on Laser Altimetry*, *in press*.



7 Annex

7.1 The variance of the spatial average.

In this annex, the behaviour of the integral of the covariance function is described more fully. When the covariance function of **Error! Reference source not found.** is stationary, its integral may be simplified by rewriting it in the following way

$$\left(\frac{1}{A}\right)^2 \int_A dA \int_A dA' C_{\varepsilon\varepsilon}(\mathbf{x} - \mathbf{x}') \equiv \int_{Earth} dA \int_{Earth} dA' W_1(\mathbf{x}) W_1(\mathbf{x}') C_{\varepsilon\varepsilon}(\mathbf{x} - \mathbf{x}')$$

Here $W_1(\mathbf{x})$ is a function that equals the constant A^{-1} inside the area extended by A , and is zero outside. By assuming that $W_1(\mathbf{x})$ is non-zero only over a small region of the Earth figure, so that Cartesian co-ordinates may be used, and changing the variable of integration with $\mathbf{s} = \mathbf{x} - \mathbf{x}'$, it is then easy to show that this integral equals

Eqn. A 1 $\int_{Earth} dA W(\mathbf{s}) C_{\varepsilon\varepsilon}(\mathbf{s})$

where $W(\mathbf{x})$ is the convolution

$$W(\mathbf{x}) = \int_{Earth} dA W_1(\mathbf{x} - \mathbf{s}) W_1(\mathbf{s})$$

Similar results may be obtained with considerably more effort working with integrals over the surface of a sphere.

One important limiting case of Eqn. A 1 occurs when the extent of the covariance function, say A_c , is very much less than that extended by A , in which case

$$\int_{Earth} dA W(\mathbf{s}) C_{\varepsilon\varepsilon}(\mathbf{s}) \sim W(\mathbf{0}) \int_{Earth} dA C_{\varepsilon\varepsilon}(\mathbf{s}) \sim \frac{A_c}{A} C_{\varepsilon\varepsilon}(\mathbf{0})$$

In this case the variance of the fluctuations in the average are reduced in proportion to the ratio of the extents. A second important limit occurs when the extent of the covariance function is very much greater than that extended by A , in which case

$$\int_{Earth} dA W(\mathbf{s}) C_{\varepsilon\varepsilon}(\mathbf{s}) \sim C(\mathbf{0}) \int_{Earth} dA W(\mathbf{s}) = C(\mathbf{0})$$

In this case, the spatial averaging has no effect on the variance of the fluctuations, because they are perfectly correlated throughout the area.

7.2 The variance of an integral of a white stationary process

In general, the covariance function $E\{x(t)x(t')\}$ of a stationary process $x(t)$ is the Fourier transform of its power spectrum $P_{xx}(\omega)$. For a white process, the power spectrum is a constant, and $P_{xx}(\omega) \equiv P_{xx}(0)$. The variance of an integral of $x(t)$ is then



$$E \left\{ \left(\frac{1}{T} \int_0^T dt x(t) \right)^2 \right\} = \int_0^T dt \int_0^T dt' E \{ x(t)x(t') \} = \frac{P_{xx}(0)}{2\pi T^2} \int_{-\infty}^{\infty} d\omega \int_0^T dt \int_0^T dt' e^{i\omega(t-t')}$$

$$= \frac{P_{xx}(0)}{2\pi T} \int_{-\infty}^{\infty} d\omega \frac{\sin^2(\omega T / 2)}{(\omega T / 2)^2}$$

The last integral is a standard form. Its value is 2π . If the variance of the integral for some particular value of T , T_0 say, is known to equal σ_0^2 , then the variance for any other value of T is $\sigma_0^2(T_0 / T)$.

7.3 The variance of a spatial average over the sea ice area.

When sea ice is present, the expression for the variance of the spatial average takes the form

$$\left(\frac{1}{A} \right)^2 \int_A dA \int_A dA' E \{ \varepsilon_c(\mathbf{x})\eta(\mathbf{x})\varepsilon_c(\mathbf{x}')\eta(\mathbf{x}') \}$$

where ε_c is some component of the error. To deal with this expression, we regard as η a stationary random variable with a covariance function $C_{\eta\eta}(\mathbf{x} - \mathbf{x}')$. In the event that the error component is independent of η and may be regarded as stationary, one has

$$\left(\frac{1}{A} \right)^2 \int_A dA \int_A dA' E \{ \varepsilon_c(\mathbf{x})\eta(\mathbf{x})\varepsilon_c(\mathbf{x}')\eta(\mathbf{x}') \} = \int_{Earth} dA W(\mathbf{s}) C_{\eta\eta}(\mathbf{s}) C_{\varepsilon\varepsilon}(\mathbf{s})$$

on following the steps of section 7.1.